DYNAMIC MODELING, CONTROL AND VERIFICATION FOR CITRUS VARIABLE-RATE TECHNOLOGY (VRT) FERTILIZATION

By

SHARATH A. CUGATI

A DISSERTATION PRESENTED TO THE GRADUATE SCHOOL
OF THE UNIVERSITY OF FLORIDA IN PARTIAL FULFILLMENT
OF THE REQUIREMENTS FOR THE DEGREE OF
DOCTOR OF PHILOSOPHY

UNIVERSITY OF FLORIDA

2006

to my parents, with appreciation and gratitude

ACKNOWLEDGMENTS

I would like to acknowledge all the people who helped make this manuscript possible.

I am grateful to Dr. William Miller, the chair of this committee, who made my research more interesting with his enthusiasm and technical inputs. He is not only my chair professor but also a good friend and a guide.

I extend my gratitude to Dr. John Schueller, who has helped and guided me in every step of my life and career during my stay here in the USA. I would like to thank him especially for acquainting me with Dr. Miller and also for introducing me to many scholars and scientists at international meetings and conferences in the field of precision agriculture.

I express my warm regards to Dr. Arnold Schumann for helping me with my experiments at CREC and working his schedule for the use of equipment to both of our advantages. Without his technical help and complementary work in the field of GPS and sensors it would have been an impossible task to complete this project in the stipulated time.

I also extend my thanks to Dr. Sencer Yeralan, Dr. Won Suk Lee and Dr. Amauri Arroyo for serving on my committee and for providing valuable inputs from time to time.

I express my gratitude to the group providing technical support at CREC. I am grateful to Sherrie Buchanon for helping me with my research and also for making my stay at Lake Alfred a pleasant one. I thank Gerald Perkins, Roy Sweeb, Kevin Hostler for

modifying the equipment as required for my research. I also thank Marjie Cody for helping me with statistical analysis of my test data.

I would like to express my gratitude to my parents for all their moral and financial support without which this task could not have been accomplished. I am grateful to my wife Inka, for her patience, encouragement and advice. Finally, I thank all of my friends for being there for me.

TABLE OF CONTENTS

LIST OF TABLES

LIST OF FIGURES

Abstract of Dissertation Presented to the Graduate School
of the University of Florida in Partial Fulfillment of the
Requirements for the Degree of Doctor of Philosophy

DYNAMIC MODELING, CONTROL AND VERIFICATION FOR CITRUS VARIABLE-RATE TECHNOLOGY (VRT) FERTILIZATION

By

Sharath A. Cugati

May 2006

Chair: William M. Miller
Cochair: John K. Schueller
Major Department: Agricultural and Biological Engineering

It is essential to conserve diminishing natural resources. Hence, precision agriculture practices such as yield monitoring and variable-rate fertilization are widely being implemented in order to minimize the potential negative effects of agriculture on the environment.

The first objective was to benchmark the performance of the commercial variable-rate controller systems with various possible configurations of hydraulic and mechanical components such as flow control valves and encoders. The second objective was to empirically model the physical components of the variable-rate spreader such as flow control valves, hydraulic motor and encoders. The third objective was to develop a PID control algorithm based on these empirical models of the components to control the response of the applicator to the fertilizer requirements of individual trees.

From this study it was determined that the present commercial controllers were not customized for citrus VRT fertilization. Features such as real-time sensor offset

compensations for speed variations in the field were not currently available. A common test procedure to benchmark the VRT systems' performance in both GPS and real-time trigger mode for all possible configurations of the commercial VRT systems and also for the model-based PID controllers was developed. Two performance criteria, the "Total Application Error" (TAE) and the "Total Single Tree-Zone Application Error" (TSAE) were proposed. The best performing commercial VRT systems' configuration was determined.

Tests were conducted to determine the dynamic characteristics of the hydraulic components of the VRT system. Based on these characteristics a model-based tuning rule was used to determine the gains for the PID controller. The benchmarking tests proved that the model-based PID controller's performance, for TAE and TSAE criteria, was 62% and 82% better than the best performing commercial VRT controller with the same system components. Additional features such as the delay time and speed compensation which greatly enhance the performance of the applicator were presented and experimentally proven for commercial scale implementation with the existing technologies.

CHAPTER 1
INTRODUCTION AND LITERATURE REVIEW

Current estimates indicate that in some years, on some soils, as much as 50 percent of the nitrogen applied by farmers is not utilized by their crops (Task force, 2001). Another study by Tillman et al. (2001) concluded that if the agricultural fertilizer consumption continues at its present rate, the increased global demand for food over the next 50 years would be accompanied by a 2.4 to 2.7 fold increase in nitrogen and phosphorus driven water pollution or eutrophication of terrestrial, freshwater and near shore marine ecosystems. Hence, it is necessary to match fertilizer application with plant requirements by implementing precision agricultural practices. This reduction of environmental impacts of farming practices will be coupled with higher economic returns.

Precision Farming

Precision farming, also known as site specific crop management, is a technology in which the farmer or production manager takes into account the variability within a field to determine the optimal inputs for the crop. The variability can be spatial, temporal and predictive. The spatial variability can be classified into physical (soil properties, plant type, tree spacing), biological (diseases, pests and weeds) and chemical (nutrients, pH) types. The temporal variability is the change that occurs from year to year or during the growth period. Changes in weather and tree canopy volume can be classified as predictive factors.

Steps in Precision Farming Practice

Precision farming practices can be developed through the following steps:

- Determining variability (Input section in Figure 1-1.)
- Identifying the cause and possible actions for this variability (Management section in Figure 1-1.)
- Implementation of profitable actions (Output section in Figure 1-1.)

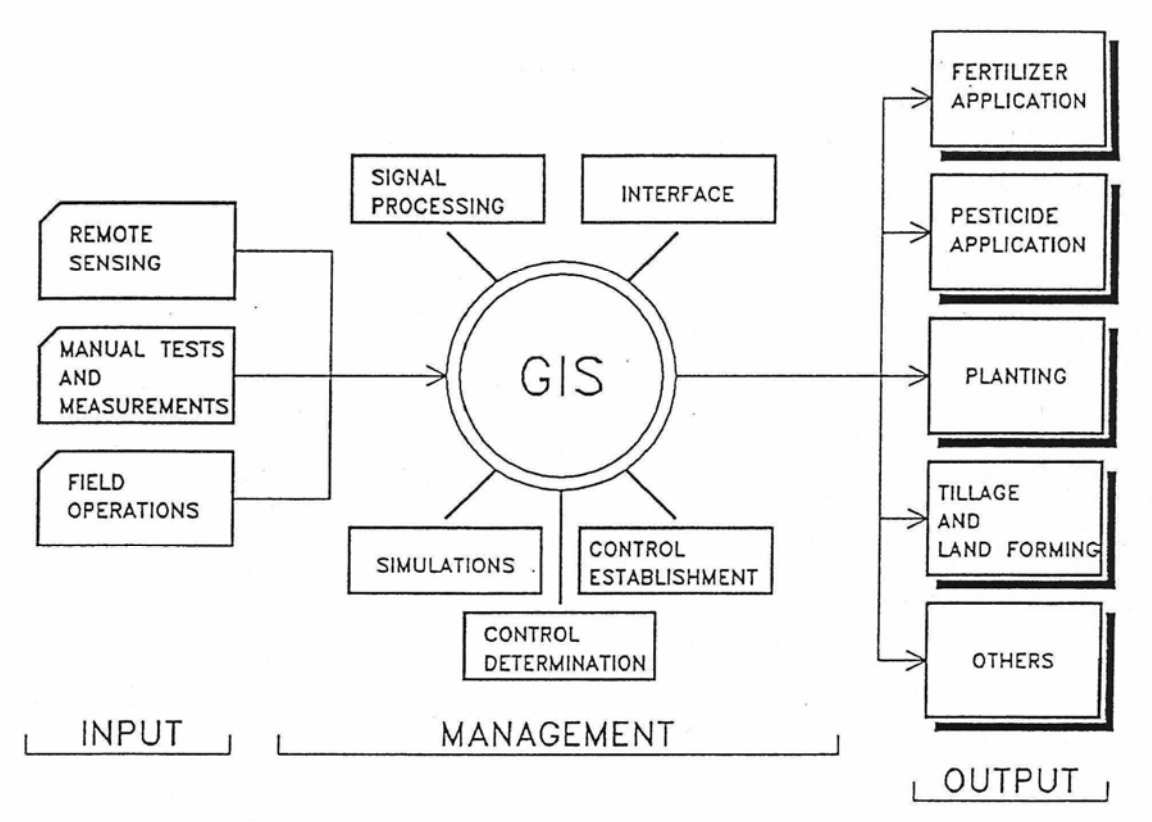

Figure 1-1. Steps in precision farming practice (Schueller, 1992).

Determining Variability

Precise crop yield data combined with soil and environmental data are essential for developing a precision crop management system. This is achieved by collecting the required data using sensors, manually or during field operations in conjunction with the use of the Global Positioning System (GPS) for spatial location or by remote sensing. Potential sensed quantities include soil properties such as pH, moisture, cation exchange

capacity (CEC), depth to water table; crop properties such as tree canopy volume, yield; pests and disease infestations.

Identification of Cause and Possible Actions

The input data are then entered into a geographic information system (GIS) where it may be post processed. GIS is a database system in which the attributes are referenced using a spatial location (latitude and longitude). Once data are analyzed in a GIS, suitable decisions can be taken by the management to deal with in-field variability. GIS is one of the many tools available to the management to decide if implementation of precision farming practices is profitable (Ess and Morgan, 2003).

Implementation of Profitable Actions

Variable-rate application (VRA) is one management approach to address in-field spatial variability. Three options for implementing VRA are described in the following subsections.

Map based approach

A map based approach is developed through use of GPS and GIS. Map based VRA systems adjust the application rate based on the information contained in a digital map of the field properties. These systems are capable of determining their position in the field with a GPS receiver, usually differentially corrected. Based on the position in the field, the controller looks for the current field conditions stored in a prescription map and changes the input (e.g., fertilizer) to the field based on these conditions. In order to compensate for the equipment lags in reacting to the controller commands and the offset between the sensors and the exit point of the fertilizer, the controller can often be programmed to “look ahead” on the map for the next change in application rate. The drawbacks of this type of system are that there are errors arising due to errors in GPS

accuracy. Also the steps involved between converting discontinuous sampled data points to continuous application maps lead to errors in estimating conditions between sample points. This method can be computer intensive with respect to memory requirements due to storage of large map data. There is also a possibility of the data being inaccurate if some field operation, for example, tree removal, was performed after the collection of the spatial data (Ess and Morgan, 2003).

Real-time or sensor based approach

In a real-time approach, the required deterministic parameters are acquired directly from the environment from the sensors and compared with set points. The control system then determines the proper application action. The sensors must provide continuous high frequency data to the controller so that inputs may be adjusted over small areas throughout the field. The concept of "look ahead" compensation in this type of application can be achieved by mounting the sensors on the front of the vehicle with the application equipment at the rear. However, errors may arise due to varying vehicle speed and insufficient lag times, available between sensing and application, necessary to achieve accurate application.

Real-time with map overlay

This approach combines the advantages of both the VRA systems mentioned above (Figure 1-2). The controller of this system obtains data from both the GPS and digital maps and real-time sensors to determine the possible actions. The positioning system can be used for data collection that can be further used for creation of control maps or for other field operations.

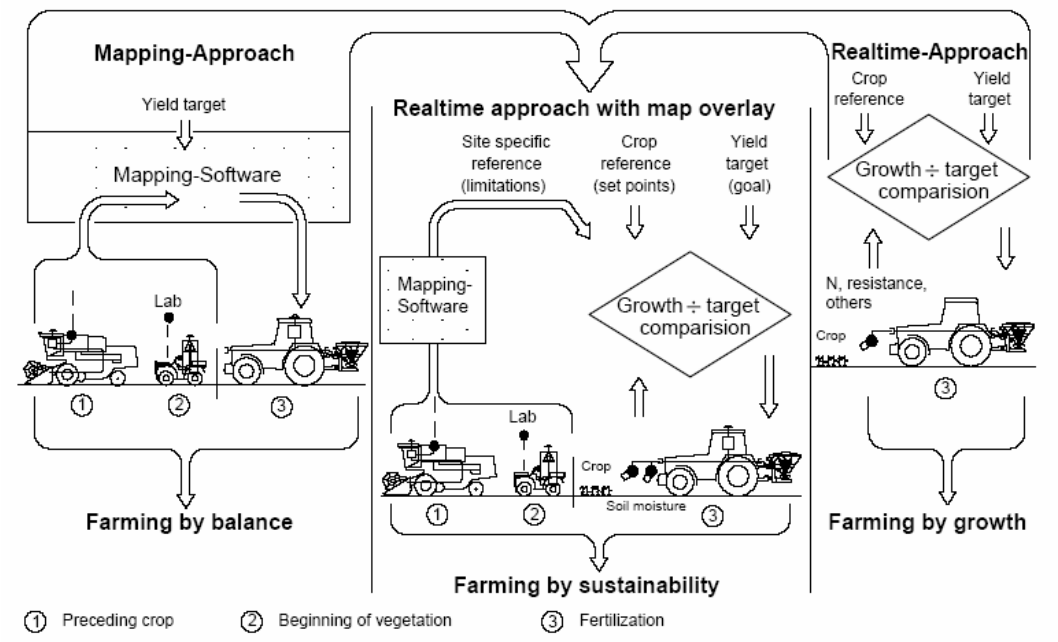

Figure 1-2. Strategies of site-specific crop management (Auernhammer, 2002).

Citrus Farming Practices in Florida

Need for Precision Agriculture Implementation in Florida

In the year 2000-2001, Florida's orange, tangerine and grapefruit production accounted for 15.1%, 1.8% and 35.8% of the world's production respectively (Food and Resource Economics Department, 2006). In that year, approximately 340,000 ha (820,000 acre) of Florida citrus were grown through Central and South Florida. The soils in these areas are predominantly a deep deposit of sand. Hence there is a need for large inputs of water, nutrients and pesticide for citrus cultivation on these soils. High average annual precipitation with sandy soils makes this area vulnerable to leaching of fertilizer and pesticides into ground water.

Typical citrus management is based on large groves or blocks ranging from one to hundreds of hectares with the assumption of minimal variability of tree canopy size, soil type, yield, texture, pH, soil drainage, etc., which has been proved otherwise by Whitney

et al. (1999). Typically in a grove, rows of citrus trees are spaced approximately 7 m apart and individual trees within each row are spaced 4 m apart. The groves in the Gulf and Indian River areas are usually bedded (Figure 1-3a) as they are typically only 1 to 1.5 m above the water table. However, the groves in the Ridge area have deep sandy soils and hence are not bedded (Figure 1-3b). Depending on different groves and tree varieties, the fertilizer application procedure also slightly varies. In the bedded groves, the applicator travels along every alternate row (avoiding the ditch) and applies the fertilizer towards the center of both the rows of trees (away from the ditch) as compared to applying it equally on both sides of the row of trees in the non-bedded groves. Diseased citrus trees and replanting practices cause significant short-range variabilities unlike small grain. These new replanted small trees are referred to as “resets”

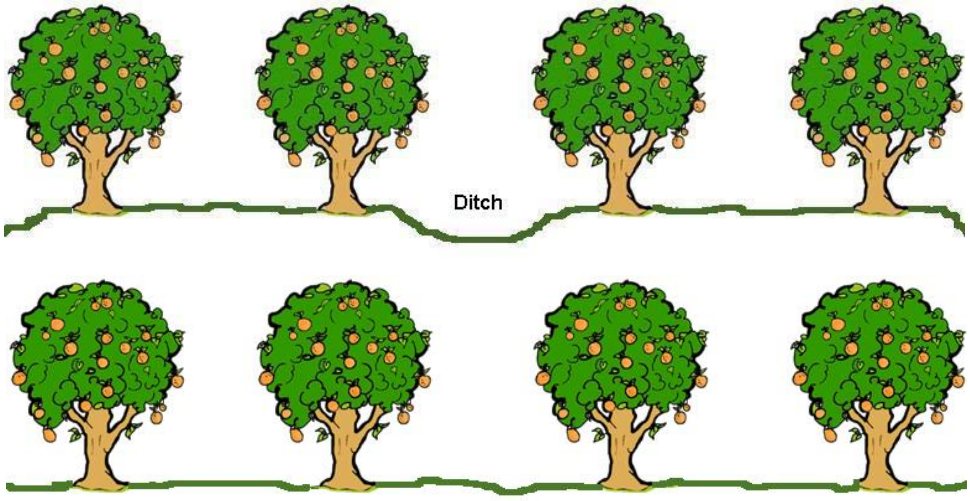

a).

b).

Figure 1-3. Types of citrus groves in Florida. a) Bedded groves and b) non-bedded groves.

Schumann et al. (2006) determined during their experiments, based on canopy volume estimates, for a central Florida ridge grove (27° 44' N, 81° 42' W) that 73.1%, 17.2%, 6.0%, and 2.0% of the fertilizer application rate zones extended over one, two, three, and four contiguous tree spaces, respectively. Remaining larger zones were

negligible (< 0.9% of total trees in the grove). Therefore, the localized spatial application and distribution of the fertilizer is essential. Due to the presence of all of the above-mentioned variability in the citrus groves, it becomes beneficial to implement variable-rate technology and precise application of granular fertilizer in Florida.

Precision Agriculture in Florida Citrus

Citrus growers in Florida are currently considering precision agriculture applications in order to comply with best management practices (BMP) and to maximize the profitability through such technologies as optimizing the use of fertilizers (Office of Agricultural Water Policy, 2006). Spatial variability implies different needs, often from tree to tree. It has been shown by Persson et al. (2003) that the working width used is inversely proportional to the amount of heterogeneity in the field. If this statement had to be adapted to tree crops, it can be concluded that maximum optimization is achieved by considering the needs of the individual tree. By implementing variable rate application of fertilizer, the grower is not only contributing to his economic benefit, but also is creating an environmental benefit through reduction of problems such as leaching of chemical fertilizers leading to contamination of ground water (Cugati, 2003). Currently, BMPs for various areas are being implemented to reduce nitrate levels in ground water (Miller et al., 2003). However, current BMP incorporates VRT on a conditional basis. BMP limits the amount of nitrogen application at any one time, increasing the frequency of application, limiting nitrogen application during rainy season, properly managing irrigation and using VRT in groves with 15% or more resets. For citrus trees 4 years or older, Tucker et al. (1995) recommended an application rate of 135-224 kg of N/ha/year for oranges and other varieties and 135-179 kg of N/ha/year for grapefruit with a minimum application frequency of 3 times per year.

Citrus yield monitors

The first step in precision agriculture implementation is to determine variability through yield mapping (Ess and Morgan, 2003). In Florida citrus yield mapping, the first component is the human component, which involves the picking of the fruit from the trees and placing it into tubs. The second portion is a truck operation when a specialized truck (goat) picks up the bins from the grove and transports it to the collection trailer (Whitney and Harrell, 1989).

There are three common methods to track the number of containers filled by each harvester. The first method involves a paper card with the harvester's name on it and once the goat driver loads the tub into the goat, the card is punched with information that depicts the number of tubs and the number of hours worked by the harvester. This involves considerable book-keeping. The second method utilizes token, where the goat driver empties the tub and leaves a token in the empty tub. At the end of the day each harvester collects all the tokens and is tallied for payroll. A third method requires touch pad entry by the goat operator. All of these methods include human interactions and are bound to have some errors. In order to reduce the amount of book-keeping and to minimize or eliminate human interaction, various sensor systems were mounted on the goat. The latest development is described based on research by Tumbo et al. (2001).

A microcontroller is interfaced with a differential Global Positioning System (DGPS) for positional information, a flash memory key for storage, two limit switches for triggering, a buzzer, and a counter for acknowledgement and counting. The microcontroller is able to track movement of the loader boom of the goat inside and outside the bed and the dumping of the tubs. Whenever a tub dumping event is detected by the microcontroller, the buzzer and counter are enabled notifying the operator that the

event is recorded. Figure 1-4b depicts the schematic of this yield monitoring system. This system did not prove to be a very effective tool as it located only the position location of the tubs and did not integrate the labor tracking system with the automated tub counting system. The yield data thus collected is used to generate the prescription map for the VRT fertilization of the groves. The yield data thus obtained was used to generate prescription maps for applicators to implement VRT fertilization of citrus groves.

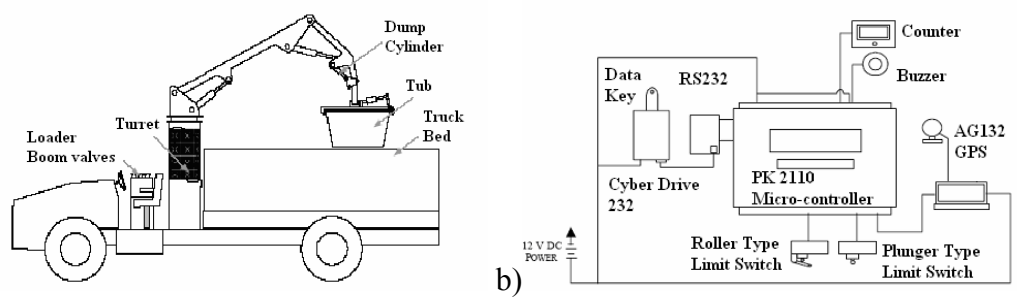

Figure 1-4. Schematic representation of a goat vehicle. a) The vehicle with hydraulic loader boom and b) the electronic circuit to record the tub-pick operation (Tumbo et al., 2001).

Variable-rate applicators

Granular fertilizer applicators are popular for agricultural field use. Application of granular materials offers several advantages over the sprayer application of liquid counterparts. Granular materials are cheaper in cost and do not have to be diluted or mixed. These granular formulations are generally safer both to the operator and environment, since there is less risk of dermal absorption, less drift and no contaminated mixing area. Another advantage of the granular fertilizer application is its capability of "slow release" or "controlled release" fertilizer material application. Most granular fertilizer applicators can be divided into two main categories, the pneumatic type and the spinner-disc type. The pneumatic applicators spread the fertilizer granules by introducing them into ducts where air is being blown at a high velocity. The fertilizer application

rates can be varied by controlling the amount of granular material that is being introduced into the air stream (Figure 1-5). The maximum discharge is limited by the air velocity.

a)  b) 

Figure 1-5. Pneumatic type variable-rate granular fertilizer applicator for citrus. a) Pneumatic type applicator and b) detailed view of the nozzle.

The concept behind the construction of the spinner-disc applicator is quite simple and robust. This applicator has a spinning disc with impellers onto which the fertilizer granules are dropped on by means of a conveyor chain. The granules on the rotating disc are under the effect of centrifugal force, gravity force, Coriolis force and the friction force as suggested by Patterson and Reece (Olieslagers et al. 1996). The friction between the particles and the disk cause a centripetal force from the disk on the particles which is overridden by the much larger centrifugal force. These forces along with the air drag affect the spread of the fertilizer granules on the ground (Mennel and Reece, 1963). A picture of the spinner disc applicator is illustrated in Figure 1-6. The required rate of the fertilizer applied can be achieved by varying the gate height and the conveyor chain speed.

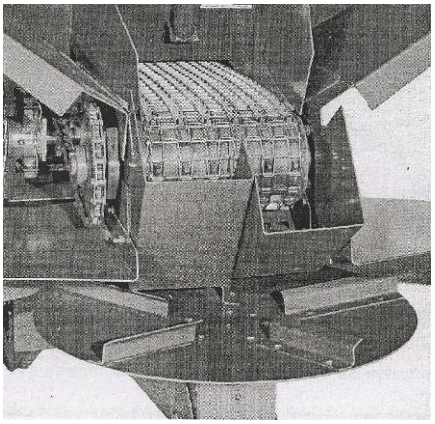

Figure 1-6. Conventional broadcast variable-rate spinner disc granular fertilizer applicator.

The variable-rate dry fertilizer applicators for citrus are a variation of the variable-rate applicators used for agronomic and vegetable production. These fertilizer applicators are modified by the addition of baffle plates to deflect the granular material towards the trees rather than spreading the fertilizer behind the applicator in the citrus grove. Due to the spinner disc enclosure and baffle plate, the spread pattern is mainly perpendicular to the direction of travel in contrast to the spinner applicators used for other crops. The applicators are equipped with two spinner discs and independent split conveyor chains to address the needs of the trees in both the left and the right rows as the applicator travels in-between these rows in the grove (Figure 1-7 a).

a)  b) 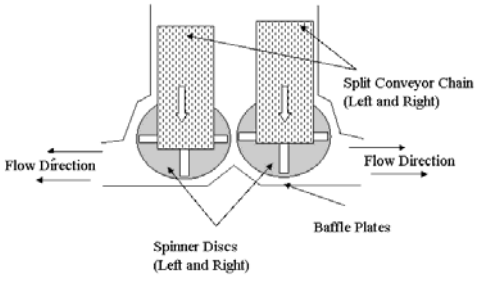

Figure 1-7. Variable-rate spinner-disc granular fertilizer applicator for citrus. a) Fertilizer applicator in a grove and b) schematic of the split conveyor chain setup.

Constant rate applicators use a ground drive of the metering chain to apply at a rate proportional to the travel speed. Electro-hydraulic systems now operated by VRT controllers vary the metering-chain speed as compared to the earlier ground driven system. The commercial VRT controller systems for citrus can operate in either map-based or a real-time mode. They are designed to accept inputs from both GPS receivers and real-time tree canopy size sensors.

Various nomenclature used during VRT fertilization of citrus groves are explained in the following. The width of the spread from the fertilizer exit point of the applicator in the direction perpendicular to the direction of travel is defined as swath width. The swath width is dependent on the spinner discs' rotational speed. Each swath can be divided into number of sections (Figure 1-8). The commercial controllers can be configured for a number of sections per swath. Typically, there will be one swath of width less than half the row spacing distance (~4 m) per side and each swath will be divided into two or more sections. The sections are used when the VRT controller is operated in real-time mode.

The real-time sensor offset is the distance along the direction of travel between the real-time tree canopy size sensor and the exit point of the fertilizer from the applicator. The GPS offset is the physical relationship (distance and direction) of a swath to the position of the GPS receiver. Presently in commercial VRT controllers, the various offsets that are being calculated are used to map the application-rate and to implement the feed-forward control actions when operating only in map-based mode. During field operations, the vehicle speed is being measured by the GPS receiver and the radar speed sensor. This measurement is used primarily to control the speed of the conveyor chain. It has been shown by Miller et al. (2004) that sensors and control, hydraulic and mechanical

components, and the drop time for the fertilizer from the conveyor chain to spinners and from the spinners to the ground, contributed to the lag in response of one of the commercial VRT systems to a change in application-rate. The present commercial controllers do not provide any compensation for lag times arising from the sensors, control or drop times. Tree-See (Roper Growers, Winter Garden, Florida) real-time canopy size sensing system compensates for the real-time sensor offset taking speed into consideration. Again in this case, the sensor does not compensate for delays arising due the various components such as GPS, valves, the controller it is interfaced with, and fertilizer drop time delays.

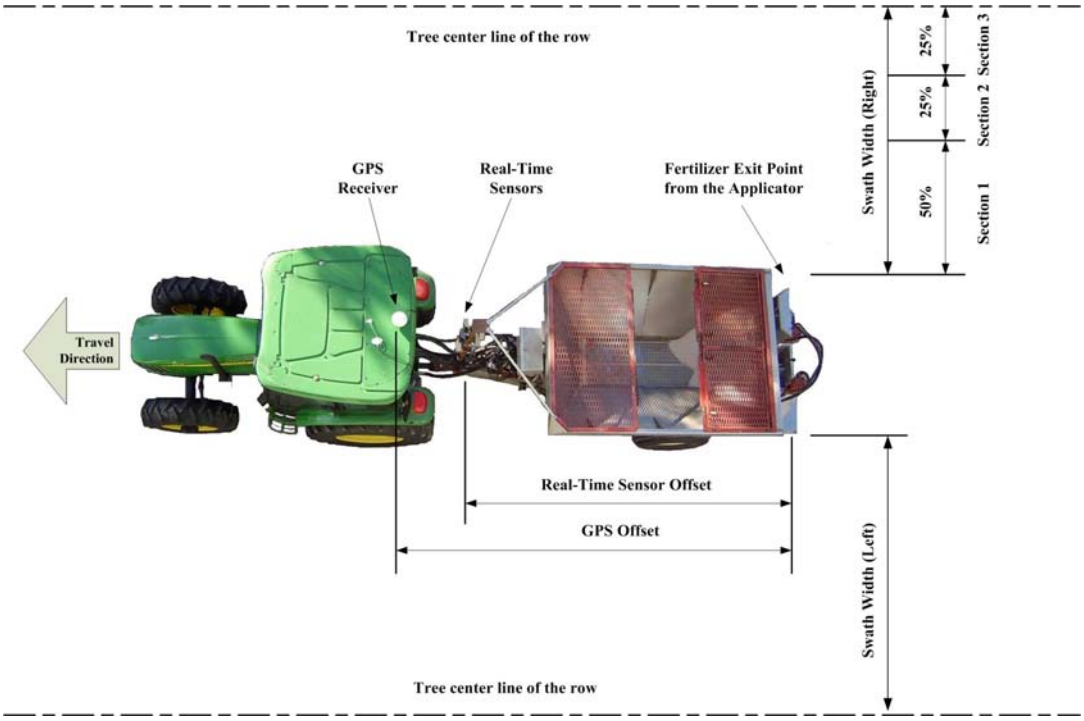

Figure 1-8. Explanation of the terms: offset, swath width and sections.

Aphale et al. (2003) presented analytical models for the on- and off-spinner distance distributions. The models reasonably predicted the distance the real fertilizer materials traveled. Olieslagers et al. (1996) provided a model to determine the spread

pattern and found that the spread pattern generated by the applicator was largely affected by variations in angular velocity of the disc as well as the change in position of the drop point. Also, changes in the mass flow lead to a fluctuating spread pattern, which resulted in large deviations from the intended application rates. All of the efforts above modeled and predicted only the steady-state operating condition of the applicator. These models cannot be used for predicting the performance of the VRT systems for citrus as these VRT systems change application rates for every tree. Hence the dynamic behavior of the components of the VRT systems has a prominent effect on the performance of the system. Fulton et al. (2001) used a sigmoid function to describe the increasing application rate changes and a linear function to describe the decreasing rate changes in a spinner disc applicator. However, this study did not address the effect of the hydraulic flow control valve on the spread pattern.

Cointault et al. (2003) developed a low-cost imaging system to determine the spatial distribution of applied fertilizer based on the measurement of initial flight conditions of fertilizer granules after their ejection by the spreading disk. A study of effect of the vane height on the distribution uniformity was performed by Yildirim et al. (2003) who found that the most uniform distribution pattern was obtained for a vane height of 35 mm. Work by Parish (2002) on the effect of PTO speed on the distribution pattern determined that a reduction of 50% in PTO speed caused pattern deterioration. Chan et al. (2003) studied the error sources affecting the variable-rate application of fertilizer. Interaction between the GPS horizontal accuracy, DGPS sampling frequencies and machine delay times of variable-rate applicator for nitrogen (N) fertilizer application was studied and it was found that the machine time delays were the most important factor

affecting the accuracy of application. An attempt to investigate various positioning systems' quality, the delays and errors involved, was made by Ehrl et al. (2003). It was determined that for a higher number of satellites, the latency was higher and settings of minimal satellite elevation, minimal azimuth or choice of filter algorithm had great influence on positioning performance.

Research Objectives

From the above literature review, it can be concluded that there is little literature available that relates the effect of the dynamic performance of the hydraulic components of the fertilizer applicator system and the controller algorithm to the final output. There are also various shortcomings in the commercial VRT controllers as stated in the previous section. There has been no prior research conducted to benchmark the performance of these commercial controllers in which they can be configured. Hence, it is important to determine the performance of the present commercial controllers so that suitable recommendations could be suggested to improve the performance of the same.

The first objective of this research was to benchmark the performance of various commercial VRT controller systems with some possible configurations of different hydraulic flow control valves and feedback encoders. The second objective was to determine the dynamic characteristics of the hydraulic components of the applicator. These results served as the basis on which a model-based Proportional Integral Derivative (PID) controller algorithm to change the application rate effectively for single tree application was developed. In the third objective, an improved controller algorithm which addressed many shortcomings listed previously about the commercial controllers was developed. Finally, the new model-based PID controller's performance was benchmarked

with the best performing commercial VRT controller configuration, determined in the first objective.

Dissertation Organization

This dissertation is organized into seven chapters each addressing various aspects of the research. Chapter 1 presented a brief introduction to the citrus production practices used in Florida and gives information about the various precision farming practices implemented in citrus cultivation. It specifically details the granular fertilizer systems that are being used for VRT and the research objectives. Chapter 2 highlights various commercial VRT controller systems that are currently available for citrus production. Chapter 3 details the procedures adopted for the various benchmarking tests that were performed on these commercial controller systems. Chapter 4 deals with experimental setup and theory referred to generate the empirical mathematical models and resultant transfer functions of the physical components of the system. Chapter 5 covers PID controller implementation and highlights the model-based tuning rules development for this type of controller. It also explains the implementation of the model-based PID controller on the existing fertilizer applicator. The final section of this chapter includes software simulations which paralleled experimental conditions. Chapter 6 compares the results of all the experiments mentioned in chapters 3-5 with respect to the performances of various controllers and system components of the granular fertilizer applicator. Conclusions, recommendations and future work are discussed in Chapter 7.

CHAPTER 2
EQUIPMENT AND EXPERIMENTAL SETUP

The 'VRT Granular Fertilizer Applicator' section describes the hydraulic system of a spinner-disc VRT granular fertilizer applicator used in field trials before the modifications that were performed before conducting this study. The 'Calculation of Application-Rate' sub-section describes how the application rates are being calculated in the commercial controller systems. The 'Commercial VRT Systems' section describes the various modules of two commercial VRT systems that were available for citrus VRT fertilizer application. The sub-sections explain the real-time tree canopy size sensor, controller modules, and the different types of flow control valves and encoder configurations that are currently available. The final section, 'Experimental Setup', describes hydraulic circuit modifications to introduce various sensors such as flowmeters and encoders. It also details the instrumentation and the interface between the hardware, the data acquisition system and the software.

VRT Granular Fertilizer Applicator

The 3-ton (2.7 metric ton) granular fertilizer applicator (M&D Spreaders, Arcadia, Florida) had a single axle frame equipped with a swivel type hitch (Figure A-1). Overall length of the applicator was 5 m and the track was 1.6 m. The hopper was constructed with 10 gauge (0.36 cm thick) 304 stainless steel sheet. A rack and pinion screw jack was used to adjust the gate height. Dual stainless steel conveyor chain, 0.25 m wide, and the conveyor roller, 0.10 m in diameter, transported the fertilizer material from the hopper to the spinner disc. The split conveyor chains were able to address different fertilizer

requirements for trees on both sides of the applicator. The vertical drop distance between the spinner discs and the conveyor chain was 0.48 m. The stainless steel spinner discs were 0.61 m in diameter with three vanes, measuring 0.18 m in length and 0.05 m in height, on each disc. The spinner discs were at a height of 0.47 m from the ground.

Hydraulic System Description

The following section details the hydraulic circuit of the commercial belt driven, dry, granular, fertilizer applicator designed for VRT application in citrus (Figure 2-1). The entire hydraulic circuit was powered by a single gear type hydraulic pump (HC-PTO-1A, Prince Manufacturing Corporation, Sioux City, South Dakota) with a specified ideal volumetric discharge of 95 L/min at a PTO speed of 540 rev/min. A three port direct acting pressure relief valve (RL-75, Brand Hydraulics, Omaha, Nebraska) protected the hydraulic circuit from overloading. Flow from the pump was directed to a Flow Divider-1 (B-50, Brand Hydraulics, Omaha, Nebraska) where the flow was divided into two equal parts, of approximately 47.5 L/min. The first output from the Flow Divider-1 powered the two hydraulic motors (M2500, Permco Inc., Streetsboro, Ohio) connected in series which turned the spinner discs of the applicator. The speed of the spinner disc motors was controlled by a needle valve limiting the flowrate to the two spinner disc motors. The second output from Flow Divider-1 was further divided into two equal parts by directing the output flow through Flow Divider-2 (B-50, Brand Hydraulics, Omaha, Nebraska). The two output flow (23.75 L/min each under ideal conditions) from Flow Divider-2 drove the two hydraulic motors (Char-Lynn H-series geroter motor, Eaton Fluid Power, Cleaveland, Ohio). Both of these low-speed, high-torque, conveyor chain motors had a volumetric displacement of 0.37 L/rev. The output shafts of these motors were connected to 6:1 speed reducing gearboxes (speed reducer, Rawson Control

Systems Inc., Oelwein, Iowa) that drove the conveyor rollers which in turn moved the split conveyor chains of the applicator to provide different application rates on the left and the right hand side of the applicator.

The flowrate to the hydraulic motors driving the split chain arrangement was controlled by DC motor operated flow control valves. The flowrate was used to control the speed of the hydraulic motors which in turn controlled the amount of fertilizer that was being dropped onto the spinner discs. There was also a 2-way, 2-position solenoid flow control valve in series with the DC motor operated flow control valve. Since, the response of the 2-way, 2-postion, solenoid flow control valve was significantly faster than the DC motor operated flow control valve, it was used to turn off the belt motor when the applicator detected a small tree or a reset. An encoder mounted on the gearbox provided the feedback signal for the system. A commercial controller system (Legacy 6000, Midwest Technologies, Springfield, Illinois) was being used on this applicator. These commercial controller systems are explained in detail in the following sections.

Calculation of Application Rate

To determine the application rate of the applicator, the density of the fertilizer material, swath width of the spread, speed of the hydraulic motor-gearbox combination, speed of the applicator and the values for the applicator's parameters mentioned in the previous section are required. The following equations show the calculation for the application rate in kg/ha:

$$Application\ Rate = \left(\frac{(k \times q) \times \pi \times D \times h \times w \times \rho}{s_w \times v \times 0.0001} \right) \tag{2.1}$$

or,

$$Application\ Rate = \left(\frac{\omega \times \pi \times D \times h \times w \times \rho}{s_w \times v \times 0.0001} \right) \quad (2.2)$$

where,

s_w = Swath width (m)

v = Current speed of the applicator (m/s)

ρ = Fertilizer material density (kg/m^3)

h = Gate height (m)

w = Conveyor chain width (m)

D = Conveyor roller diameter (m)

$\omega = k \times q$ = Speed of the motor-gearbox shaft (rev/s)

where,

k = Gain of the hydraulic motor-gearbox combination (rev/L)

q = Flowrate input (L/min)

Rate of coverage area of fertilizer (ha/s) for the given swath width and a vehicle speed =

$$(s_w \times v \times 0.0001) \quad (2.3)$$

Rate of fertilizer deposition (kg/s) at the stated speed of motor-gearbox shaft =

$$(\omega \times \pi \times D \times h \times w \times \rho) \quad (2.4)$$

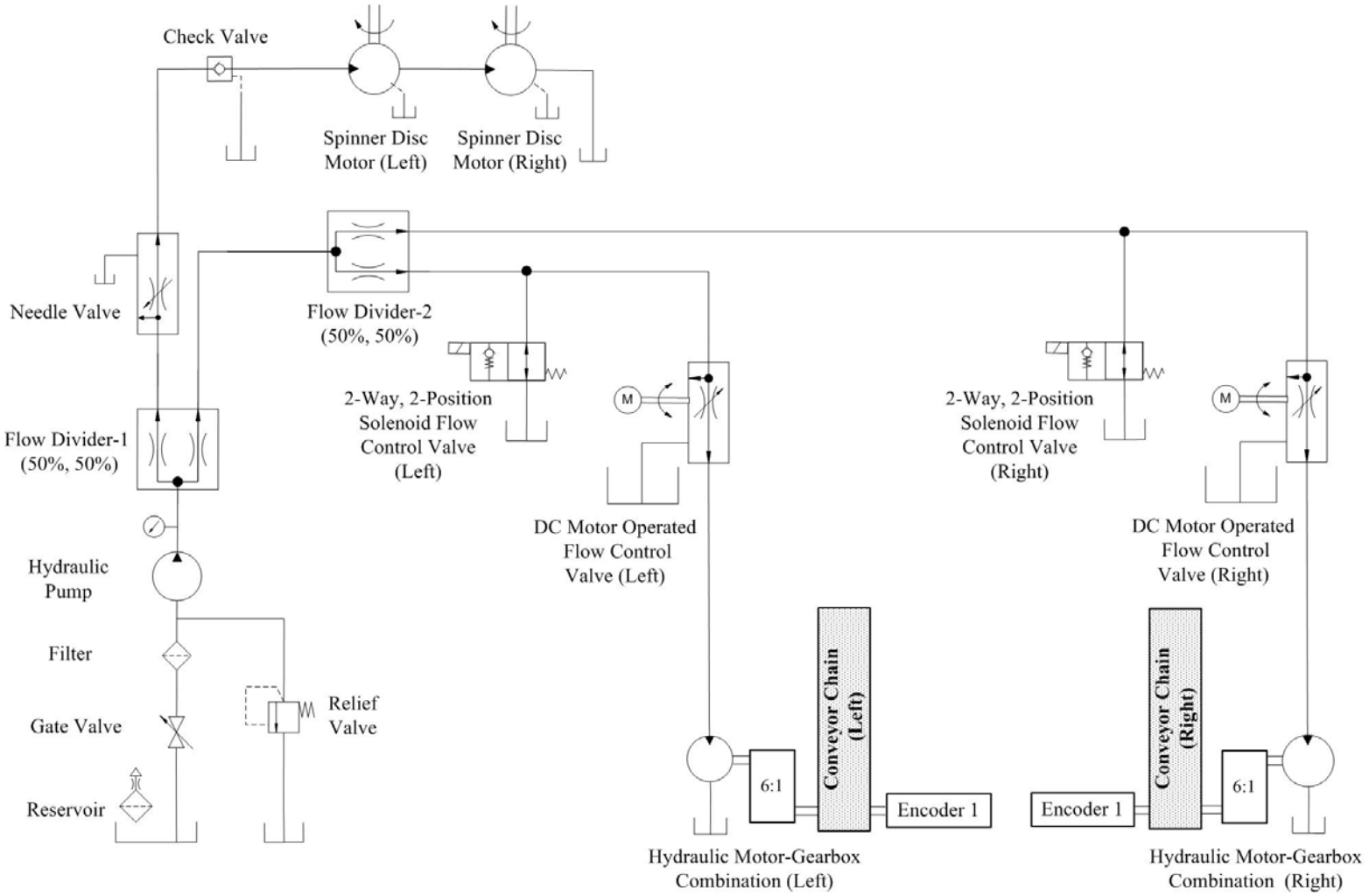

Figure 2-1. Schematic of the hydraulic system of the commercial VRT system of the fertilizer applicator.

Commercial VRT Systems

The commercial systems available for VRT application were comprised of various subsystems.

- The real-time tree canopy size sensors.
- A controller module, usually having various ports for inputs from real-time sensors and GPS receivers.
- The electro-hydraulic component, usually the hydraulic flow-control valves for granular applications.
- The feedback component, usually rotary encoders for granular applications.

In granular fertilization for citrus VRT, the principal electro-hydraulic components were the various types of flow control valves. In case of the feedback component, it was the various types of encoders that were used to determine the number of revolutions of the conveyor chain roller shaft.

Real-time Tree Canopy Size Sensor

Three infrared sensors (QMT 42, Banner Engineering, Minneapolis, Minnesota) formed the real-time tree canopy size sensing system for each side. The sensors were pointed at the trees in the direction perpendicular to the direction of travel. The sensors were mounted on a vertical pole, or directly on the applicator body, such that their infrared light beam was emitted and was reflected back to the sensors after striking the tree in front of it. Detection of the reflected infrared light denoted the presence of the tree at that level. By having three sensors, it was possible to have four classes of tree canopy size. When all of the sensors did not detect any reflected infrared light then there was no tree, if only the bottom sensor detected the infrared light then it was a small tree, if both the bottom and the middle sensors detected the infrared light then it was a medium tree and if all of the sensors detected the infrared light then it was classified as a large tree.

The sensors were designed such that they were not energized by reflected infrared light that is not emitted by their source. By increasing the number of sensors it is possible to have more intermediate classes of tree canopy size.

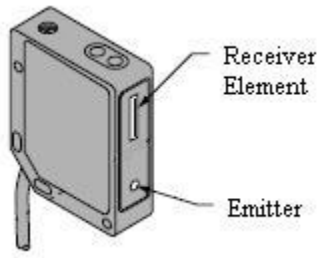

Figure 2-2. Real-time infrared sensors for tree canopy size determination.

Each section of the swath width described in the previous chapter can be associated with any particular sensor and each section can have a percentage of the maximum application rate assigned to it. For example, sections one, two and three maybe assigned percentages of 50%, 25% and 25% of maximum application rate and were associated to the bottom, middle and upper real-time sensor respectively. When only the bottom sensor was triggered (small tree), the output application rate will equal 50% of the maximum application rate, when the bottom and the middle sensors were triggered (medium tree), the output application rate will be 75% of the maximum application rate and when all three sensors were triggered, the output will be equal to the maximum application rate.

Commercial Controller Modules

The controller modules had various communication ports and other low level components to effectively interface with subsystems such as GPS receivers, electro-hydraulic valves, speed sensors, encoders, flowmeters, PDAs, etc. These modules formed the human machine interface (HMI) between the operator and the system. The HMI was used to load a prescription map, to set the gains of the controller, to calibrate

the system or to download the "as applied" data. Various levels of automation can be implemented depending upon the manufacturer and the cost. However, these controller modules' interfaces were not adapted specifically to a citrus application. In the following, different commercial controller modules that were benchmarked in this study and their features are described.

Calibration Procedure: The calibration number is defined as the volume of the material deposited per unit encoder pulse. The commercial controller units take into consideration a hypothetical speed of the applicator that was set by the operator. Then the unit was set to apply the fertilizer at a constant application-rate for a fixed amount of time in a stationary mode. The output material during this time was collected and weighed. The controller displayed the mass of the actual amount of fertilizer output calculated based on the old calibration number (equation 2.5). After the first run, the actual weight of the material deposited was entered by the operator into the system. The controller calculated the new calibration number for the new run based on this entry and the test was repeated again. This procedure was performed until the weight displayed by the controller module and the weight (kg) of the actual material deposited were equal.

$$\textit{Mass of the fertilizer output} = (pr \times t \times \rho) / cn \tag{2.5}$$

where,

pr = Encoder pulse rate (p/s)

t = time (s)

ρ = Fertilizer material density (kg/m^3)

cn = Calibration number (p/m^3)

Commercial Controller Module-1

The commercial controller module (Legacy 6000, Midwest Technologies, Springfield, Illinois) will be referred to as the Commercial Controller Module-1 henceforth. The controller had a 32-bit Intel StrongArm processor operating at 206 MHz running a Microsoft Windows CE 3.2 operating system. It had 32 MB of DRAM and 32 MB flash memory. The controller module had two RS232 and one USB ports. The serial string output from the GPS receiver was connected to one of these RS232 ports of the controller module. The module was compatible with differentially-corrected GPS (DGPS) receivers which output the NMEA 0183 GGA sentence at 2 Hz or greater. The controller communicated with the various subsystems by means of a proprietary CAN bus protocol (Figure 2-3). The various subsystems are:

1. The Power Speed Module (PSM), which was the primary arbitrator for the bus and the gateway for parallel networks. It accepted two speed sensor digital inputs optimized for 50% duty cycle, with a range from 0-5 kHz.

2. The Switch Sense Module (SSM), which monitored the status of switches aboard the vehicle. It can sense up to 20 digital switches (0 V / 12 V DC) per module. In these tests, digital inputs from the real-time canopy sensors were utilized with three sensors for each side.

3. The Product Control Module (PCM) controlled the product delivery system by connecting to the actuator and the sensor. One PCM was required for each application. Each PCM module had four digital inputs (0-12 V DC) with a range of 0-5 kHz and two analog inputs (0-5 V DC) for the sensors. The output signal can be a 12 V DC pulse width modulation (PWM) signal or a current control signal, depending upon the valve being controlled. The PCM could control only one output at any instance. All the other inputs were used only for monitoring.

The Controller module was configured for dual channel granular spreader (Midwest Technologies, n.d.). The controller could be used either in a map-based mode or in a real-time mode or in a real-time with map-overlay mode. The system was configured in various steps before citrus grove VRT fertilization. The first setup was the GPS. Then

information such as the type of application – liquid or granular; drive type – servo (for DC motor operated flow control valve) or solenoid (for proportional solenoid flow control valve); valve properties such as gain; units being used for measurement (kg/ha) and the type of sensor – encoder with a certain calibration number (e.g., 18000 p/m^3) formed the PCM setup.

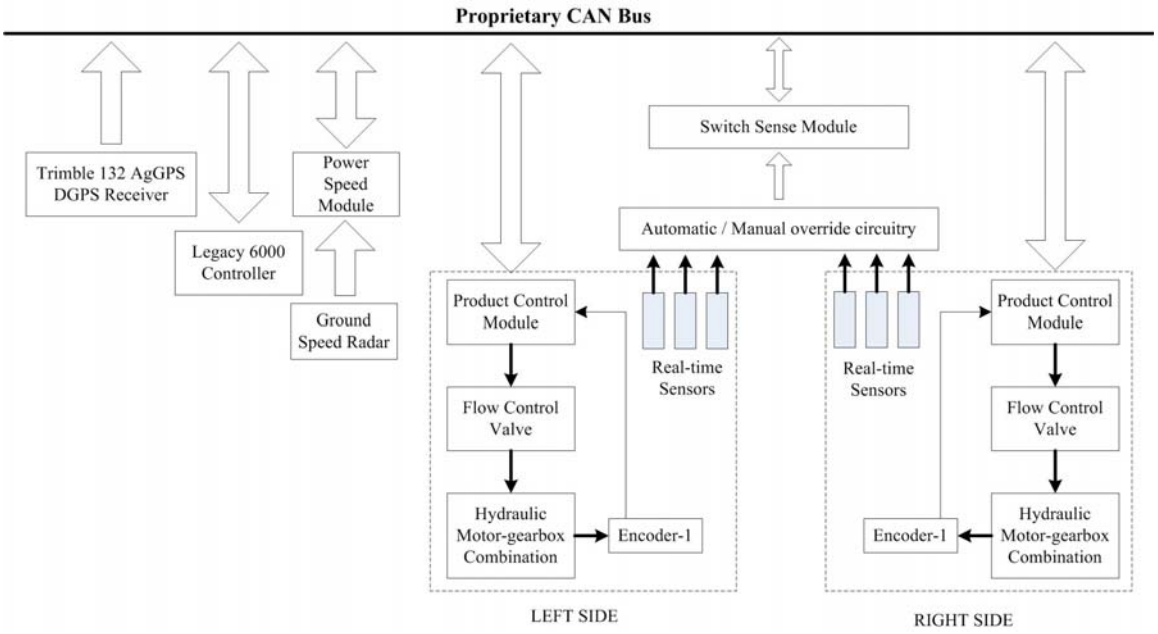

Figure 2-3. The Legacy 6000 controller system interfaced with the fertilizer spreader.

Commercial Controller Module-2

The commercial controller module (Land Manager II, DICKEY-john Corporation, Auburn, Illinois) will be referred to as the Commercial Controller Module-2 henceforth. The Commercial Controller Module-2 was comprised of six basic components: a display console, a master switch module, a ground speed sensor, a feedback device to monitor application rate (rotary encoder), an actuator device to regulate the application rate (proportional solenoid flow control valve) and the harness system. A maximum of ten digital input channels could be configured as inputs. In citrus application, three of these

inputs were connected to the three infrared real-time tree canopy size sensors for each side.

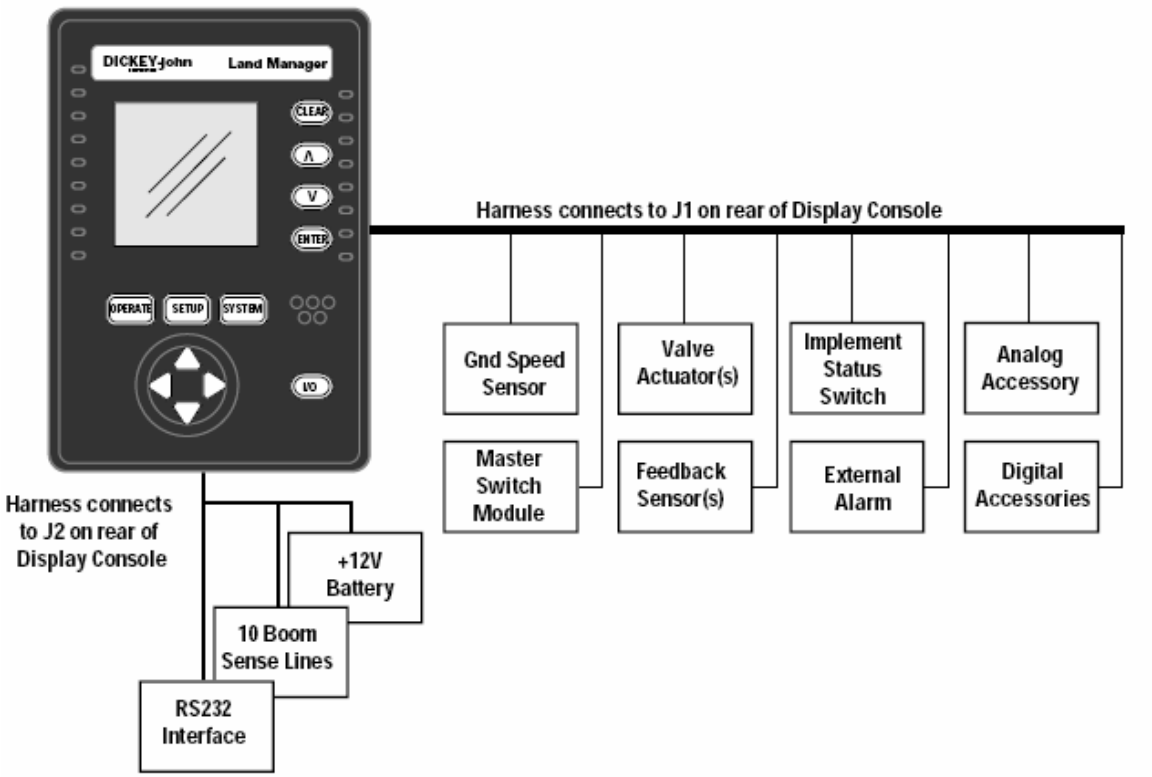

Figure 2-4. The Land Manager II controller system. (DICKEY-john Corporation, 2003)

This controller had the capability to control two independent channels, i.e., left and right side of the applicator in the real-time mode but only one channel in the GPS mode. The module obtained its current speed from a GPS receiver operating at 5 Hz. The module was also equipped with a RS232 serial port. Map-based mode operation could be achieved by connecting the controller module to a PDA loaded with Farm Site Mate software (Farmworks, Hamilton, Indiana) through the RS232 port. This module without the PDA was capable of operating in only real-time mode. Another interesting feature of this controller module was the 'Automatic Gain Calibration'. Automatic Gain Calibration tuned the gain values for the control loop for a particular solenoid valve. The results

established determined good working values which could be fine-tuned based upon field operation. The setup of this controller was similar to Commercial Controller Module-1 in terms of calibration.

Flow Control Valves

In the following sub-sections the various types of flow control valves that control the speed of the hydraulic motor-gearbox combination which moves the conveyor chain are described in detail.

DC motor operated flow control valve

A DC motor with gear reduction, which rotated at a constant speed, controlled the operation of the DC motor operated flow control valve (Midtech EXR II, Midwest Technologies, Springfield, Illinois). The angle of turn from completely closed to completely open was 90º with the flowrates ranging from 0 L/min to a rated full flowrate respectively. The design of the valve provided for a linear increase or decrease in flow for a constant valve stem speed. This was achieved by the placement the valve stem with a circular orifice into a concentric cylinder with a rectangular slot which converts the variable circular orifice into a variable rectangular orifice (Figure 2-5b and 2-5c). It took three seconds for the valve to turn from a completely closed state to completely open position. Hence the change in the rotational speed of the valve stem was 30º/s. The input command to the valve was a 12 V pulse width modulated DC supply. Reversing the polarity of the signal changes the direction of the rotation. For example, if the valve stem was given a rotational input of 15º then the command signal should be a pulse of 12 V for the duration of 0.5 s with a duty-cycle of 100%. In controlling the valve with the commercial controller modules, the valve was directly connected through the wiring harness provided along with the controller modules.

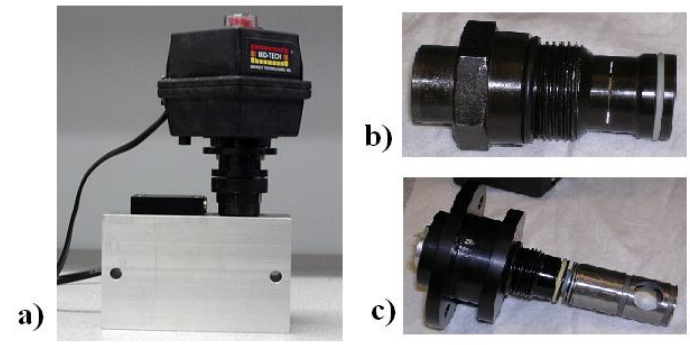

Figure 2-5. DC motor operated flow control valve. a) Complete valve assembly. b) Valve-stem housing with a rectangular slot. c) Valve stem with circular orifice.

Proportional solenoid flow control valve

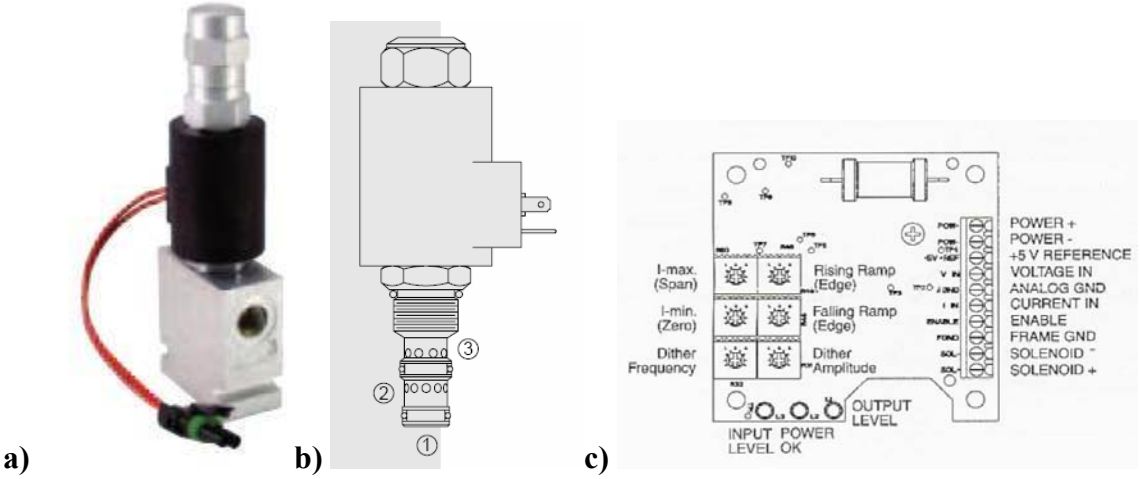

Figure 2-6. Proportional solenoid flow control valve. a) Complete valve assembly. b) Port nomenclature. c) Valve controller board.

The proportional solenoid flow control valve (DICKEY-john Corporation, Illinois) consisted of a spool that was spring loaded and also had an electromagnet. The valve was normally closed when de-energized. The regulated flowrate was from 0-15 L/min. The flowrate, with pressure compensation, could be regulated by controlling the current that was being supplied to the electromagnet's coil. The spool was drawn against the spring force when a current was being supplied to the electro-magnet regulating the flow from port 1 to port 3 (Figure 2-6 b). The flow rate was directly proportional to the supplied

current. For commercial controllers, the valve was directly connected to the harness provided by the controller modules.

2-way, 2-postion, solenoid flow control valve

The 2-way, 2-postion, solenoid flow control valve (Vickers SV3-16-O, Eaton, Grand Rapids, Michigan) in the hydraulic circuit was operated by switching on/off a 12 V power to the valve. Maximum flowrate rating for this valve was 133 L/min under a maximum pressure load of 20 MPa. For commercial controllers, the valve was directly connected to the harness provided by the controller modules. When this valve was not supplied with power, the complete oil flow was diverted into the reservoir. The total flow was diverted to the hydraulic circuit downstream when the solenoid valve was energized with 12 V DC.

Encoders

The encoders were used for feedback of the actuator state, in this case the motor-gearbox combination, to the control module. The control algorithm accepted this feedback and then determined the necessary action needed to be taken to obtain the desired output from the actuator. The encoder shaft was coupled with the motor-gearbox combination shaft. The rotation of the motor-gearbox combination was thus converted to a digital pulse train with a 50% duty cycle, either a 0-5 V or a 0-12 V, based on the power input to the encoder. By determining the frequency of this pulse, it was possible to calculate the speed of the shaft, if the number of pulses per revolution of the shaft was known.

There were two types of encoders provided with the commercial VRT controller systems based upon the method used to generate the pulse. The first type of encoder was known as the Hall Effect sensor. This sensor was mounted on the gearbox in close

proximity to the gear teeth. In this type of encoder, a pulse was generated when the magnetic flux generated by the sensor was disturbed by the moving gear tooth causing the flux field to expand and collapse. These sensors can be used in very hostile environments and are proven to be sturdy. This type of encoder (GS101201, Cherry Corporation, Pleasant Prairie, Wisconsin) was used in conjunction with the motor-gearbox combination and was mounted on the gearbox casing. It generated 67 pulses per revolution of the shaft. Henceforth, this encoder will be addressed as Encoder-1.

An incremental optical rotary encoder consisted of an illumination source, a rotating grating or code wheel, and a set of optical detectors. The grating structures were created by deposition of an opaque material on the glass surfaces in a controlled and repeatable manner. The number of alternating clear and opaque patterns placed upon the perimeter of the rotating disk defined the number of pulses the encoder will generate per revolution. Encoders of this type compared the light detector output with a threshold level via a comparator circuit. This allowed a digital signal to be generated with a period equal to the cyclic fluctuation of the incident light. The commercial encoder (Application Rate Sensor, DICKEY-john Corporation, Auburn, Illinois) of this type, bundled with the VRT Commercial Controller Module-2, generated 360 pulses per revolution of the shaft. This encoder will be addressed as Encoder-2. A similar incremental optical encoder (F14, Dynapar, Gurnee, Illinois) was used for experimental purposes. It generated 5000 pulses per revolution of the shaft and will be addressed as Encoder-3. Both Encoder-2 and Encoder-3 were connected to the tail shaft of the conveyor chain.

Experimental Setup

As the fertilizer applicator had to be operated in its original configuration for other field tests, it was decided to redesign the hydraulic circuit such that the spreader could be operated in any required configuration without having to re-plumb the hydraulics. Figure 2-7 illustrates the hydraulic circuit of the applicator after its modification. Experimental data were acquired from the operation of the hydraulic system on one side (right) of the applicator. The flow coming out of the right side output of Flow Divider-2 passed through a 6-port double selector valve (DS-4A1E, Prince Manufacturing Corporation, North Sioux City, South Dakota). By operating the hand-lever on the direction control valve, the flow was directed to either the DC motor operated flow control valve or the proportional solenoid flow control valve. The output flow from both of these valves was connected to the input of the hydraulic motor-gearbox combination. A flowmeter (Flowmeter-1 or Flowmeter-2), a needle valve and a pressure transducer were placed in series between the flow control valves' output and the input to the hydraulic-motor gearbox combination. Data from the hydraulic pressure transducer, flowmeter (Flowmeter-1 or Flowmeter-2) and the encoder (Encoder-1, Encoder-2 or Encoder-3) were acquired at a rate of 50 Hz with a laptop computer with a PCMCIA data acquisition card (Table 2-1) and LabView software (Ver. 7.1, National Instruments Corporation, Austin, Texas.). Table 2-1 lists the specifications of all the sensors and data acquisition hardware used for the study. The signal from the pressure transducers were filtered for noise with a low-pass active filter with a cut-off frequency of 100 Hz.

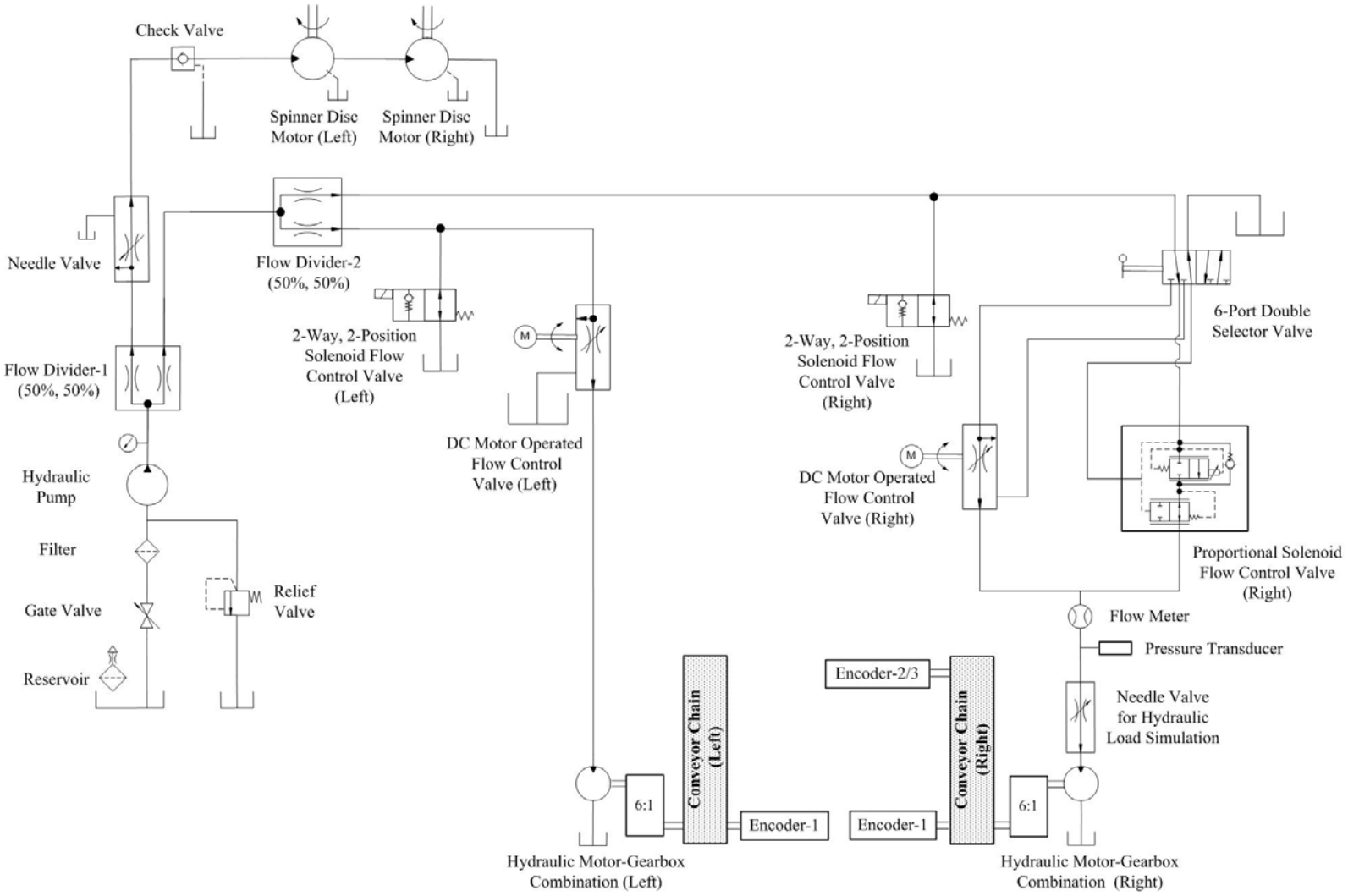

Figure 2-7. Modified hydraulic circuit of the VRT applicator for the experimental setup.

Table 2-1. Sensors and data acquisition card specifications

Type of transducer	Manufacturer	Model	Input Range	Output Range
Pressure	Barksdale	426-10	0 – 6.8 MPa	1 – 11 V
Flow (Flowmeter-1)	Hedland	RAM 520-100	0 – 23 L/min	0 – 5 V
Flow (Flowmeter-2)	AW Company	JVA-60KG	0.19 – 75.71 L/min	926 p/L
Angular speed (Encoder-1)	Cherry Corporation	GS101201		67 p/rev
Angular speed (Encoder-2)	DICKEY-john Corporation	Application-Rate Sensor	2– 2500 rev/min	360 p/rev
Angular speed (Encoder-3)	Dynapar	F14 (Incremental)	0 – 6000 rev/min	5000 p/rev
Data acquisition	National Instruments	DAQ-6036E	Analog:±10 V, 8 channels, 16 bit Digital: 0 – 5 V, 8 ports, 2 digital counters	Analog:±10 V, 2 channels, 16 bit Digital: 0 – 5 V, 8 ports

Controlling the speed and direction of the rotation of the valve stem of the DC motor operated flow control valve was achieved by providing the valve controller board (Figure 2-8) with a voltage ranging between 0 and 6 V. 0 V corresponded to the maximum speed (30º/s) in close direction and 6 V corresponded to the maximum speed (30º/s) in the open direction. Providing the controller with a voltage between 3.06 and 3.26 V would keep the motor shaft of the flow control valve stationary. Figure 2-9 depicts the DC motor operated flow control valve's angular speed and direction for any commanded voltage input to the controller board from LabView. This controller board was used only for LabView interface with the valve.

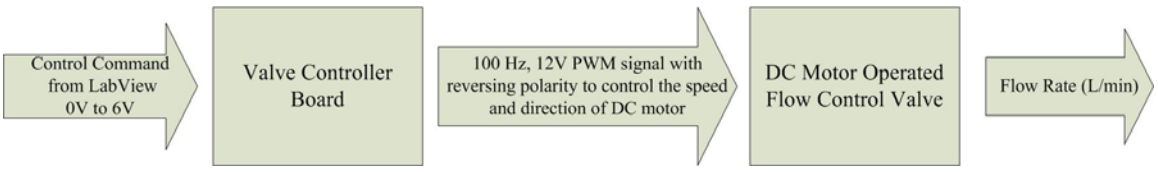

Figure 2-8. Command signal flow for the DC motor operated flow control valve.

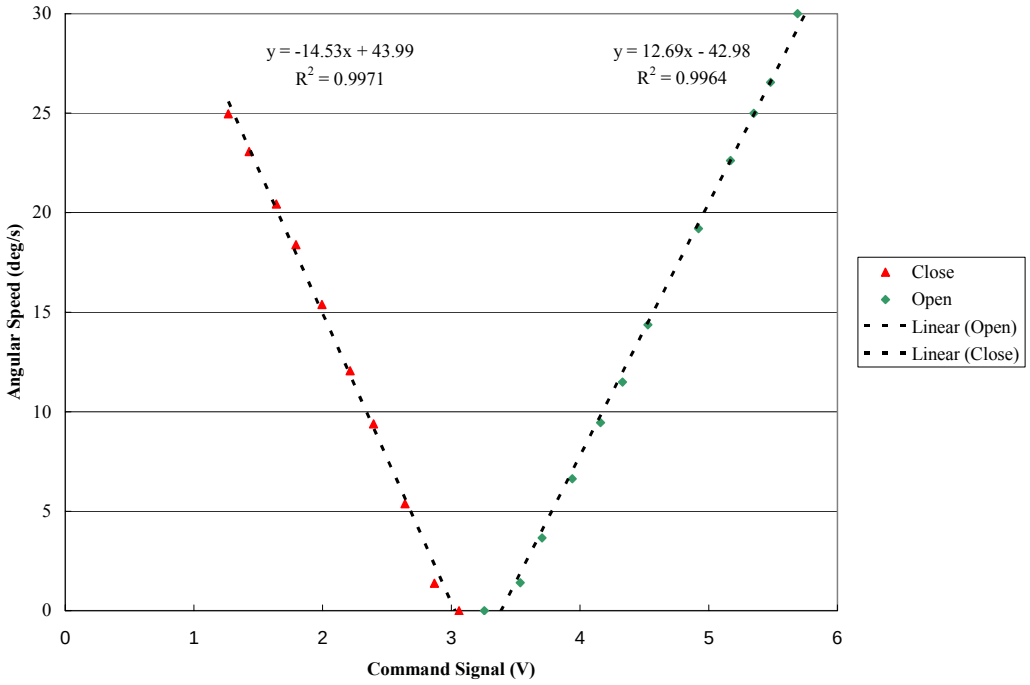

Figure 2-9. Calibration of controller board for the DC motor operated flow control valve.

The current control for the proportional solenoid flow control valve in LabView was achieved by a controller board (Figure 2-6c), where the analog voltage command ranged between 0 V and 5 V. Potentiometers were provided on the board for fine tuning for rising ramp, falling ramp, dither level, dither frequency, maximum and minimum current. The minimum or the threshold current was specified as 300 mA ± 100 mA while the specified maximum current was 1500 mA ± 100 mA.

Optically isolated relays (G4ODC5A, Opto 22, Temecula, California) were used to separate the signal level logic from the high current and voltage circuit used to control the 2-way, 2-position flow control valve in LabView.

A combination of the various commercial controller modules, flow control valves and encoders resulted in various system combinations. Apart from the above mentioned commercial controllers, two control algorithms were coded in LabView software

(LabView Controller-1 and LabView Controller-2) to control the proportional solenoid flow control valve and the DC motor operated flow control valve respectively. Hence, due to various combinations of controllers, flow control valves and encoders, a set of generic names were assigned to all of these combinations and will be referred to by 'System Number'. Each 'System Number' and its corresponding configuration is listed in Table 2-2.

Table 2-2. Designation for various VRT control systems that were evaluated.

System Number	Controller Module	Valve Combination	Feedback	Trigger Mode
01	Commercial Controller Module-1	DC motor operated flow control valve	Encoder-1 67 p/rev	GPS
02	Commercial Controller Module-1	DC motor operated flow control valve + 2 way, 2 position solenoid valve	Encoder-1 67 p/rev	GPS
03	Commercial Controller Module-1	DC motor operated flow control valve	Encoder-1 67 p/rev	Real-time
04	Commercial Controller Module-1	Proportional solenoid flow control valve	Encoder-1 67 p/rev	GPS
05	Commercial Controller Module-1	Proportional solenoid flow control valve	Encoder-1 67 p/rev	Real-time
06	Commercial Controller Module-2	Proportional solenoid flow control valve	Encoder-2 360 p/rev	GPS
07	Commercial Controller Module-2	Proportional solenoid flow control valve	Encoder-2 360 p/rev	Real-time
08	Commercial Controller Module-2	Proportional solenoid flow control valve	Encoder-1 67 p/rev	Real-time
09	LabView Controller-1	Proportional solenoid flow control valve	Flowmeter-2 926 p/L	Real-time
10	LabView Controller-2	DC motor operated flow control valve	Flowmeter-2 926 p/L	Real-time

CHAPTER 3
BENCHMARKING OF COMMERCIAL CONTROLLER SYSTEMS

There is an engineering need for standardization for all aspects of VRT applications and yield monitoring and a framework for the development of a new standard for characterizing and reporting performance of VRT systems was proposed by Shearer et al. (2002). The ASABE standard S341.3 measures the distribution uniformity and calibrates granular broadcast spreader. Currently the ASABE PM-54 precision agriculture committee is working on standardizing procedures for evaluating yield monitoring and variable-rate granular material application accuracy. Miller et al. (2003) developed a test procedure using the ASAE standard S341.3 and a field-testing facility to generate 2D dynamic performance information for the variable-rate granular fertilizer applicator. It was not possible to use this method to evaluate the control system performance as the effect of external variables such as wind, vehicle speed change, etc. could not be controlled. Also, it was only possible to evaluate the overall performance of the applicator as the sub-component elements such as controller, hydraulic valves and sensors could not be isolated and analyzed. It would be very labor intensive to conduct this test for multiple rate changes. In this chapter, a new test procedure to benchmark various commercial controllers and their configurations are presented. These tests were performed to determine the effect of the components on the performance of the applicator. Also the performance difference when operating in map-based or real-time mode was determined.

Experimental Concept

In order to perform an unbiased comparison between the performances of different configurations of the VRT systems described in Table 2-2. All the tests were performed in a stationary condition. An input to simulate the applicator traveling at a constant speed of 1.34 m/s across fifteen tree zones, 5.3 m in length, in series from north to south was used (Figure 3-1).

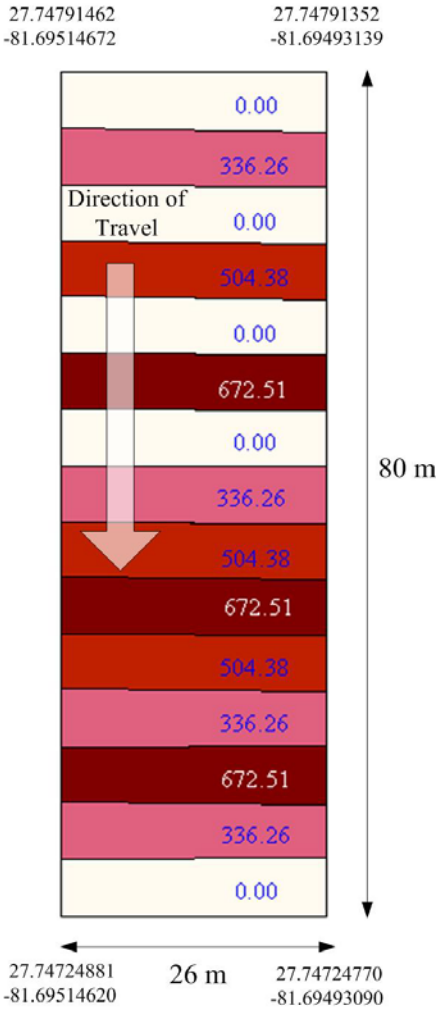

Figure 3-1. Application rates in kg/ha for the fifteen tree zones.

The initial and the final tree zones were assumed to be “resets” and were assigned 0 kg/ha application rates. There were three intermediate application rates selected,

336.26 kg/ha, 504.38 kg/ha and 672.51 kg/ha. These rates corresponded to the commercial controller modules when operating in real-time mode distinguishing only 3 classes of trees (small, medium or large) due to the limitation on the number of real-time tree canopy size infrared sensors. The controller modules were calibrated such that an application rate of 336.26 kg/ha corresponded to a flow rate of 6 L/min from the flow control valve at a constant applicator travel speed of 1.34 m/s. This relationship was linear for a constant applicator travel speed and hence a flow rate of 12 L/min corresponded to an application rate of 672.51 kg/ha. From Equation 2.1, the application rate is directly proportional to the flowrate output from the flow control valve for a constant applicator travel speed. At a speed of 1.34 m/s, it takes approximately 60 seconds for the applicator to travel a distance of 80 m. Figure 3-2 depicts the position of the applicator at any instant of time and the corresponding application rate matches the tree zones depicted in Figure 3-1.

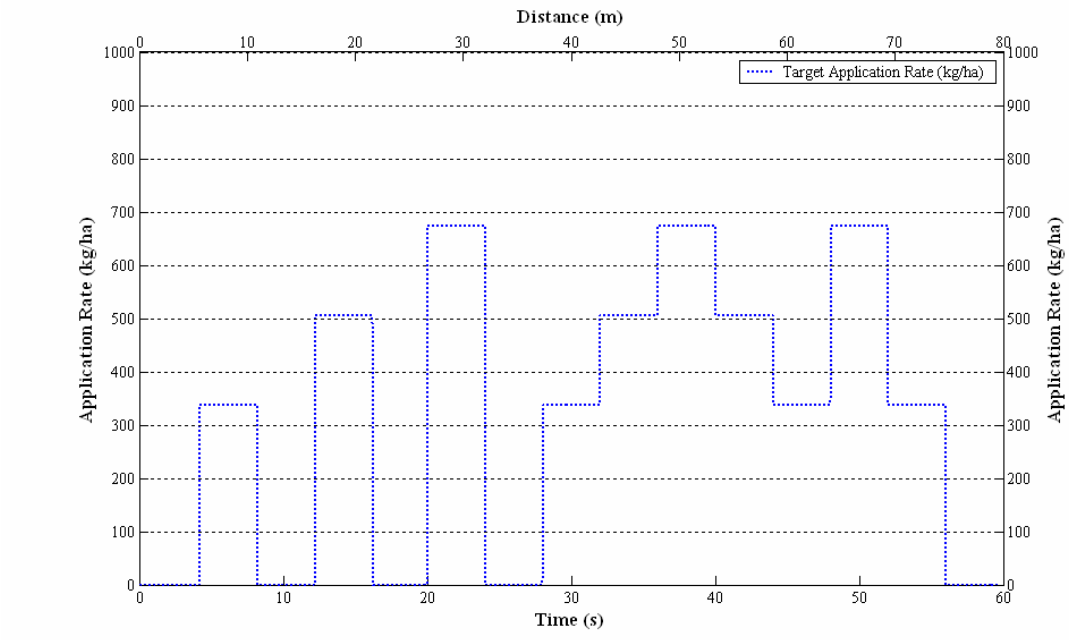

Figure 3-2. Prescribed or commanded application rate at any instant of time or position during the test run.

The setup of the pattern of change in application rates ensured that all permutations (12) of the transitions in the application rates were included i.e. 0-336.26 kg/ha, 336.26-0 kg/ha; 0-504.38 kg/ha, 504.38-0 kg/ha, 0-672.51 kg/ha, 672.51-0 kg/ha, 336.26-504.82 kg/ha, 504.82-672.51 kg/ha, 672.51-504.82 kg/ha, 504.82-336.26 kg/ha, 336.26-672.51 kg/ha and 672.51-336.26 kg/ha. Five repetitions of all the experiments described in the following sections and chapters were performed.

Trigger Mode

The application rate change in commercial controller modules could be triggered either by the GPS signal or real-time sensors. In the GPS mode the controller module received the position location data from the GPS receiver. The controller then executed a search algorithm and determined from the previously loaded prescription map, the applicator's current location and the prescribed application rate at that location. In the real-time trigger mode, the controller module determined the application rate by monitoring the inputs from the infrared sensors triggered by tree size. In the following, the details of the experimental and software setup for performance evaluation in GPS triggered mode is described.

GPS

A GGA (GPS Fix Data) string from a GPS receiver contains the time, position, and fix related data. Each field in the string is separated by a comma. GGA strings are transmitted at a frequency of 5 Hz. Table 3-1 explains each of the fields for the GGA message. A GGA message example is:

$GPGGA,151924,3723.454444,N,12202.269777,W,2,09,1.9,–17.49,M,–25.67,M,1,0000*57

Table 3-1. GGA message structure.

Field	Description
1	UTC of position fix in HHMMSS.SS format
2	Latitude in DD MM,MMMM format (0-7 decimal places)
3	Direction of latitude N: North S: South
4	Longitude in DDD MM,MMMM format (0-7 decimal places)
5	Direction of longitude E: East W: West
6	GPS Quality indicator 0: fix not valid 4: Real-time kinematic, fixed integers 1: GPS fix 5: Real-time kinematic, float integers 2: DGPS fix
7	Number of SVs in use, 00-12
8	HDOP
9	Antenna height, MSL reference
10	"M" indicates that the altitude is in meters
11	Geoidal separation
12	"M" indicates that the geoidal separation is in meters
13	Correction age of GPS data record, Type 1; Null when DGPS not used
14	Base station ID, 0000-1023

(Source: Trimble Navigation Limited, p.10)

A VTG (Velocity True Ground) message identifies the actual track made good and speed over ground. VTG strings are transmitted at a frequency of 1 Hz. Table 3-2 explains each of the fields for the VTG message. The VTG message example is:

$GPVTG,0,T,,,1.87,N,3.46,K*33

Table 3-2. VTG message structure.

Field	Description
1	Track made good
2	Fixed text "T" shows that track made good is relative to true north
3	Not used
4	Not used
5	Speed over ground in knots (0–3 decimal places)
6	Fixed text "N" shows that speed over ground is in knots
7	Speed over ground in kilometers/hour (0–3 decimal places)
8	Fixed text "K" shows that speed over ground is in kilometers/hour

(Source: Trimble Navigation Limited, p.19)

The end of each GGA and VTG sentences are marked by a * symbol. The number present after this termination symbol is of hexadecimal base and is known as the

checksum used to verify the integrity of the GPS message. The checksum on any GPS string can be obtained by an XOR operation of the ASCII values of all the characters after the $GPGGA up to the * symbol excluding the symbol. For a VRT controller module, the information that is necessary to determine the flow rate setpoint is the latitude and longitude from the GGA string plus speed from the VTG string.

A laptop connected to a GPS receiver mounted on a vehicle was used to collect raw GPS data in GGA and VTG string mode at 5 Hz as the vehicle drove down the row in a grove at a constant speed, writing this previously acquired raw GPS data to the serial port of the controller module. However, on the examination of the speed information in the GPS strings, it was found that the speed was not constant and it was impossible to drive the vehicle at a constant speed. Changes in speed results in a change in total area covered per second. Therefore the controller would then change the flow rate to compensate for change in speed to maintain the same application rate. Hence in order to remove the effect of speed, it was decided to generate synthetic raw GPS strings.

ArcView 3.2 (ESRI, Redlands, California) was used to generate synthetic points in a row in north-south direction (Figure 3-3) 0.268 m apart. These points transversed across fifteen tree zones, each 5.3 m in length. The points denoted the position of the applicator at every 0.2 s increment assuming a velocity of 1.34 m/s. The latitude and longitude information of each point was imported to a spreadsheet (Excel, Microsoft Corporation, Redmond, Washington). The information was in decimal degrees format. These values were then converted into degree decimal minutes format used to represent latitude and longitude in a raw GPS signal.

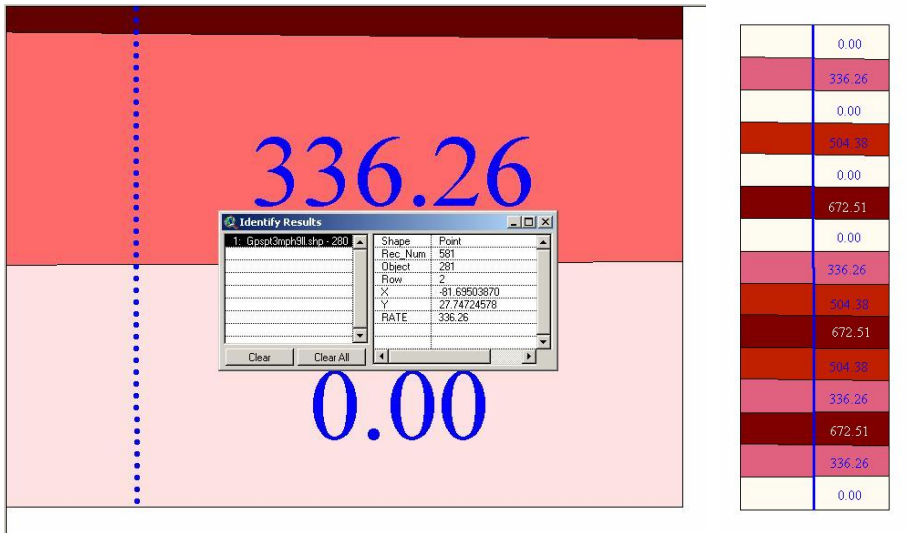

Figure 3-3. Generation of the synthetic GPS points using ArcView 3.2 for the benchmarking tests in the GPS triggered mode.

These data were then imported to a LabView program, specifically developed to embed these points to generate the synthetic GPS signals. Apart from generating the synthetic GGA and the VTG string, the code also generated the correct checksums for each of these strings and concatenated it at the end of each string. A partial extract of the synthetic strings generated by the above method is listed below:

$GPGGA,205643.20,2744.874880,N,08141.702345,W,2,09,1.9,-17.49,M,-25.67,M,1,0000*71
$GPGGA,205643.40,2744.874737,N,08141.702345,W,2,09,1.9,-17.49,M,-25.67,M,1,0000*74
$GPGGA,205643.60,2744.874593,N,08141.702345,W,2,09,1.9,-17.49,M,-25.67,M,1,0000*7A
$GPGGA,205643.80,2744.874450,N,08141.702345,W,2,09,1.9,-17.49,M,-25.67,M,1,0000*7A
$GPGGA,205644.00,2744.874307,N,08141.702345,W,2,09,1.9,-17.49,M,-25.67,M,1,0000*70
$GPVTG,180.0,T,,,2.607,N,4.828,K*21
$GPGGA,205644.20,2744.874163,N,08141.702345,W,2,09,1.9,-17.49,M,-25.67,M,1,0000*72
$GPGGA,205644.40,2744.874020,N,08141.702345,W,2,09,1.9,-17.49,M,-25.67,M,1,0000*72
…

The system configurations listed in Table 2-2 that were triggered by the GPS signals were System 01, System 02, System 04 and System 06.

Procedure: The prescription map with the application rates as specified in Figure 3-1 was prepared and loaded in to the controller module. For Controller Module-2 the prescription map was loaded into the PDA that was connected to the serial port of the

controller module. LabView code, specifically developed for this project, acquired the data at a rate of 50 Hz from Flowmeter-2. This code also output the GPS string to the RS232 port of the controller modules at the rate of 5 Hz. A commanded application-rate at each sampling instance was also acquired. The results of this experiment are discussed in Chapter 6.

Real-time

In case of the real-time trigger mode, digital inputs of the commercial controller module which accepts the signal from the tree canopy size sensors were connected to the digital output ports of the data acquisition card through the optically isolated modules. The digital ports of the data acquisition cards are configured to write data to the digital input lines of the commercial controller modules. The commercial controller modules' software was configured for swath width sections with a small tree application rate set to 336.26 kg/ha, a medium tree 504.38 kg/ha, a large tree 672.51 kg/ha and 0 kg/ha for no tree or "resets". LabView code was used to simulate tree size sensing in real-time mode by switching the respective digital ports of the data acquisition card on or off. The states of the real-time sensors to simulate the respective tree sizes were read from the text file that had the information of the states of the real-time sensors in an array format for every 0.2 s for the entire length of the experiment (~60 s). This provided the real-time input to commercial controller modules. The code updated the sensor status every 0.2 s similar to the GPS signal update in the GPS trigger mode. The data acquisition was at a rate of 50 Hz. Hydraulic flowrate and the commanded application rate data were acquired. The flowrate was calibrated to the application rate as explained at the beginning of this chapter. The system configurations listed in Table 2-2 that were triggered by the real-time signals were System 03, System 05, System 07 and System 08.

Flow Control Valves

To determine the effect of the flow control valves on the performance of the applicator, an experiment was performed in both real-time and GPS trigger mode. All tests for the flow control valves' comparison were performed using the commercial controller module-1. The results of the system configurations of System Number 01 and System Number 04 can be compared for the GPS triggered mode and System Number 03 and System Number 05 for the real-time trigger mode. The results of these tests are discussed in detail in Chapter 6.

Encoders

To determine the effect of the encoder resolution, the applicator was operated in real-time trigger mode. The commercial controller module-2 was used for this purpose. The proportional solenoid flow control valve was used to control the flowrate to the hydraulic motor-gearbox combination. The two encoders that were used for comparison were the Encoder-1 and Encoder-2. The auto-tune function described in Chapter 2 was executed on commercial controller module-2 before the first test runs for both the configurations (System Number 07 and System Number 09) to obtain new optimized gains with the new encoder resolutions. The calibration number was also changed appropriately based on the encoder resolution. Results of the System Number 07 and System Number 09 are used to compare encoder performance of the applicator. The results of all these tests are discussed in detail in Chapter 6.

CHAPTER 4
DYNAMIC MODELLING OF THE PHYSICAL COMPONENTS OF THE HYDRAULIC SYSTEM

Introduction

The Laplace transform provides a one to one correspondence between a signal, or a time function (f(t)) and a function of a complex frequency variable, *s*, called the Laplace transform of the signal which in turn converts the differential equation describing a system to an algebraic expression (Dorf, 1996). The Laplace transforms of some of the common time functions are listed in Table 4-1.

$$\mathcal{L}[f(t)](s) \equiv F(s) = \int_0^\infty f(t)\, e^{-st} dt \tag{4.1}$$

Table 4-1. Laplace transforms of some of the common time functions.

Time Function f(t)	**Laplace Transform $\mathcal{L}$ [f (t)](s) = F(s)**
1	$\frac{1}{s}$
t^n	$\frac{n!}{s^{(n+1)}}$
$\delta(t - T_d)$	e^{-sT_d}
$\tau \frac{dy(t)}{dt} + y(t) = Kx(t)$	$Y(s)(\tau s + 1) = KX(s)$

The relationship between the input and output of a system, subsystem, or equipment in terms of the transfer characteristics is defined as a transfer function. It can also be defined as the ratio of the Laplace transform of the output to the Laplace transform of the input of a fixed linear system. Figure 4-1 depicts the input and the output

signals of the proportional solenoid flow control valve and the hydraulic motor-gearbox combination.

The mathematical model was based on the hypothesis that the flow control valves and the hydraulic motor-gearbox combination behave as a linear first order systems. For the flow control valves, the output flowrates of the valves are proportional to the valves' orifice areas. Time domain analyses of the valves' and hydraulic motor-gearbox combination's response to the step input under various load conditions were performed. The data collected from these tests were used to determine the transfer functions of these hydraulic components of the applicator (Figure 4-1).

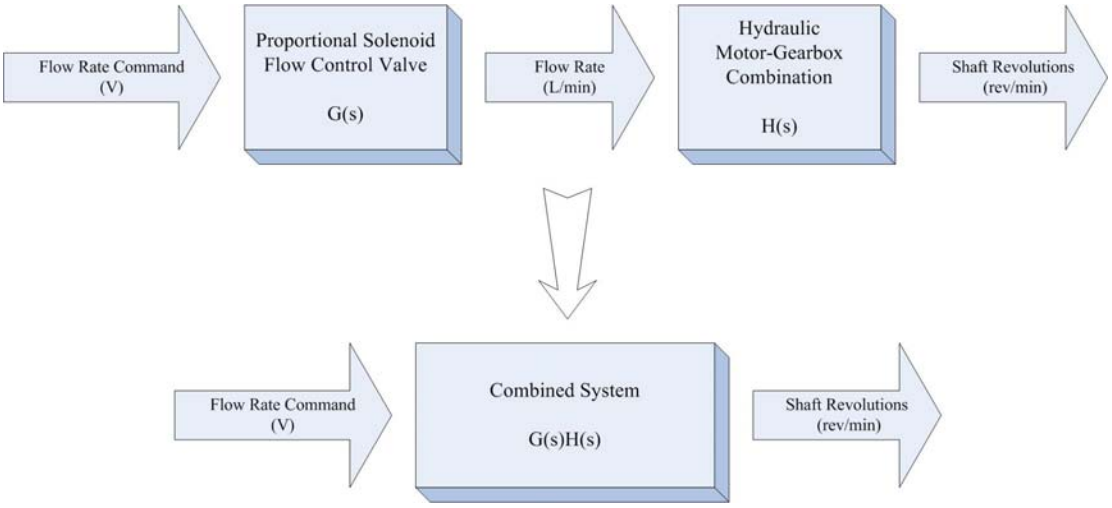

Figure 4-1. Transfer functions.

This makes it possible to design the model based controller to optimize the performance of the applicator. The development of the model based controller is described in detail in Chapter 5. The following sections explain the experimental procedure and the determined transfer functions of the various hydraulic components of the VRT applicator.

Effect of Loading

The pressure in the hydraulic system (at the motor) exerted by the fertilizer material when the hopper was completely filled was recorded at the maximum application rate during one of the field applications. To determine the steady-state and transient response of the motor-gearbox combination and the 2-way, 2-position solenoid flow control valve in loaded condition, three drums (total mass = 225 kg with one third of each drum volume filled with water) were placed on a 2 m x 0.24 m x 38 mm wooden platform (covered by 9.5 mm thick Ultra High Molecular Weight polyethylene (UHMW) sheet) placed on the belt chain (Figure 4-2). This setup exerted a comparable load (0.55 MPa) on the hydraulic system as the full load of fertilizer material in the hopper. Flowrate, pressure and motor-gearbox combination speed data were collected from the respective transducers for minimal and maximum loading conditions.

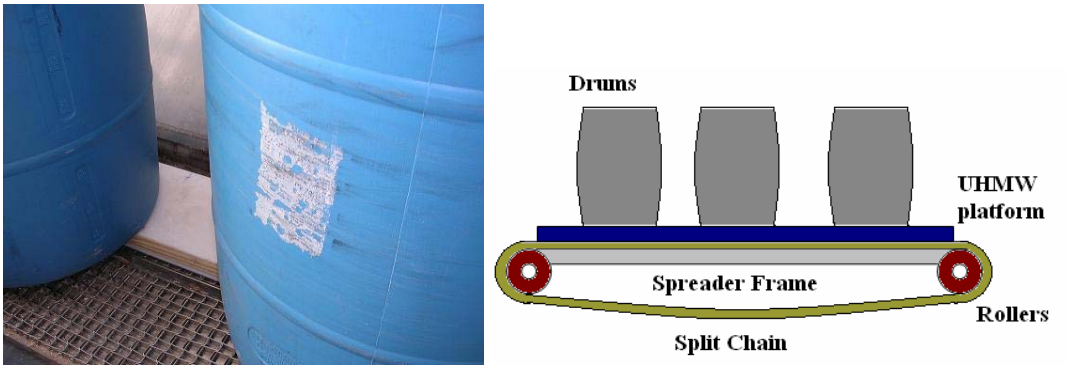

Figure 4-2. Placement of water filled drums on the conveyor chain to simulate fertilizer loading.

Hydraulic Motor-Gearbox Combination

Steady-state behavior

Experimental Procedure: In order to analyze the steady state response of the hydraulic motor-gearbox combination, the flow control valve was set to completely closed position and the solenoid valve energized. Experimental data were collected by

rotating the DC motor operated flow control valve stem by a series of pre-determined angles and monitoring the flowrate output (Flowmeter-1) of the valve and shaft speed of the motor-gearbox combination (Encoder-3). The data were then post-processed by aggregating encoder count samples of 0.004 s to encoder count samples of 0.04 s. Then these aggregated encoder counts were converted to rev/min (Cugati et al. 2005a).

Results: Figure 4-3 and 4-4 depict the steady state response of the motor-gearbox combination for the commanded step inputs from the DC motor operated flow control valve for no load and fully loaded condition respectively. It was concluded that loading of the conveyor chain had a negligible effect on the performance of the motor-gearbox combination. The steady-state speed response was determined to be 0.44 rev/L $\left(\frac{rev/min}{L/min}\right)$ for input flowrates between 2 L/min and 19 L/min (Figure 4-5).

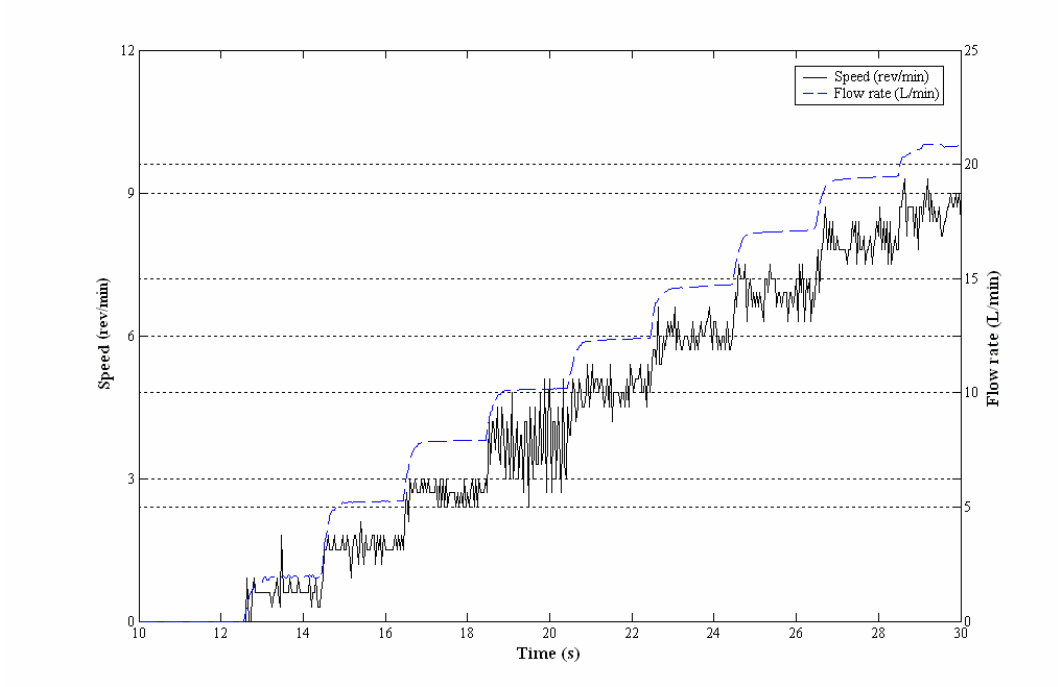

Figure 4-3. Response of the hydraulic motor-gearbox combination to incremental flowrate commands under no load conditions.

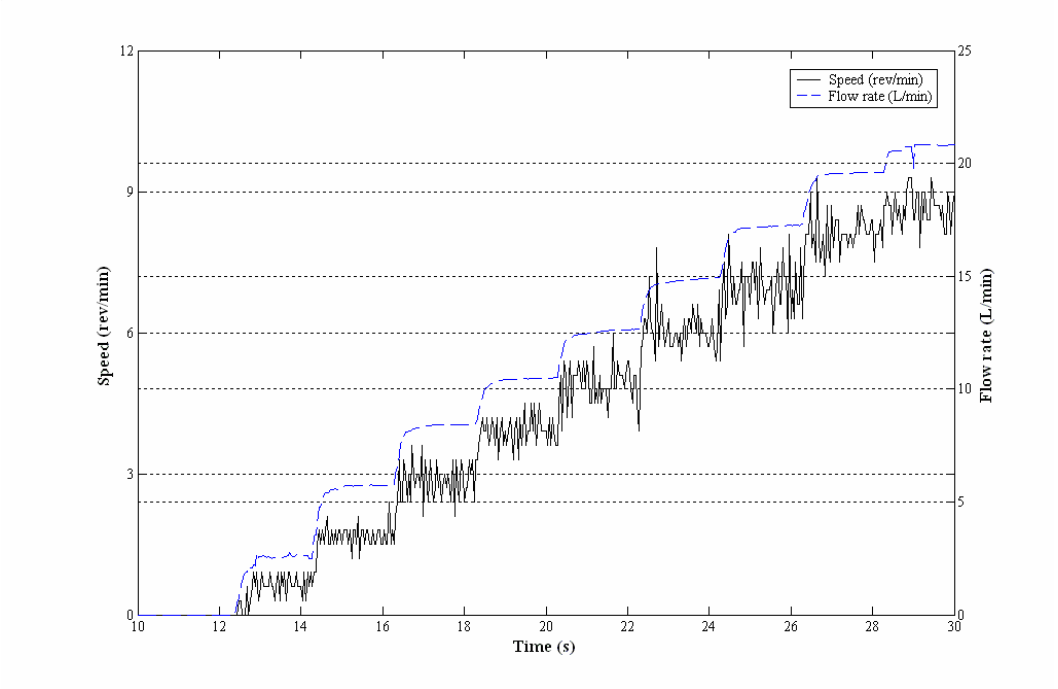

Figure 4-4. Response of the hydraulic motor-gearbox combination to incremental flowrate commands under full load conditions.

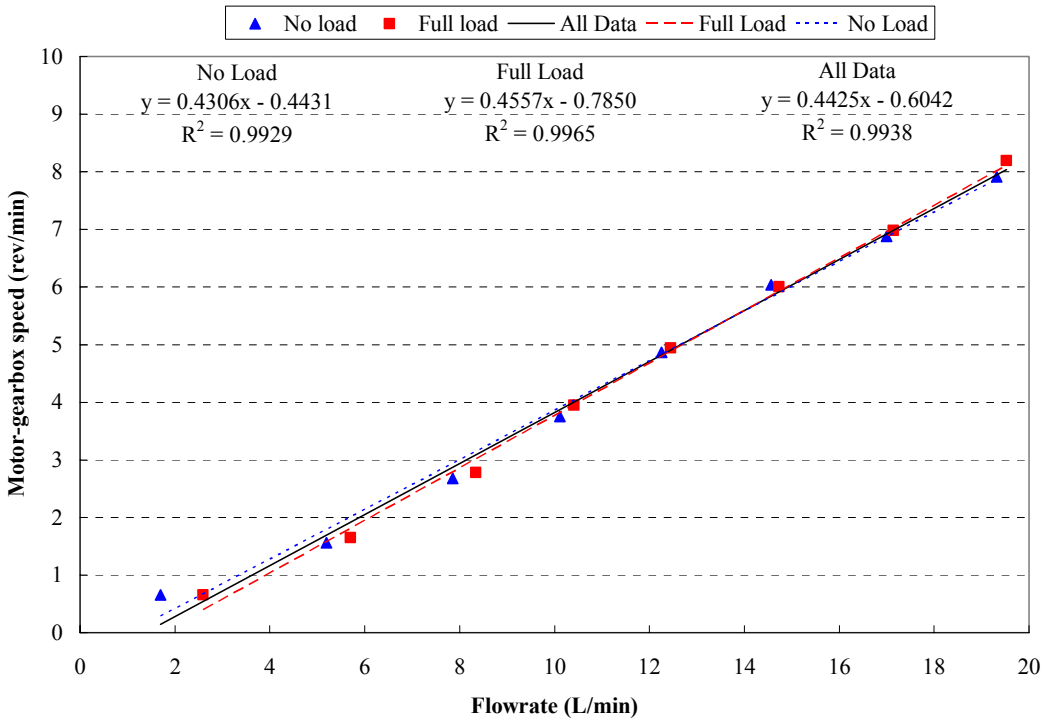

Figure 4-5. Steady state relationship of the flowrate vs. the speed of-motor gearbox combination.

From the above steady-state slope and the gear box reduction ratio (6:1), the apparent hydraulic motor volumetric displacement was then calculated to be 0.38 L/rev which is consistent with the 0.37 L/rev cited in the manufacturer's specification.

Dynamic behavior

Experimental Procedure: The DC motor operated flow control valve was set in a completely open position and the 2-way 2-position solenoid valve was initially set to a closed position. The data acquisition was initiated in this state. The 2-way, 2-position solenoid valve was switched on after 2 s and the flow from the pump was directed to the hydraulic motor-gearbox combination. The Encoder-3 cumulative counts at each sampling instance were acquired along with the flowrate (using Flowmeter-1) and pressure. This control condition was maintained for a period of 3 s. The 2-way 2-position solenoid valve was then switched off while the data acquisition continued for 4 additional seconds. Figure 4-6 and 4-7 are plots of the transient and the steady-state response of the 2-way 2-position solenoid valve for the commanded step input for no load and full load conditions respectively (Cugati et al. 2005a).

Results: It was again observed from Figure 4-6 and 4-7 that the loading of the conveyor chain had little or no effect on the speed and flowrate. The dynamic response of the hydraulic motor-gearbox combination is relatively fast compared to the valves and the needs of the system. Hence, the transient response of the motor-gearbox combination could be modeled as a pure gain (K) of 0.44 derived from the steady-state slope in Figure 4-5. The combination therefore has adequate transient response. The transfer function of the hydraulic motor-gearbox combination is depicted in Figure 4-8.

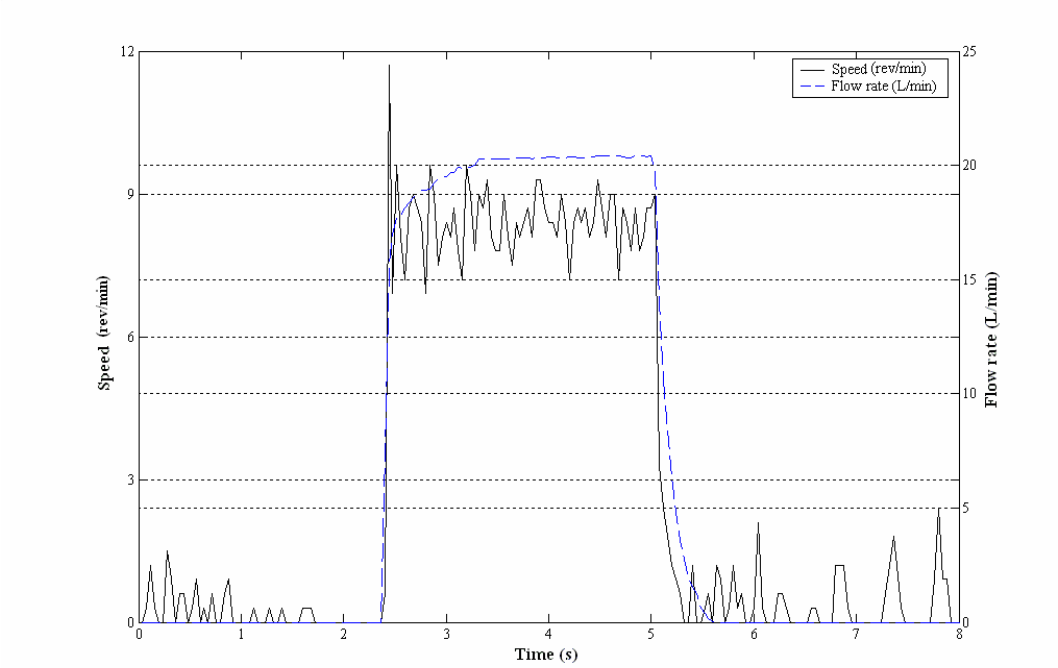

Figure 4-6. Response of the hydraulic motor-gearbox combination to an open command of the 2-way, 2-position solenoid flow control valve under no load conditions

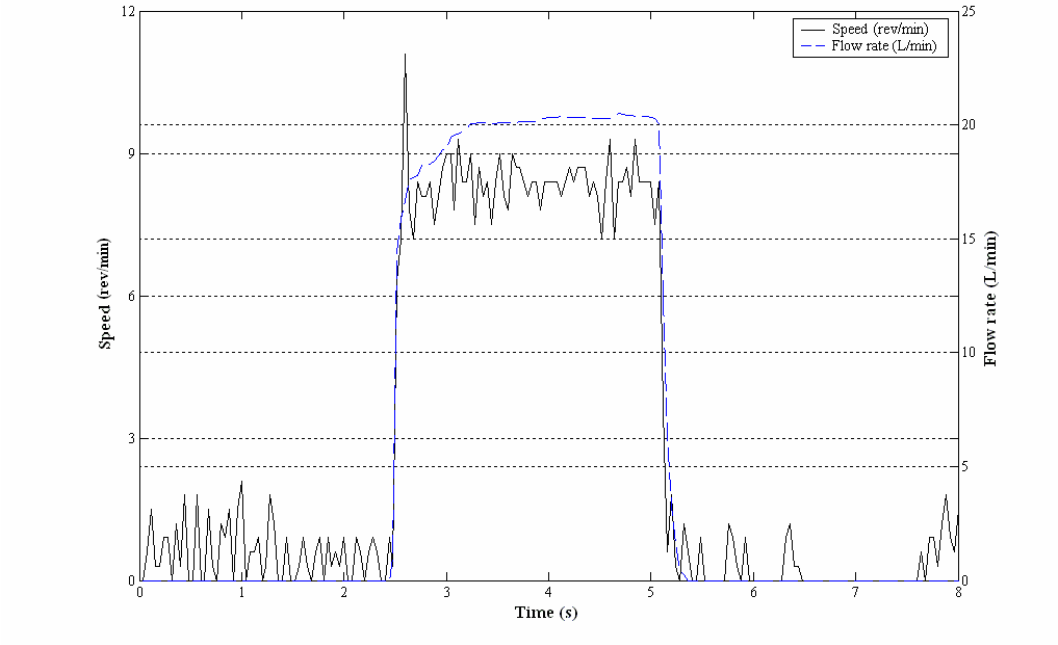

Figure 4-7. Response of the hydraulic motor-gearbox combination to an open command of the 2-way, 2-position solenoid flow control valve under full load conditions

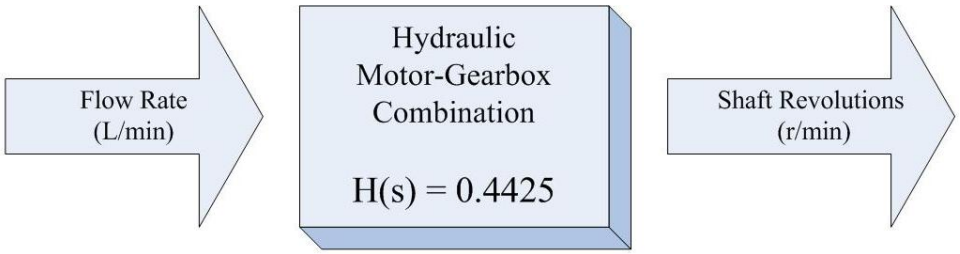

Figure 4-8. Transfer function of the hydraulic motor-gearbox combination.

Flow Control Valves

Various parameters that define the mathematical model of the flow control valves are discussed in this section.

Solenoid 2-Way, 2-Position Flow Control Valve

Experimental Procedure: The experimental procedure to determine the various parameters that are necessary to define the transfer function of the solenoid 2-way, 2-position flow control valve was similar to the procedure described to determine the dynamic behavior of the hydraulic motor-gearbox combination. Flowrate (using Flowmeter-1), pressure, and command state readings of this valve were acquired. Figure 4-9 and 4-10 are plots of the transient and the steady state response of the 2-way 2-position solenoid flow control valve for a commanded step input in no load and full load conditions respectively (Cugati et al. 2005a).

Steady-state behavior

Results: Since a 2-way 2-position solenoid valve has only two positions in its operation, it was only possible to have two steady-state flowrates. When the 2-way 2-position solenoid valve is closed, the flowrate is 0 L/min and when open, the flowrate is the maximum flowrate delivered through the Flow Divider-2. From Figures 4-9 and 4-10, it was determined to be approximately 20 L/min.

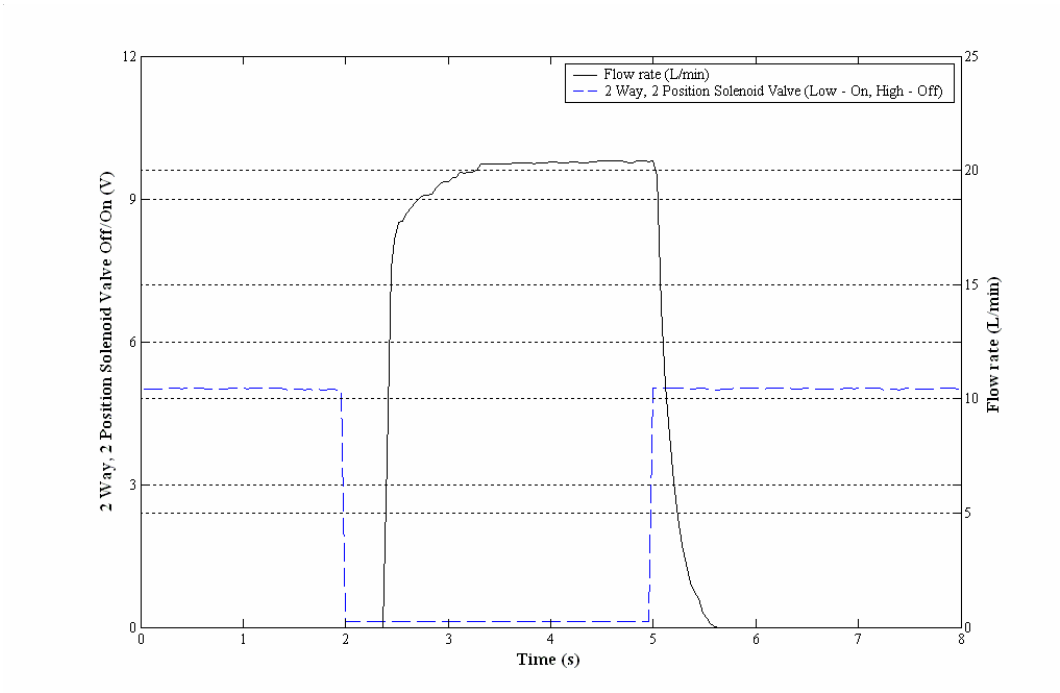

Figure 4-9. Response of the 2-way, 2-position solenoid flow control valve to the open and close command under no load conditions

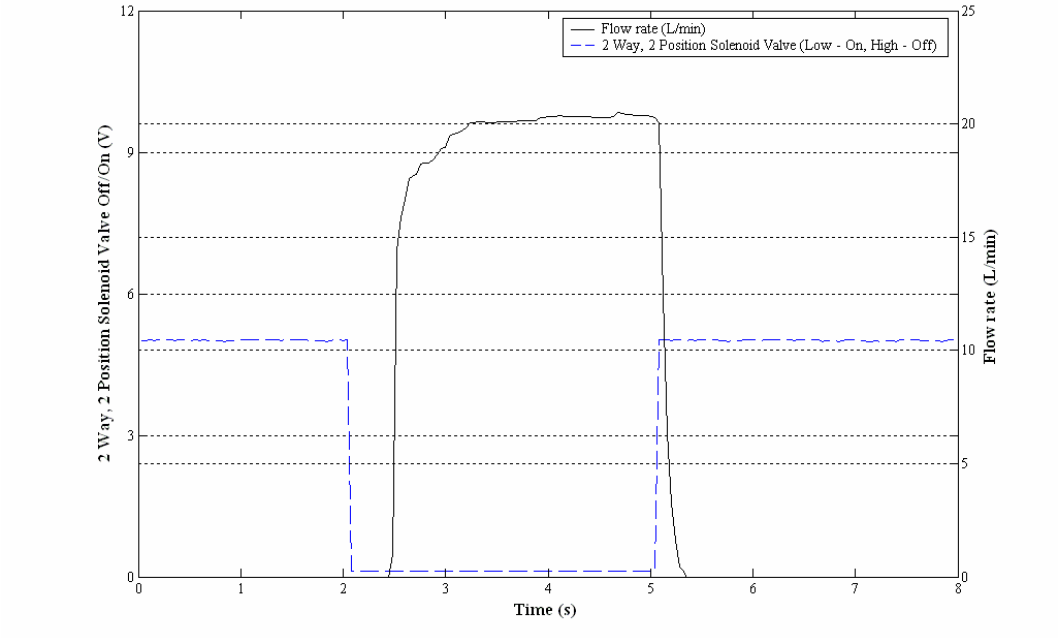

Figure 4-10. Response of the 2-way, 2-position solenoid flow control valve to the open and close command under full load conditions

Dynamic behavior

Results. There was a delay time (τ) of 0.4 s from issuing an open command signal until the flow response started, and a delay time (τ) of 0.036 s from issuing a close command signal until the flow response began (Figure 4-9 and 4-10). It was also observed that the motor gearbox combination's speed reached steady-state even before the flowrate reached steady-state (Figure 4-6 and 4-7). Hence, it can be concluded that the time constant observed in the flowrate data were not the time constant of the 2-way 2-position solenoid valve but rather a time constant for Flowmeter-1 itself. The 2-way 2-position solenoid flow control valve can therefore be modeled as a pure delay component. The transfer function of this valve is depicted in Figure 4-11.

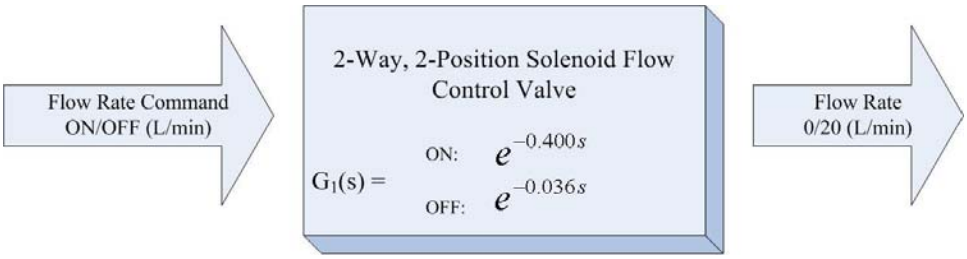

Figure 4-11. Transfer function of the 2-way 2-position solenoid flow control valve.

DC Motor Operated Flow Control Valve

Steady-state behavior

Experimental Procedure. Experimental data were collected by rotating the valve stem by a series of predetermined angle of 1.5° and by monitoring the flow output from the valve using Flowmeter-2. The valve was returned to the initial state by issuing similar open loop close commands by the same predetermined angular steps. Figures 4-12 and 4-13 show the open loop response of the DC motor operated flow control valve for the open and close command in steps of 1.5° respectively (Cugati et al. 2005b).

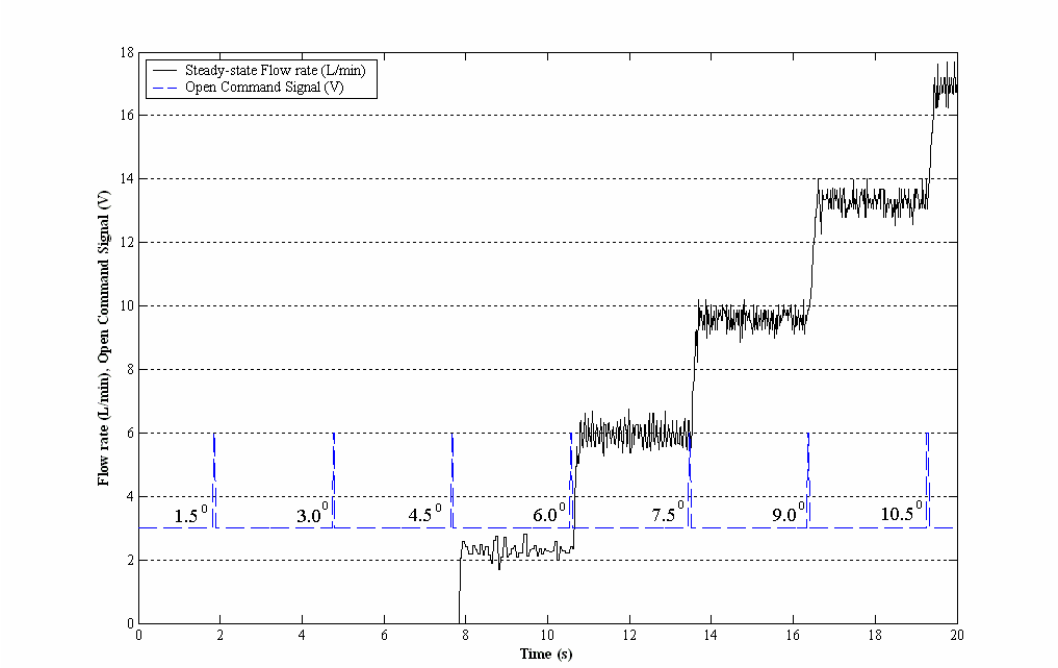

Figure 4-12. Response of the DC motor operated flow control valve to 1.5° step open commands.

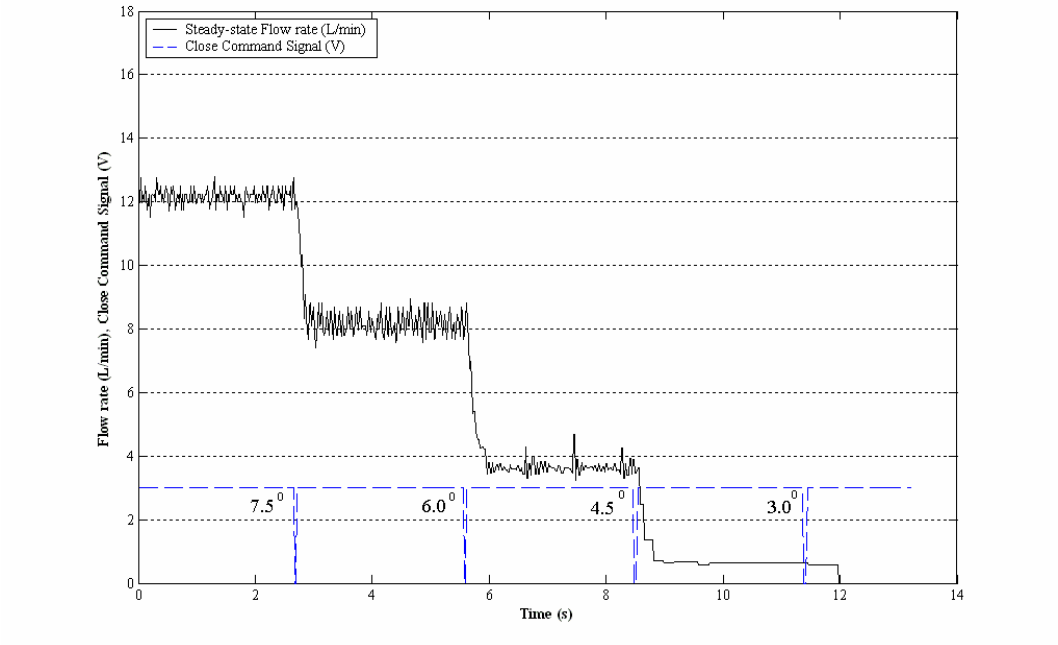

Figure 4-13. Response of the DC motor operated flow control valve to 1.5° step close commands.

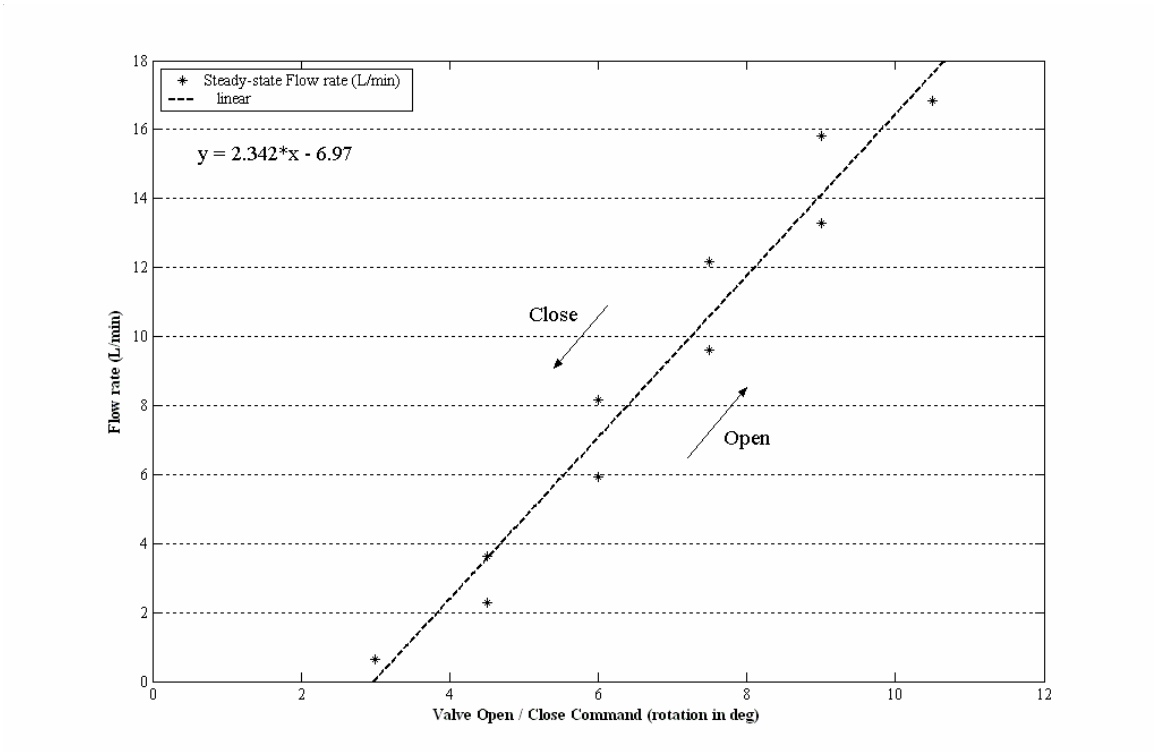

Figure 4-14. Steady-state behavior of the DC motor operated flow control valve.

Results: Figure 4-14 depicts the steady-state behavior of this valve. From Figures 4-12 and 4-13, there was no flow observed for the rotation of valve stem from 0° to 3°. Also, the flowrates for the same commanded position during the open cycle and the close cycle were not the same due to hysteresis. This hysteresis was measured to be an average value of 2.38 L/min or 1°. The flowrate was found to be linear from 3° to 10.5° and this could be represented by the linear relation:

$$y = 2.34*x - 6.97 \quad (4.1)$$

where,

y = Flowrate (L/min)

x = Commanded valve stem position (deg)

Even though the valve stem was able to rotate beyond 10.5° and up to 90° and the maximum flowrate from the flow divider was 21 L/min, the rotations were limited to

10.5°. At that position, the DC motor operated flow control valve had the maximum flowrate rating of 16 L/min which corresponded with the maximum flowrate of the proportional solenoid flow control valve when completely opened. It was decided to operate the DC motor operated flow control valve only within this linear range so that an unbiased comparison of these two types of valves could be performed.

Dynamic behavior

Experimental Procedure: From the previous experiment it is possible to determine the steady-state flowrate output from the DC motor operated flow control valve for any valve stem position between 3° and 10.5°. The valve stem was rotated to a position where the steady-state flowrate was 4 L/min and the data acquisition was initiated at this point. Flowmeter-2 was used to acquire the flowrate data. Then the valve stem was rotated by a 1.3° step such that the change in the steady-state flowrate from the previous command to the next command was equal to 3 L/min, as calculated from Equation 4.1. The valve stem was held in this position for about 3 s. This procedure was repeated two more times. The response of the DC motor operated flow control valve for this step change is depicted in Figure 4-15.

Results: From Figure 4-15 it can be determined that that there was a delay time (τ) of 0.08 s from issuing a command signal until the flow response started. Then there was a near-linear transient response. The response represents an approximate first order response with a time constant (T) of 0.09 s for the step input change of 3 L/min (Figure 4-16). This transfer function is of a first-order lag plus dead time (FOLPD) model.

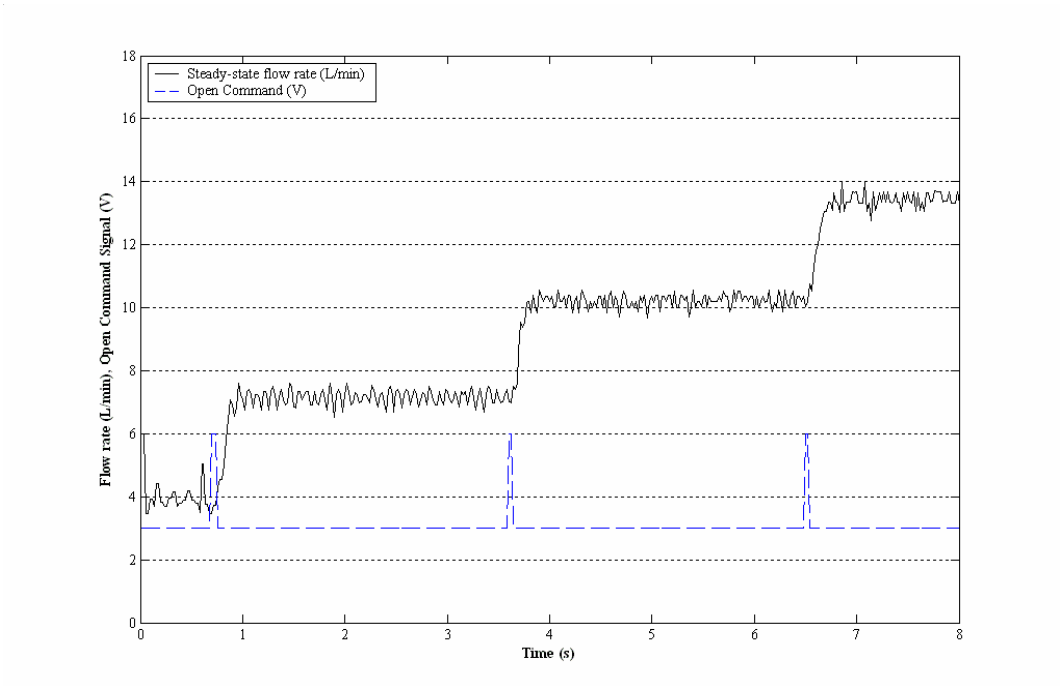

Figure 4-15. Response of the DC operated flow control valve for step input change of 3 L/min.

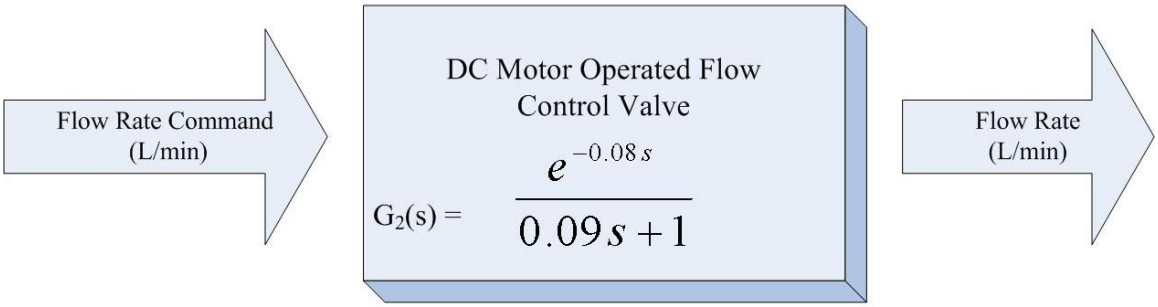

Figure 4-16. Transfer function of the DC motor operated flow control valve.

Proportional Solenoid Flow Control Valve

Steady-state behavior

Experimental Procedure: Experimental data were collected by moving the valve spool by a series of predetermined steps of 0.5 V open commands and by monitoring the flow output from the valve using Flowmeter-2. The valve was brought back to the initial state by issuing similar open loop close commands by the same predetermined steps of

0.5V. Figures 4-17 and 4-18 show the open loop response of the proportional solenoid flow control valve for the open and close command in steps of 0.5 V respectively.

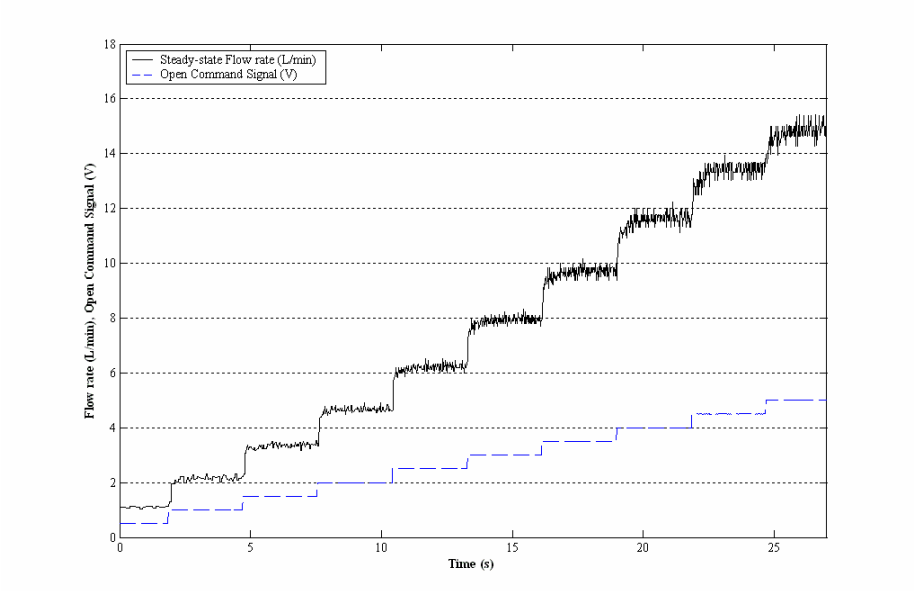

Figure 4-17. Response of the proportional solenoid flow control valve to 0.5 V step open commands.

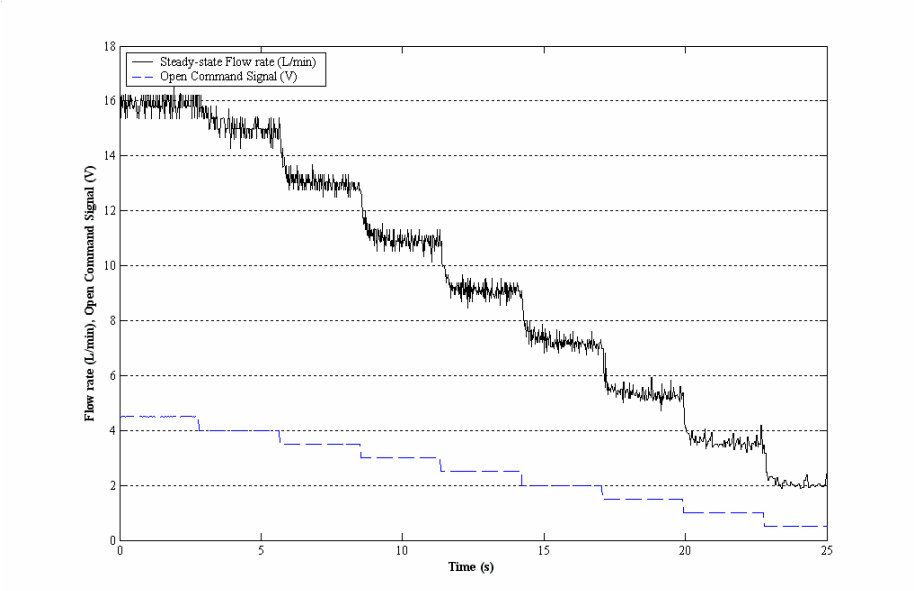

Figure 4-18. Response of the proportional solenoid flow control valve to 0.5 V step close commands.

Result. Figure 4-19 depicts the steady-state behavior of this valve. It is observed from figures 4-17 and 4-18 that the flowrates for the same commanded position during the open cycle and the close cycle were not the same due to the effect of hysteresis. This hysteresis was measured to be an average value of 2 L/min or 0.7 V.

The flowrate was found to be linear in 0 V to 5 V range and represented by the linear relation:

$$y = 3.26*x - 0.29 \quad (4.1)$$

where,

y = Flowrate (L/min)

x = Commanded voltage (V)

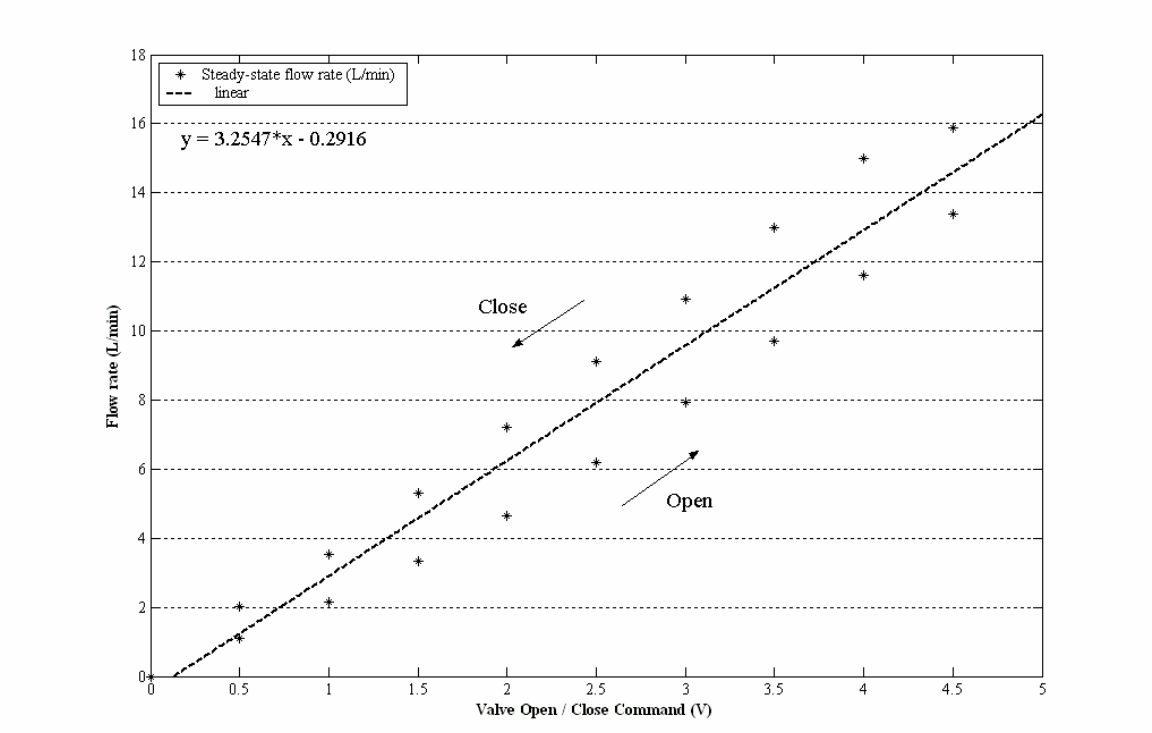

Figure 4-19. Steady-state behavior of the proportional solenoid flow control valve.

Dynamic behavior

Experimental Procedure: From the previous experiment it was possible to determine the steady-state flowrate output from the proportional solenoid flow control valve. The valve spool was moved to a position by issuing the voltage command such that the steady-state flowrate was 3 L/min and the data acquisition was initiated at this point. Flowmeter-2 was used to acquire the flowrate data. Then the valve spool was moved to positions, calculated from equation 4.2, such that the change in the steady-state flowrate from the previous command to the next command was equal to 3 L/min. This procedure was repeated two more times. The valve spool was held in these positions for about 3 s. The response of the proportional solenoid flow control valve for this step change is depicted in Figure 4-20.

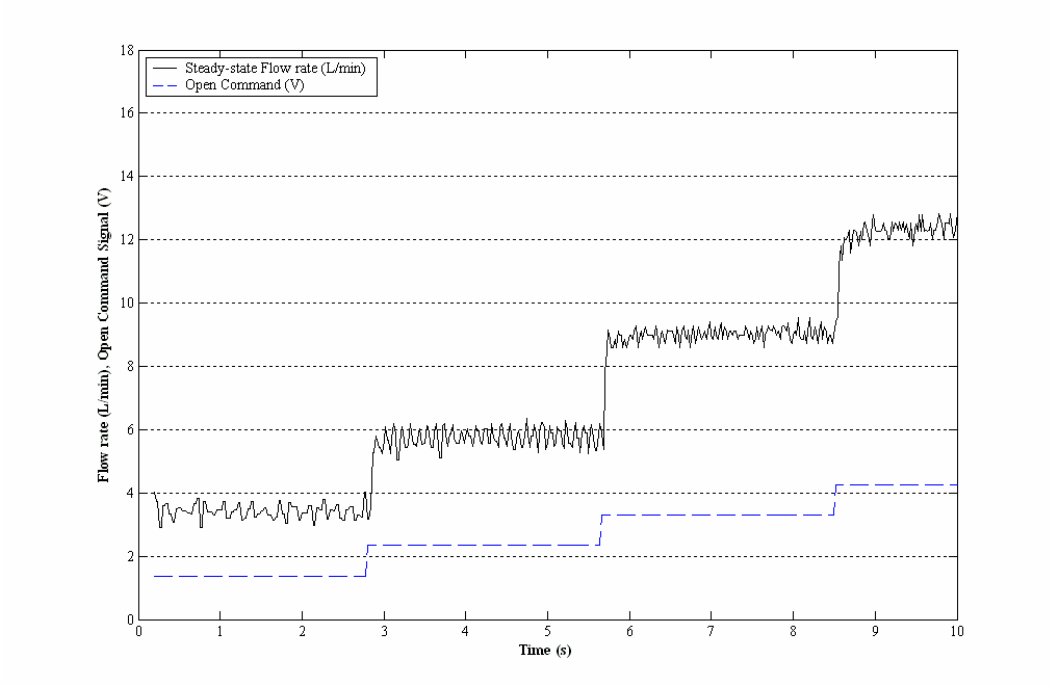

Figure 4-20. Response of the proportional solenoid flow control valve for step input change of 3 L/min.

Results: From Figure 4-20, it was calculated that there was a delay time (τ) of 0.04 s from issuing a command signal until the flow response starts. Then there is a near-linear transient response modeled as an approximately first order response with a time constant (T) of 0.024 s for the step input change of 3 L/min. A first-order lag plus dead time (FOLPD) model was used to determine the transfer function.

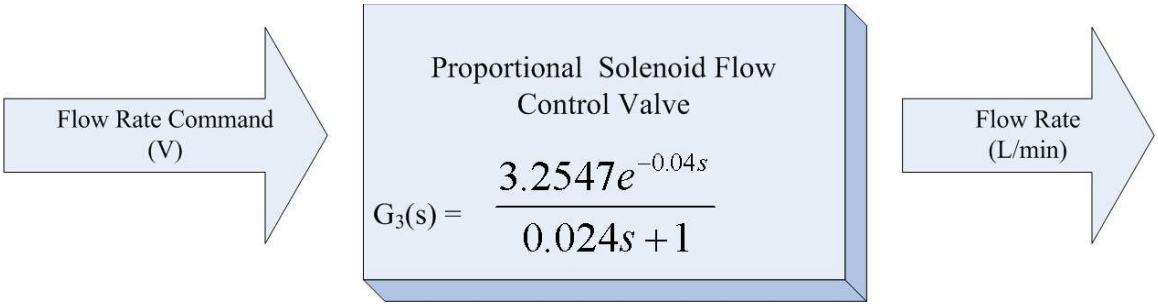

Figure 4-21. Transfer function of the proportional solenoid flow control valve.

Summary

The dynamic characteristics of the various flow control valves and the hydraulic motor-gearbox combination of the applicator are summarized in Table 4-2. From Table 4-2 it can be observed that the initial time delay (τ) and the time constant (T) of the proportional solenoid flow control valve is less than the initial time delay and the time constant of the DC motor operated flow control valve. It is possible to have a better performance if the values of these two parameters were smaller. Hence it can be stated that proportional solenoid flow control valve has a better performance as compared the DC motor operated flow control valve. This can be verified in the results of the benchmarking tests discussed in Chapter 6.

Table 4-2. Dynamic characteristics of the hydraulic components of the applicator.

Components	Gain K	Delay Time (s) τ	Time Constant (s) T	Transfer Function
Hydraulic Motor-Gearbox Combination	0.44	0	0	0.44
2-Way, 2-Position Solenoid Flow Control Valve	1	ON: 0.4 OFF: 0.036	0	$ON: e^{-0.4s}$ $OFF: e^{-0.036s}$
DC Motor Operated Flow Control Valve	1	0.08	0.09	$\frac{e^{-0.08s}}{0.09s+1}$
Proportional Solenoid Flow Control Valve	3.26	0.04	0.024	$\frac{3.26\,e^{-0.04s}}{0.024s+1}$

CHAPTER 5
DEVELOPMENT OF A MODEL BASED PID CONTROLLER

PID Controller Basics

Process control is defined as the necessary action to bring a parameter to the desired value by observation of the parameter. Any physical parameter which can change either spontaneously or from external influences is a dynamic variable. A controller is defined as a process control element that performs the operation of measurement evaluation and initiation of an appropriate action on the dynamic variable based on the evaluation (Johnson, 1977). This dynamic variable being controlled is also referred to as the process variable. Error is defined as the difference between the actual process variable to the setpoint.

The controller can operate in a two-position mode or a multi-position mode. In a two-position mode, if the measured value is greater than the setpoint, then the controller outputs the first state, when less than the setpoint, the controller outputs the second state. A good example is the conventional room thermostat. In case of the multi-position mode, there are several intermediate rather than only two settings of the controller output. Various algorithms are available to implement the multi-position mode (Johnson, 1977). The most commonly used multi-position mode control algorithm is the Proportional Integral Derivative (PID) type. The representation of a PID control is illustrated in Figure 5-1, where $G_c(s)$ is the controller transfer function and $G_m(s)$ is the process transfer function.

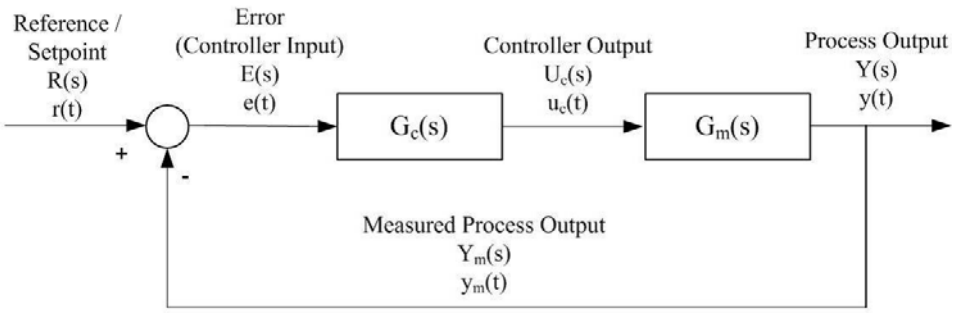

Figure 5-1. Block diagram of a process control.

The proportional control is used when the controller action is to be proportional to the size of the process error signal ($e(t) = r(t) - y_m(t)$). The proportional control is represented as,

$$u_c(t) = k_p\, e(t) \tag{5.1}$$

in time domain and as,

$$U_c(s) = k_p\, E(s) \tag{5.2}$$

in the Laplace domain (Figure 5-2a), where, k_p is defined as the proportional gain.

Integral control is used to correct any steady-state offset of the process output from a constant reference signal value. It eliminates steady-state offsets without the use of excessively large controller gains. The integral control is represented as,

$$u_c(t) = k_i \int^{t} e(t)dt \tag{5.3}$$

in time domain and as,

$$U_c(s) = \frac{k_i}{s}\, E(s) \tag{5.4}$$

in Laplace domain (Figure 5-2b), where, k_i is defined as the integral gain.

Derivative control uses the rate of change of an error signal to perform the corrective action. The derivative control is represented as,

$$u_c(t) = k_d \frac{d}{dt} e(t) \tag{5.5}$$

in time domain and as,

$$U_c(s) = k_d \, s \, E(s) \tag{5.6}$$

in the Laplace domain (Figure 5-2c) where, k_d is defined as the derivative gain.

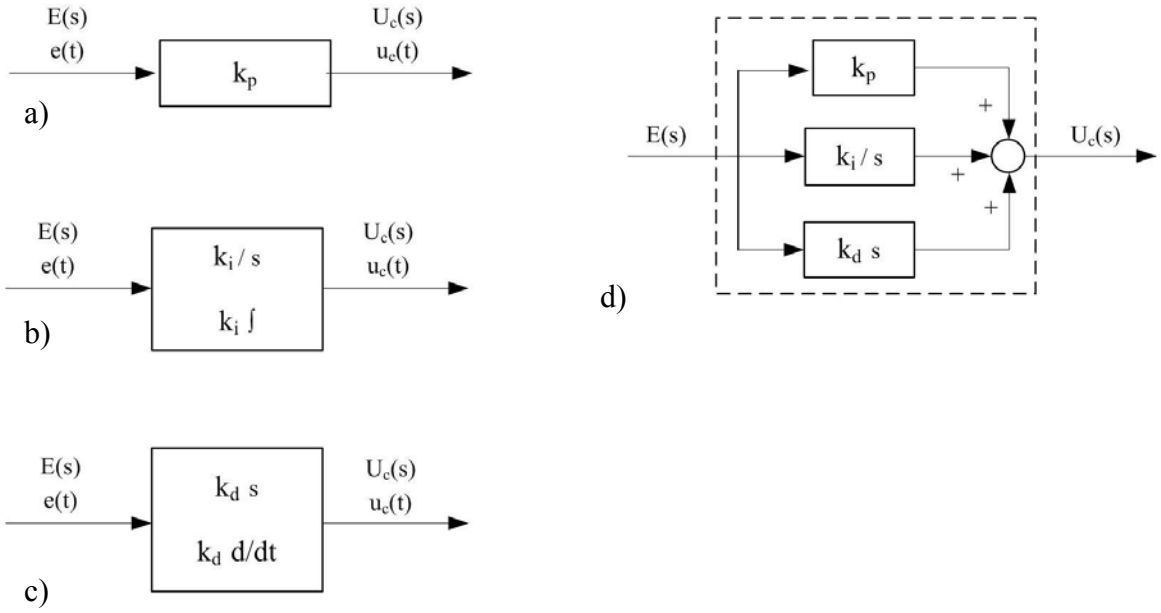

Figure 5-2. Various modules of the PID controller. a) Proportional module, b) Integral module, c) derivative module and d) PID modules.

Figure 5-2d represents a parallel PID control structure obtained from the individual proportional, integral and derivative modules. This structure can be represented in time domain by the equation,

$$u_c(s) = k_p e(t) + k_i \int^{t} e(t)dt + k_d \frac{d}{dt} e(t) \tag{5.7}$$

and in Laplace domain by the equation,

$$U_c(s) = \left[k_p + k_i \frac{1}{s} + k_d s \right] E(s) \tag{5.8}$$

However, industrial representations of the PID controller often use a time-constant form for the PID parameters instead of the decoupled form detailed above (Johnson and Moradi, 2005). The time-constant form of the PID controller in time domain becomes:

$$u_c(s) = k_p\left[e(t) + \frac{1}{T_i}\int^{t} e(t)dt + T_d\frac{d}{dt}e(t)\right] \tag{5.9}$$

and in Laplace domain:

$$U_c(s) = k_p\left[1 + \frac{1}{T_i s} + T_d s\right]E(s) \tag{5.10}$$

where,

$T_i = \frac{k_p}{k_i}$ and $T_d = \frac{k_d}{k_p}$

Therefore the term $k_p\left[1 + \frac{1}{T_i s} + T_d s\right]$, is the transfer function of the PID controller.

The ability of PID controllers to compensate most practical industrial processes has led to their wide acceptance in industrial applications. Åström and Hägglund (O'Dwyer, 2003, p.1) estimated that more that 95% of the controllers in process control applications are of PID type.

Tuning of PID Controllers

Van Overschee and De Moor (O'Dwyer 2003) reported that 80% of the PID controllers are badly tuned. The authors also stated that 25% of all the PID controller loops are used in factory default settings. Even though there is a wealth of information available in the literature regarding the tuning rules, it has not been effectively implemented in industrial applications. Hence the main objective of this study was to implement and validate the available tuning rules, in the literature, in a PID controller

that would change the application rates for VRT fertilization of individual trees taking into account the varying speed and spatial location of the applicator in the grove.

Model Based Tuning Rules

From Chapter 4, it was determined that the transfer function of the proportional solenoid flow control valve was a first-order lag plus dead time (FOLPD) type, $G(s) = \frac{Ke^{-s\tau}}{Ts+1}$, as depicted in Table 4-2, where, $K = 3.26$, $\tau = 0.04$ s and $T = 0.02$ s. One tuning rule to obtain the gains for the PID controller, proposed by Zhuang and Atherton (1993), is based on time weighted integral performance criteria. They stated that "When the plant transfer function is known, the parameters of the PID controller may be optimised by minimizing an integral performance criterion." They chose an integral performance index denoted by:

$$J_n(\theta) = \int_0^\infty \{t^n e(\theta,t)\}^2 dt \tag{5.11}$$

where, θ denotes the variable parameters chosen to minimize $J_n(\theta)$. It was also stated by Zuhang and Atherton (1993, p. 216) that 'minimisation of $J_1(\theta)$, often gave quite similar results to minimisation of the integral of time absolute error.' They found that the choice of $n = 1$ in Equation 5.11, which is known as the Integral Squared Time Error (ISTE) criterion, provided satisfactory results. But the optimization of the PID parameters by this process is dependent on the knowledge of the overall transfer function. Hence it becomes essential to accurately determine the transfer function of the component that is being controlled, in this case, the transfer function of the proportional solenoid flow control valve.

The optimizations were carried were carried out for different values of normalized dead time (τ /T) to determine optimal PID control parameters to minimize Integral Squared Error(ISE), when $n = 0$ in Equation 5.11; Integral Squared Time Error (ISTE), when $n = 1$ in Equation 5.11, and Integral Squared Time Squared Error (IST^2E), when $n = 2$ in Equation 5.11, performance criteria. The following relationships to determine the k_p, T_i and T_d terms of the PID controller are mentioned by Zhuang and Atherton (1993, p. 217):

$$k_p = \frac{a_1}{K}\left(\frac{\tau}{T}\right)^{b_1} \tag{5.12}$$

$$T_i = \frac{T}{a_2 + b_2\left(\frac{\tau}{T}\right)} \tag{5.13}$$

$$T_d = a_3 T\left(\frac{\tau}{T}\right)^{b_3} \tag{5.14}$$

The values of the coefficients a_1, b_1, a_2, b_2, a_3 and b_3 in Equations 5.12, 5.13 and 5.14 are listed in Table 5-1.

Table 5-1. PID tuning constants for set-point changes.

τ /T range	**0.1 − 1.0**			**1.1 − 2.0**		
Criterion	**ISE**	**ISTE**	**IST^2E**	**ISE**	**ISTE**	**IST^2E**
a_1	1.048	1.042	0.968	1.154	1.142	1.061
b_1	-0.897	-0.897	-0.904	-0.567	-0.579	-0.583
a_2	1.195	0.987	0.977	1.047	0.919	0.892
b_2	-0.368	-0.238	-0.253	-0.220	-0.172	-0.165
a_3	0.489	0.385	0.316	0.490	0.384	0.315
b_3	0.888	0.906	0.892	0.708	0.839	0.832

(Source: Zhuang and Atherton 1993, p. 218)

From Table 4-2 the transfer function of the proportional solenoid flow control valve was found to be $\frac{3.26\, e^{-0.04s}}{0.024s + 1}$. Therefore the value of τ /T was equal to 1.67. The

coefficients $a_1 = 1.142$, $b_1 = -0.597$, $a_2 = 0.919$, $b_2 = -0.172$, $a_3 = 0.384$ and $b_3 = 0.839$ in Equations 5.12, 5.13 and 5.14 for the value of τ /T equal to 1.67 from Table 5-1. Given the above, it was possible to calculate the parameters of the PID controller, used to control the proportional solenoid flow control valve, for minimum ISTE criteria.

$$k_p = \frac{a_1}{K}\left(\frac{\tau}{T}\right)^{b_1} = \frac{1.142}{3.255}\left(\frac{0.04}{0.024}\right)^{-0.579} = 0.27 \tag{5.15}$$

$$T_i = \frac{T}{a_2 + b_2\left(\frac{\tau}{T}\right)} = \frac{0.024}{0.919 - 0.172\left(\frac{0.04}{0.024}\right)} = 0.038 \tag{5.16}$$

$$T_d = a_3 T\left(\frac{\tau}{T}\right)^{b_3} = 0.384 \times 0.024\left(\frac{0.04}{0.024}\right)^{0.839} = 0.014 \tag{5.17}$$

From Equations 5.15, 5.16 and 5.17, the proportional gain (0.27), the integral time constant (0.038 s) and the derivative time constant (0.014 s) were calculated for a PID controller to control the proportional solenoid flow control valve. The resultant transfer function of this PID controller was $0.27\left[1 + \frac{1}{0.038s} + 0.014s\right]$. Figure 5-3 details the process and the controller as a complete system.

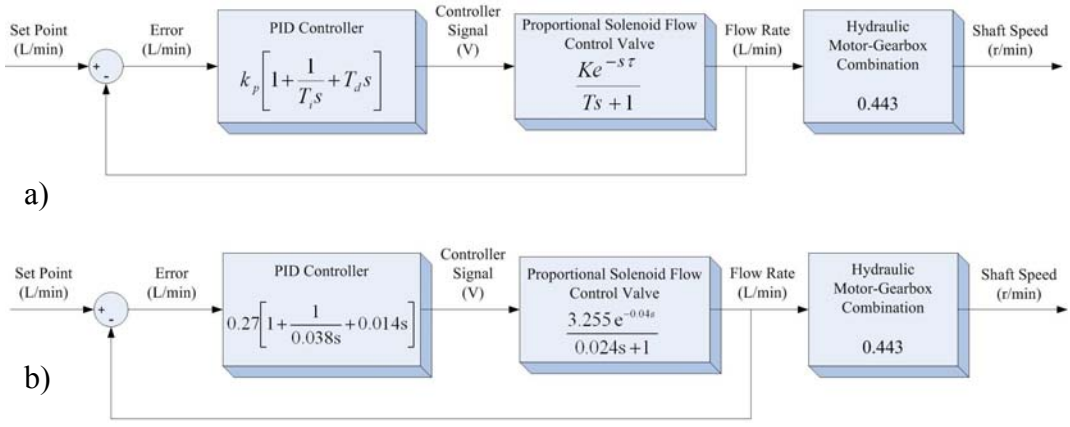

Figure 5-3. Block diagrams of the process and the controller as a complete system. a) Transfer function of the various components of the system, b) The controller gains, time constant and the time delay of the flow control valve.

The above section explains the derivations of one of the tuning rules for the parameter optimization of the PID controller based on the dynamic characteristics of the FOLPD process being controlled with ISTE criteria. In a similar manner, the PID controller parameters for ISE and IST^{2}E criteria were also calculated using Table 5-1.

A similar PID controller parameter tuning approach was performed by Wang et al. (1995). But in this case, the error criteria minimized were Integral Squared Error (ISE), Integral Absolute Error (IAE) and Integral Time Absolute Error (ITAE) where,

$$ISE = \int_0^\infty e^2(t)dt \tag{5.18}$$

$$IAE = \int_0^\infty |e(t)|dt \tag{5.19}$$

$$ITAE = \int_0^\infty t|e(t)|dt \tag{5.20}$$

Wang et al. (1995) determined that only the proportional gain was observed to be dependent on the implemented tunable parameter. The tuning parameters determined by their study are listed below,

$$k_p = \frac{(1+\beta K)(T+0.5\tau)}{(T+\tau)K} \tag{5.21}$$

$$T_i = (T+0.5\tau) \tag{5.22}$$

$$T_d = \frac{0.5T\tau}{(T+0.5\tau)} \tag{5.23}$$

Equations 5.21, 5.22 and 5.23 were simplified and the appropriate terms substituted from the Equations 10, 11 and 12 as detailed by Wang et al. (1995, p. 19). The numerical

value for β in Equation 5.21 was determined from Equation (55) stated by Wang et al. (1995, p. 26),

$$\beta = \frac{\delta_0 - 1 + \frac{\delta_1}{\theta}}{K} \tag{5.24}$$

where,

$\theta = \tau/T$

and δ_0 and δ_1 were determined from Table 5-2. By substituting for β and θ in Equations 5.21 and 5.24, the following expression for proportional gain k_p was obtained:

$$k_p = \frac{\left(\delta_0 + \frac{\delta_1}{\tau/T}\right)(T + 0.5\tau)}{(T+\tau)K} \tag{5.25}$$

Table 5-2. Coefficients of tuning formula to determine k_p.

	ISE	**IAE**	**ITAE**
δ_0	0.9155	0.7645	0.7303
δ_1	0.7524	0.6032	0.5307

(Source: Wang et al., 1995, p.26)

The six tuning rules to control the proportional solenoid flow control valve, (FOLPD process) selected from all considered tuning rules, are listed in Table 5-3. The rules were assigned generic names for convenient referencing in the following chapters. Table 5-4 lists the values of the PID controller parameters obtained by substituting for the coefficients (K = 3.26, τ = 0.04 s and T = 0.024 s) in the equations listed in Table 5-3.

Table 5-3. Tuning rules for the FOLPD systems.

Generic Name	Rule	k_p	T_i	T_d
Tuning Rule-01	Zhuang and Atherton (1993) – minimum ISTE	$\frac{1.142}{K}\left(\frac{\tau}{T}\right)^{-0.579}$	$\frac{T}{0.919-0.172\left(\frac{\tau}{T}\right)}$	$0.384\times T\left(\frac{\tau}{T}\right)^{0.839}$
Tuning Rule-02	Zhuang and Atherton (1993) – minimum ISE	$\frac{1.154}{K}\left(\frac{\tau}{T}\right)^{-0.567}$	$\frac{T}{1.047-0.220\left(\frac{\tau}{T}\right)}$	$0.490\times T\left(\frac{\tau}{T}\right)^{0.708}$
Tuning Rule-03	Zhuang and Atherton (1993) – minimum IST^{2}E	$\frac{1.061}{K}\left(\frac{\tau}{T}\right)^{-0.583}$	$\frac{T}{0.892-0.165\left(\frac{\tau}{T}\right)}$	$0.315\times T\left(\frac{\tau}{T}\right)^{0.832}$
Tuning Rule-04	Wang et al. (1995) – minimum ITAE	$\frac{\left(0.730+\frac{0.531}{\tau/T}\right)(T+0.5\tau)}{K(T+\tau)}$	$T+0.5\tau$	$\frac{0.5T\tau}{T+0.5\tau}$
Tuning Rule-05	Wang et al. (1995) – minimum IAE	$\frac{\left(0.765+\frac{0.603}{\tau/T}\right)(T+0.5\tau)}{K(T+\tau)}$	$T+0.5\tau$	$\frac{0.5T\tau}{T+0.5\tau}$
Tuning Rule-06	Wang et al. (1995) – minimum ISE	$\frac{\left(0.916+\frac{0.752}{\tau/T}\right)(T+0.5\tau)}{K(T+\tau)}$	$T+0.5\tau$	$\frac{0.5T\tau}{T+0.5\tau}$

Table 5-4. Numerical values for the PID control gains.

Generic Name	Rule	k_p	T_i	T_d
Tuning Rule-01	Zhuang and Atherton (1993) – minimum ISTE	0.2689	0.0384	0.0142
Tuning Rule-02	Zhuang and Atherton (1993) – minimum ISE	0.2734	0.0357	0.0170
Tuning Rule-03	Zhuang and Atherton (1993) – minimum IST^{2}E	0.2494	0.0394	0.0116
Tuning Rule-04	Wang et al. (1995) – minimum ITAE	0.2278	0.0446	0.0110
Tuning Rule-05	Wang et al. (1995) – minimum IAE	0.2447	0.0446	0.0110
Tuning Rule-06	Wang et al. (1995) – minimum ISE	0.2970	0.0446	0.0110

PID Controller Implementation for the Proportional Solenoid Flow Control Valve

Procedure: The proportional solenoid flow control valve was controlled for a setpoint flowrate with the controller board through LabView as explained in Chapter 2. The feedback of the flowrate was obtained from Flowmeter-2, which generated 926 p/L

of flow. This translated to 2093 p/rev of the hydraulic motor-gearbox combination shaft. The LabView program was executed with a loop time of 0.02 s. The test configuration was similar to the setup explained for the benchmarking test of commercial controllers in real-time mode. One module in the loop read the simulated states of the real-time sensors from the text file that had the status information of the real-time sensors in an array format for every 0.2 s for the entire length of the experiment (~60 s). The vehicle was assumed to travel at a speed of 1.34 m/s. By reading the simulated states of the real-time sensors, it was possible to determine the commanded application-rate which was scaled to the setpoint flowrate (Equation 2.1). Inputs to the PID module in the program were the commanded flowrate and actual flowrate obtained from Flowmeter-2 and the output was the voltage command to the proportional solenoid flow control valve's controller board. The gains in the PID module could be set at the beginning of the experiment. All of the values from Table 5-3 of the PID controller parameters obtained from the tuning rules stated in Table 5-2 were substituted in the code and the data were acquired. These results are discussed in detail in Chapter 6.

Implementation of Delay Algorithm to Compensate for Speed Variation, Distance Offset and Delay Time

As discussed in the previous chapters, the present commercial controllers vary the conveyor-chain speed based on the commanded application rate (Equation 2.1). It can be concluded that the application rate was inversely proportional to the vehicle speed with all the other parameters in Equation 2.1 being constant. The real-time sensors had distance offset compensation incorporated in them on the assumption that the applicator was traveling at a constant speed. It did not account for the variation in the vehicle speed which occurred in field conditions for every execution of the control loop.

The flowchart described in Figure 5-4 compensated for the various offsets depending on operating mode (GPS or real-time). Currently, the code can only work in real-time mode. If a point search algorithm can be implemented, this code can execute in GPS mode and hence can compensate for GPS offsets. This delay module was incorporated into the same control algorithm as described in the previous section (PID Controller Implementation for the Proportional Solenoid Flow Control Valve). However, in this case, the additional inputs would be the GPS or real-time sensor offsets (Figure 1-9); delay time, vehicle speed inputs from either the GPS or the radar ground speed sensor. The delay time was a sum of proportional solenoid flow control valve initial delay time (0.04 s), GPS point search algorithm delay time, the GPS receiver delay time (Miller et al. 2004, Table 5, p. 165) and fertilizer particles drop delay time (explained in the following section). For the benefit of easier understanding, in all of the test cases, simulated ground speed values were input into the code at a rate of 50 Hz (speed update for every control loop execution). The output from the delay module was a commanded flowrate which had compensation for all the above mentioned parameters. This commanded flowrate and the actual flowrate measured from Flowmeter-2 were the input to the PID control module.

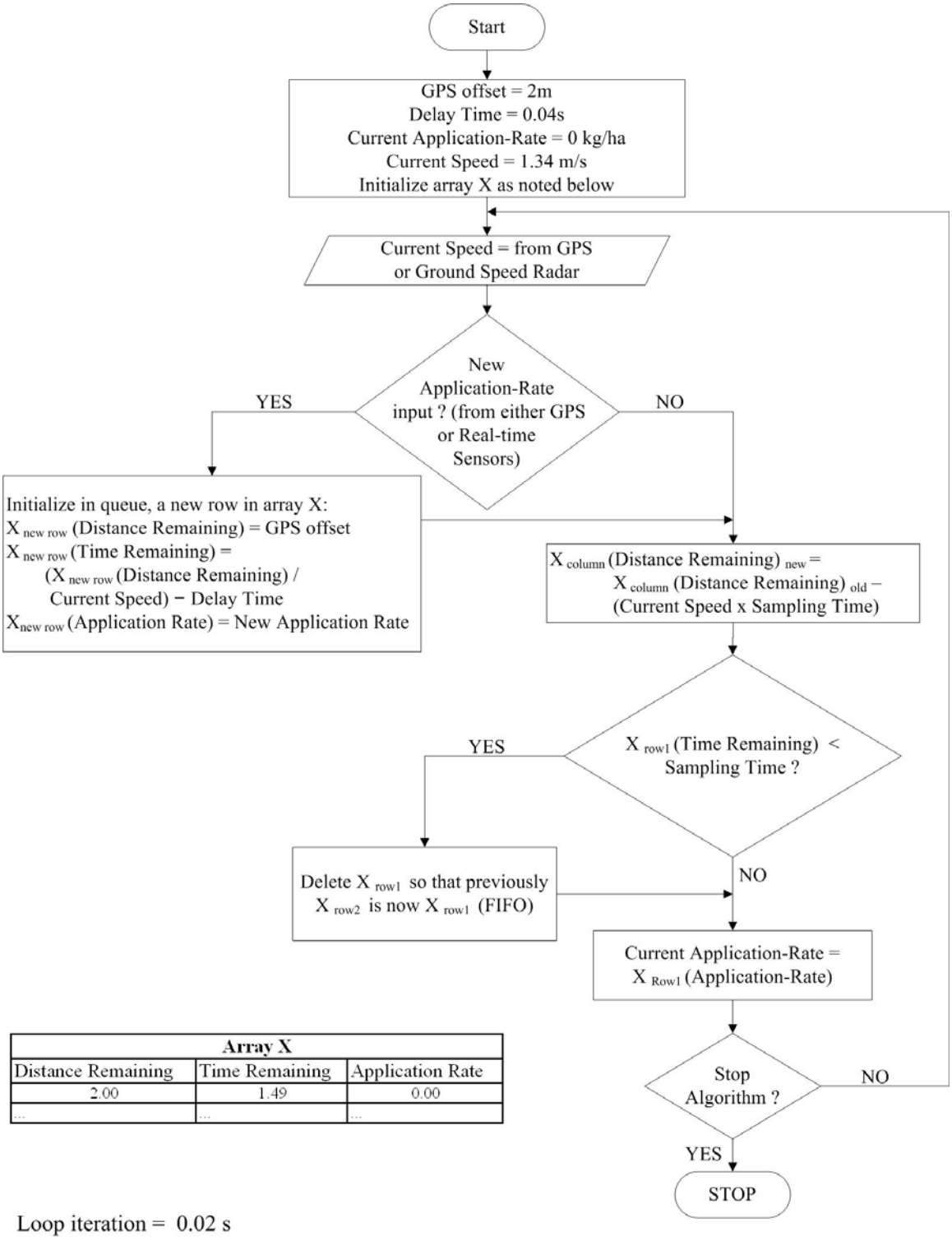

Figure 5-4. Flow chart for the speed, distance offsets and delay times compensation.

Fertilizer Particle-Drop Delay Time Determination

In this section, the time (T_{Travel}) required for the fertilizer particle to travel from the hopper of the applicator to the tree base was calculated. In order to determine the total time required by the fertilizer particle to travel from the conveyor-chain to the ground, the solution was divided in to 3 parts, namely:

- The travel of the fertilizer material from the belt to the spinner disc (free fall)
- The fertilizer material and spinner disc interaction (rolling and sliding)
- The travel of the fertilizer material from the spinner disc to the ground (projectile)

Free-fall calculation

In this case, the negative drag force along the y axis was not considered. The free fall time was determined by the equation stated below,

$$d = \tfrac{1}{2}\, g\, T_{Belt2Disc}^{2} \qquad (5.26)$$

where,

d = Vertical distance traveled by the particle = 0.48 m

g = Acceleration due to gravity = 9.807 m/s^2

$T_{Belt2Disc}$ = time (s)

Therefore, by rearranging the terms in the above equation to solve for $T_{belt2disc}$,

$$T_{Belt2Disc} = \left| \pm \sqrt{2d/g} \right| = 0.31 \text{ s} \qquad (5.27)$$

Fertilizer material on spinner-disc calculation

The time ($T_{SpinnerDisc}$) required for the fertilizer particles to travel radially from the point of the deposit on the spinner disc to the perimeter of the spinner disc was calculated by averaging the times determined by 2 methods of motion between the disc and the material, pure rolling (t_{roll}) and pure sliding (t_{slide}).

Case of Pure Sliding: Equations (2 and 4) from Aphale et al. (2003)

$$\frac{r}{R} = \frac{r_0}{R}\left[\left(\frac{1}{\beta_1 - \alpha}\right)\left(1 - \frac{\mu g}{\omega_1^{\,2} r_0}\right)\left[\beta_1 exp(\alpha\, \omega_1\, t_{slide}) - \alpha exp(\beta_1\, \omega_1\, t_{slide})\right] + \frac{\mu g}{\omega_1^{\,2} r_0}\right] \qquad (5.28)$$

$$\alpha, \beta_1 \;\; = -\mu \pm \sqrt{\mu^2 + 1}$$

where,

r = Radial position from the center of the spinner disc (m)

R = Outer radius of the spinner disc = 0.305 m

r_0 = Radial distance from the spinner disc center where a particle is dropped (assumed the particles are dropped at the midpoint of the disc) = 0.153 m

ω_1 = Rotational speed of the spinner disc = 47.12 rad/s

g = Acceleration due to gravity (m/s^2) = 9.807 m/s^2

μ = Friction coefficient between particle and the spinner disc and the particle and a spinner vane = 0.4 for limestone filler, urea, etc.

α, β_1 = Characteristic roots of pure sliding equation

Since, we needed to determine the time (t_{slide}) at which the particle was at the outer tip of the disc (i.e. r=R), the above equation can be written as:

$$1 = \frac{r_0}{R}\left[\left(\frac{1}{\beta_1 - \alpha}\right)\left(1 - \frac{\mu g}{\omega_1^{\,2} r_0}\right)\left[\beta_1 exp(\alpha\omega_1 t_{slide}) - \alpha exp(\beta_1\omega_1 t_{slide})\right] + \frac{\mu g}{\omega_1^{\,2} r_0}\right] \qquad (5.29)$$

The above equation was further simplified to:

$$\left[\beta_1 \exp(\alpha\omega_1 t_{slide}) - \alpha exp(\beta_1\omega_1 t_{slide})\right] = \left(\frac{R}{r_0} - \frac{\mu g}{\omega_1^{\,2} r_0}\right)\left((\beta_1 - \alpha)\Big/\left(1 - \frac{\mu g}{\omega_1^{\,2} r_0}\right)\right) \qquad (5.30)$$

The above equation was in the explicit form; hence it was solved for t_{slide} by the method of substitution using Solver function in Excel. t_{slide} was determined to be 0.023 s.

Case of Pure Rolling: Equation (9) from Aphale et al. (2003),

$$\frac{r}{R} = \frac{r_0}{R}\left[\left(1 - \frac{\mu g}{\omega_1^{\,2} r_0}\right)\cosh\left(\sqrt{\frac{5}{7}}\omega_1 t_{roll}\right) + \frac{\mu g}{\omega_1^{\,2} r_0}\right] \tag{5.31}$$

where,

r = Radial position from the center of the spinner disc

R = Outer radius of the spinner disc = 0.305 m

r_0 = Radial distance from the spinner disc center where a particle is dropped (assumed the particles are dropped at the midpoint of the disc) = 0.153 m

ω_1 = Rotational speed of the spinner disc = 47.12 rad/s

g = Acceleration due to gravity = 9.807 m/s^2

μ = Friction coefficient between particle and the spinner disc and the particle and a spinner vane = 0.4 for limestone filler, urea, etc.

Since, we needed to determine the time (t_{roll}) at which the particle was at the outer tip of the disc (i.e. r=R), the above equation can be written as:

$$1 = \frac{r_0}{R}\left[\left(1 - \frac{\mu g}{\omega_1^{\,2} r_0}\right)\cosh\left(\sqrt{\frac{5}{7}}\omega_1 t_{roll}\right) + \frac{\mu g}{\omega_1^{\,2} r_0}\right] \tag{5.32}$$

The above equation was further simplified to get,

$$t_{roll} = \frac{1}{\omega_1\sqrt{5/7}}\cosh^{-1}\left[\left(\frac{R}{r_0} - \frac{\mu g}{\omega_1^{\,2} r_0}\right)\frac{1}{\left(1 - \frac{\mu g}{\omega_1^{\,2} r_0}\right)}\right] = 0.033 \text{ s} \tag{5.33}$$

Therefore,

$$T_{SpinnerDisc} = \frac{t_{slide} + t_{roll}}{2} = 0.028 \text{ s} \tag{5.34}$$

Fertilizer particle as a projectile calculation

This section describes the procedure to calculate the time required by the fertilizer particle to travel from the perimeter of the spinner disc to the ground based on the assumption that the spinner discs are parallel to the ground. Assuming the drag forces on the particle to be negligible and hence the time ($T_{Projectile}$) required by the fertilizer particle to reach the ground from the spinner disc is,

$$h_1 = g\,(T_{Projectile}^{2}) \tag{5.35}$$

where,

h_1 = Vertical distance of the spinner-discs from ground = 0.47 m

g = Acceleration due to gravity = 9.807 m/s^2

$T_{Projectile}$ = time (s)

Therefore,

$$T_{Projectile} = \left| \pm \sqrt{\frac{2h_1}{g}} \right| = 0.31 \text{ s} \tag{5.36}$$

Therefore total time of travel for the particle from the conveyor chain to the ground is given by,

$$T_{Travel} = T_{Belt2Disc} + T_{SpinnerDisc} + T_{Projectile} = 0.65 \text{ s} \tag{5.37}$$

Implementation of a Simple Control Algorithm for the DC Motor Operated Flow Control Valve

A simple algorithm was implemented to control the DC motor operated flow control valve. In this case, the actual flowrate was determined using Flowmeter-2 for every execution of the control loop at a frequency of 50 Hz. In case of the DC motor operated flow control valve operation, it was possible to control the angular speed of the valve stem rotation. A simple proportional control was implemented such that larger errors generated faster valve stem rotation.

The steady-state slope of the valve was 2.34 L min^{-1} deg^{-1} rotation of the valve stem (between 3° and 10.5°) from Figure 4-14. Maximum speed of rotation of the valve stem in either direction was 30°/s which corresponded to 0.6° for every 0.02 s. From the above calculations, it can be concluded that the maximum flowrate change that can occur in a single control loop execution was 1.4 L/min (0.6° x 2.34 L/min). Hence if the error between the commanded and the actual flowrate was greater than or equal to 1.4 L/min, then the valve stem was either opened or closed at full speed. If the error was less than 1.4 L/min, then the speed of the motor was determined such that the valve stem would rotate by that correction rotation in 0.02 s. For example, if the actual flowrate was determined to be 9.5 L/min instead of the commanded 9 L/min, then the valve stem was commanded to rotate at a speed of 0.21° (0.5/2.34) in 0.02 s, which corresponded to 10.68°/s. This speed was scaled (Figure 2-7) to a corresponding voltage issued to the valve controller board. The implementation of this control algorithm is illustrated in Figure 5-5.

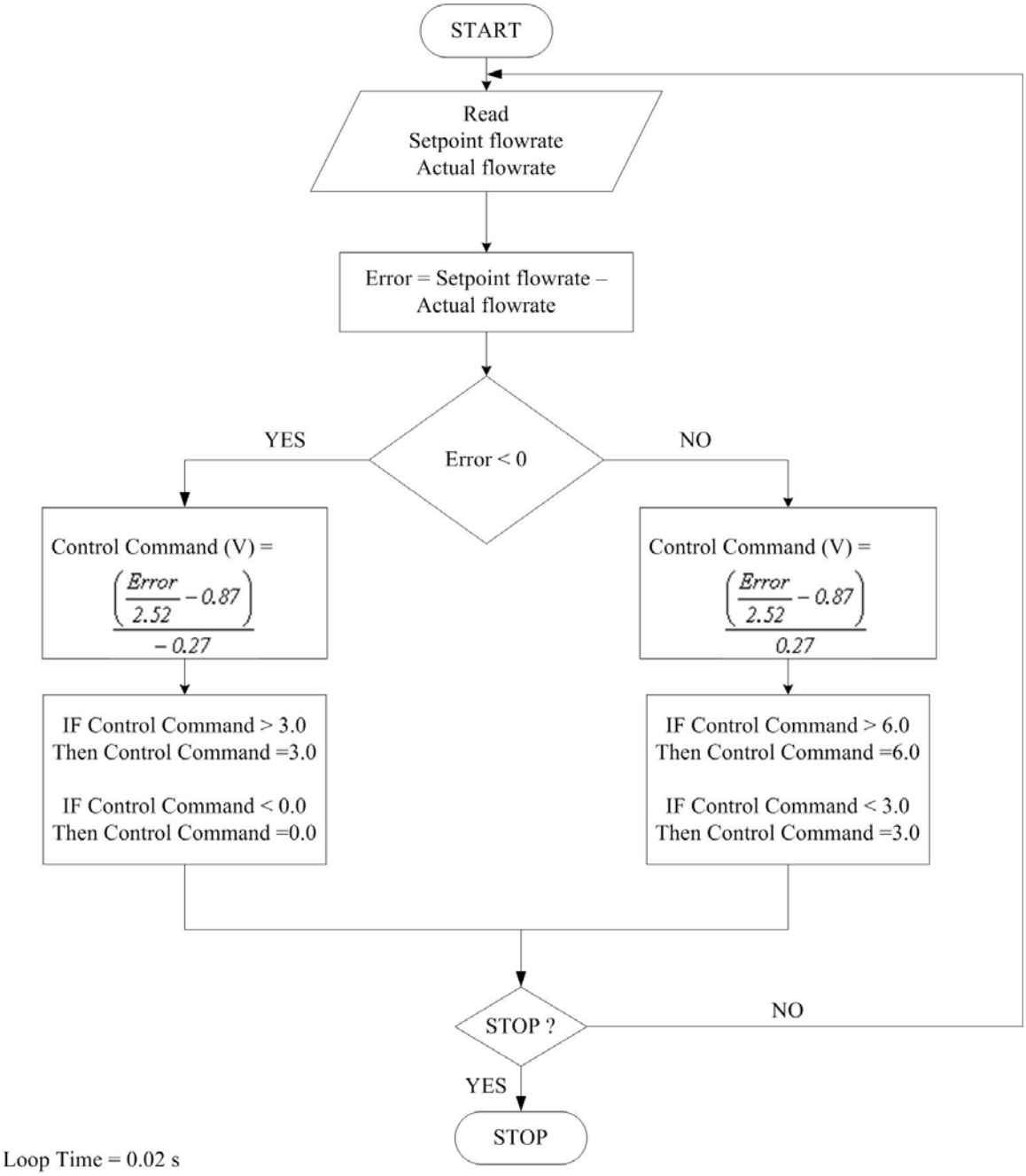

Figure 5-5. Control algorithm for the DC motor operated flow control valve.

CHAPTER 6
RESULTS AND DISCUSSION

Performance Evaluation Estimation

The new test procedure presented in Chapter 3 to benchmark the commercial and model-based PID control VRT system configurations mentioned in Table 2-2 were executed to acquire experimental data from these systems. To benchmark the performance, it was necessary to develop new evaluation methods. The two new methods to evaluate the experimental data are proposed in this chapter. The first method will be addressed as the "Total Application Error" (TAE) and the second designated as "Total Single Tree-Zone Application Error" (TSAE).

Total Application Error (TAE): is a measure of how well the system followed the application-rate change pattern issued by the controller over time. It accounts for dynamic performance of the control system. This is a sum total of the absolute errors measured by the control loop in each iteration. The error, in terms of flowrate (L/min), measured during each control loop iteration is converted to the amount of material applied (kg) by multiplying the quantity of fertilizer deposited per second (kg/s) at the stated speed of motor-gearbox shaft (Equation 2.4) and the loop time or data sampling time (0.02 s). The yellow area in Figure 6-1 represents the application error calculated for a single tree zone. The sum total of this individual application error (kg) determined for the entire test run is the TAE (Equation 6.1).

$$Total\ Application\ Error = \sum_{t_{beg}}^{t_{end}} \left| \left(\omega_c - \omega_a\right) \times \pi \times D \times h \times w \times \rho \times t_s \right| \tag{6.1}$$

where,

ρ = Fertilizer material density (kg/m^3)

h = Gate height (m)

w = Conveyor chain width (m)

D = Conveyor roller diameter (m)

t_s = Data sampling time (s) = 0.02 s

$\omega_c = k \times q_c$ = Commanded Speed of the motor-gearbox shaft (rev/s)

$\omega_a = k \times q_a$ = Actual speed of the motor-gearbox shaft (rev/s)

where,

k = Gain (rev/L) of the hydraulic motor-gearbox combination

q_c= Commanded flowrate (L/min)

q_a = Actual flowrate (L/min)

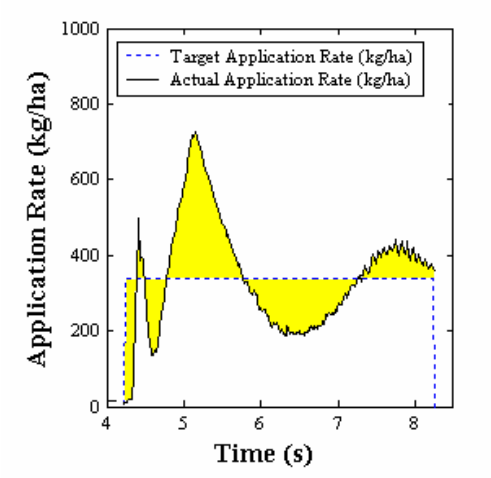

Figure 6-1. Application Error for one tree-zone.

All system configurations stated in Table 2-2 were subjected to five repetitions of the test described in chapters 3 and 5 for statistical analysis. Table 6-1 summarizes the TAE of all the commercial systems' configuration listed in Table 2-2. The TAE (kg)

within each tree zone and for each repetition of the tests was calculated using Equation 6.1.

Table 6-1. TAE for the commercial systems' configuration.

Commanded Application-rate (kg/ha)	**0.00**	**336.24**	**0.00**	**504.36**	**0.00**	**672.48**	**0.00**	**336.24**	**504.36**	**672.48**	**504.36**	**336.24**	**672.48**	**336.24**	**0.00**	**Total (kg)**
Commanded quantity of fertilizer (kg)	**0.00**	**0.62**	**0.00**	**0.94**	**0.00**	**1.25**	**0.00**	**0.62**	**0.94**	**1.25**	**0.94**	**0.62**	**1.25**	**0.62**	**0.00**	**9.06**
								Application Error (kg) ↓								
System 01																
Repetition 1	0.05	0.47	0.34	0.72	0.36	0.83	0.59	0.56	0.21	0.27	0.16	0.09	0.43	0.24	0.10	**5.42**
Repetition 2	0.05	0.49	0.19	0.63	0.36	0.80	0.46	0.55	0.22	0.26	0.30	0.09	0.59	0.29	0.22	**5.50**
Repetition 3	0.06	0.50	0.13	0.55	0.20	0.59	0.27	0.39	0.24	0.25	0.15	0.22	0.49	0.18	0.15	**4.37**
Repetition 4	0.06	0.50	0.24	0.62	0.36	0.88	0.59	0.57	0.24	0.33	0.17	0.10	0.47	0.17	0.05	**5.36**
Repetition 5	0.02	0.49	0.21	0.69	0.43	0.83	0.56	0.51	0.19	0.27	0.18	0.08	0.40	0.22	0.12	**5.21**
System 02																
Repetition 1	0.01	0.54	0.07	0.65	0.06	0.70	0.08	0.37	0.28	0.29	0.31	0.06	0.45	0.34	0.04	**4.26**
Repetition 2	0.00	0.45	0.04	0.61	0.06	0.81	0.08	0.51	0.30	0.29	0.11	0.17	0.40	0.14	0.04	**4.02**
Repetition 3	0.00	0.62	0.04	0.62	0.08	0.74	0.07	0.52	0.20	0.21	0.18	0.21	0.50	0.29	0.04	**4.33**
Repetition 4	0.00	0.42	0.04	0.62	0.06	0.75	0.07	0.55	0.24	0.30	0.23	0.14	0.52	0.22	0.05	**4.22**
Repetition 5	0.00	0.45	0.04	0.62	0.10	0.79	0.07	0.53	0.26	0.23	0.13	0.24	0.55	0.21	0.03	**4.24**
System 03																
Repetition 1	0.00	0.35	0.05	0.55	0.13	0.58	0.13	0.38	0.19	0.13	0.21	0.06	0.50	0.18	0.06	**3.47**
Repetition 2	0.00	0.44	0.06	0.53	0.14	0.54	0.13	0.43	0.19	0.11	0.14	0.11	0.40	0.13	0.07	**3.43**
Repetition 3	0.00	0.36	0.06	0.53	0.11	0.53	0.14	0.42	0.26	0.13	0.18	0.12	0.45	0.17	0.07	**3.53**
Repetition 4	0.00	0.42	0.07	0.50	0.13	0.57	0.16	0.41	0.21	0.16	0.21	0.10	0.40	0.24	0.05	**3.63**
Repetition 5	0.09	0.38	0.06	0.50	0.08	0.59	0.13	0.36	0.30	0.18	0.17	0.14	0.40	0.20	0.06	**3.65**
System 04																
Repetition 1	0.00	0.25	0.16	0.30	0.18	0.41	0.28	0.28	0.10	0.13	0.10	0.12	0.24	0.39	0.16	**3.09**
Repetition 2	0.00	0.28	0.12	0.26	0.12	0.37	0.26	0.32	0.06	0.13	0.07	0.10	0.18	0.17	0.10	**2.53**
Repetition 3	0.00	0.45	0.15	0.39	0.20	0.50	0.37	0.31	0.16	0.11	0.10	0.14	0.37	0.27	0.15	**3.66**
Repetition 4	0.00	0.35	0.20	0.41	0.31	0.47	0.40	0.34	0.14	0.14	0.13	0.16	0.36	0.24	0.15	**3.80**
Repetition 5	0.00	0.39	0.21	0.38	0.33	0.59	0.54	0.32	0.15	0.19	0.09	0.09	0.28	0.15	0.09	**3.79**
System 05																
Repetition 1	0.01	0.20	0.04	0.22	0.08	0.24	0.09	0.28	0.09	0.10	0.16	0.12	0.23	0.24	0.05	**2.14**
Repetition 2	0.10	0.26	0.08	0.25	0.07	0.23	0.09	0.29	0.08	0.13	0.09	0.12	0.15	0.17	0.05	**2.16**
Repetition 3	0.00	0.23	0.06	0.26	0.07	0.28	0.08	0.24	0.12	0.14	0.08	0.14	0.16	0.32	0.04	**2.22**
Repetition 4	0.08	0.22	0.09	0.27	0.08	0.27	0.09	0.24	0.15	0.14	0.14	0.11	0.23	0.21	0.04	**2.36**
Repetition 5	0.00	0.28	0.08	0.26	0.07	0.29	0.09	0.23	0.08	0.16	0.14	0.12	0.19	0.22	0.07	**2.29**
System 06																
Repetition 1	0.00	0.26	0.18	0.41	0.26	0.52	0.46	0.25	0.13	0.05	0.13	0.05	0.25	0.25	0.08	**3.27**
Repetition 2	0.00	0.23	0.24	0.33	0.31	0.54	0.51	0.31	0.24	0.22	0.09	0.04	0.27	0.24	0.08	**3.65**
Repetition 3	0.00	0.27	0.23	0.37	0.28	0.63	0.40	0.23	0.14	0.05	0.14	0.06	0.36	0.18	0.09	**3.45**
Repetition 4	0.01	0.22	0.21	0.41	0.28	0.61	0.43	0.30	0.17	0.06	0.15	0.09	0.29	0.25	0.10	**3.56**
Repetition 5	0.01	0.27	0.21	0.36	0.27	0.63	0.49	0.25	0.21	0.09	0.13	0.07	0.25	0.24	0.11	**3.59**
System 07																
Repetition 1	0.00	0.11	0.07	0.19	0.09	0.24	0.11	0.11	0.13	0.11	0.04	0.06	0.13	0.07	0.06	**1.51**
Repetition 2	0.00	0.13	0.06	0.22	0.09	0.23	0.12	0.09	0.10	0.04	0.09	0.06	0.10	0.07	0.06	**1.47**
Repetition 3	0.01	0.15	0.07	0.12	0.10	0.21	0.13	0.13	0.16	0.13	0.12	0.09	0.16	0.06	0.07	**1.71**
Repetition 4	0.00	0.13	0.06	0.17	0.08	0.20	0.13	0.07	0.06	0.06	0.07	0.04	0.08	0.13	0.06	**1.34**
Repetition 5	0.00	0.14	0.08	0.23	0.08	0.14	0.13	0.15	0.10	0.06	0.14	0.04	0.16	0.08	0.07	**1.58**
System 08																
Repetition 1	0.00	0.27	0.10	0.45	0.12	0.79	0.11	0.29	0.09	0.13	0.14	0.16	0.27	0.24	0.07	**3.23**
Repetition 2	0.00	0.32	0.06	0.48	0.10	0.70	0.12	0.31	0.06	0.12	0.13	0.16	0.26	0.26	0.07	**3.15**
Repetition 3	0.00	0.32	0.09	0.56	0.09	0.69	0.11	0.31	0.20	0.20	0.14	0.17	0.23	0.26	0.07	**3.44**
Repetition 4	0.08	0.33	0.07	0.48	0.11	0.79	0.10	0.30	0.20	0.24	0.14	0.15	0.26	0.17	0.12	**3.54**
Repetition 5	0.05	0.28	0.08	0.55	0.09	0.79	0.11	0.26	0.13	0.12	0.08	0.17	0.24	0.27	0.07	**3.31**

Total Single Tree Zone Application Error (TSAE): is defined as the measure of performance of the controller to deposit the required amount of fertilizer under each tree. It does not take into account the spread pattern in the direction of travel under the tree zone, but only the quantity of fertilizer deposited. This error (kg) was determined for each

tree zone. The total amount of fertilizer to be deposited under each tree zone was determined by the commanded application-rate (blue area in Figure 6-2 a) and the total amount of fertilizer deposited was determined by the actual application-rate (brown area in Figure 6-2 b). The difference between these areas was the error within a single tree-zone. It can either have an under application (blue area > brown area) or an over application (blue area < brown area). TSAE is the sum total of all absolute single tree-zone errors in the test run (Equation 6.2).

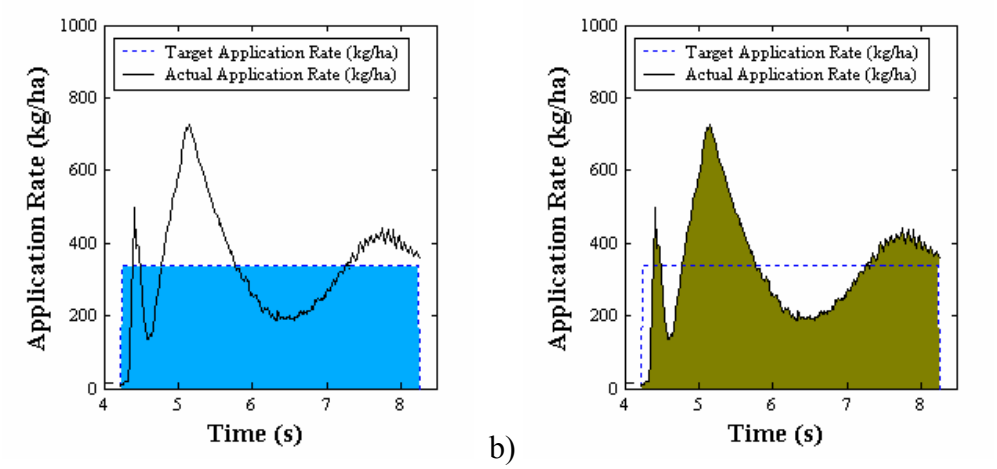

Figure 6-2. Components of a Single Tree-Zone Application Error. a) Commanded quantity of fertilizer applied and b) actual quantity of fertilizer applied.

Total Single Tree-Zone Application Error =

$$\sum_{AllTreeZones}\left|\sum_{SingleTreeZone}\left(\omega_c\times\pi\times D\times h\times w\times\rho\times t_s\right)-\sum_{SingleTreeZone}\left(\omega_a\times\pi\times D\times h\times w\times\rho\times t_s\right)\right| \qquad (6.2)$$

where,

ρ = Fertilizer material density (kg/m^3)

h = Gate height (m)

w = Conveyor chain width (m)

D = Conveyor roller diameter (m)

t_s = Data sampling time (s) = 0.02 s

$\omega_c = k \times q_c$ = Commanded Speed of the motor-gearbox shaft (rev/s)

$\omega_a = k \times q_a$ = Actual speed of the motor-gearbox shaft (rev/s)

where,

k = Gain (rev/L) of the hydraulic motor-gearbox combination

q_c = Commanded flowrate (L/min)

q_a = Actual flowrate (L/min)

Table 6-2 depicts the TSAE of all the commercial systems' configuration listed in Table 2-2. The TSAE (kg) within each tree-zone and for each repetition of the tests was determined using Equation 6.2. Figure 6-3 compares the TAE and the TSAE of the various commercial controller systems. These averaged errors (kg) for five repetitions, of each system, was depicted as a percentage of the total commanded quantity (kg) of fertilizer applied in one test run.

Table 6-2. TSAE for the commercial systems' configuration.

Commanded Application-Rate (kg/ha)	**0.00**	**336.24**	**0.00**	**504.36**	**0.00**	**672.48**	**0.00**	**336.24**	**504.36**	**672.48**	**504.36**	**336.24**	**672.48**	**336.24**	**0.00**	**Total (kg)**
Commanded quantity of fertilizer (kg)	**0.00**	**0.62**	**0.00**	**0.94**	**0.00**	**1.25**	**0.00**	**0.62**	**0.94**	**1.25**	**0.94**	**0.62**	**1.25**	**0.62**	**0.00**	**9.06**
								Single Tree-Zone Application Error (kg) ↓								
System 01																
Repetition 1	0.05	0.07	0.34	0.15	0.36	0.47	0.59	0.06	0.21	0.10	0.07	0.07	0.42	0.21	0.10	**3.26**
Repetition 2	0.05	0.01	0.19	0.15	0.36	0.44	0.46	0.02	0.22	0.07	0.00	0.09	0.59	0.29	0.22	**3.17**
Repetition 3	0.06	0.16	0.13	0.02	0.20	0.36	0.27	0.04	0.24	0.04	0.08	0.22	0.49	0.15	0.15	**2.61**
Repetition 4	0.06	0.03	0.24	0.22	0.36	0.45	0.59	0.07	0.24	0.05	0.07	0.07	0.47	0.12	0.05	**3.10**
Repetition 5	0.02	0.07	0.21	0.17	0.43	0.43	0.56	0.12	0.19	0.24	0.06	0.07	0.39	0.00	0.12	**3.07**
System 02																
Repetition 1	0.01	0.14	0.07	0.12	0.06	0.25	0.08	0.02	0.28	0.03	0.09	0.06	0.45	0.34	0.04	**2.05**
Repetition 2	0.00	0.07	0.04	0.25	0.06	0.47	0.08	0.09	0.30	0.29	0.01	0.17	0.40	0.12	0.04	**2.39**
Repetition 3	0.00	0.11	0.04	0.04	0.08	0.25	0.07	0.05	0.20	0.09	0.08	0.21	0.50	0.20	0.04	**1.96**
Repetition 4	0.00	0.03	0.04	0.13	0.06	0.41	0.07	0.05	0.24	0.15	0.02	0.14	0.52	0.21	0.05	**2.13**
Repetition 5	0.00	0.11	0.04	0.04	0.10	0.27	0.07	0.07	0.26	0.10	0.07	0.24	0.55	0.12	0.03	**2.06**
System 03																
Repetition 1	0.00	0.08	0.05	0.13	0.13	0.01	0.13	0.11	0.19	0.03	0.17	0.02	0.49	0.06	0.06	**1.65**
Repetition 2	0.00	0.16	0.06	0.09	0.14	0.09	0.13	0.16	0.19	0.03	0.02	0.11	0.40	0.12	0.07	**1.76**
Repetition 3	0.00	0.09	0.06	0.08	0.11	0.10	0.14	0.14	0.26	0.05	0.08	0.09	0.44	0.15	0.07	**1.88**
Repetition 4	0.00	0.16	0.07	0.06	0.13	0.05	0.16	0.15	0.21	0.02	0.16	0.10	0.39	0.17	0.05	**1.88**
Repetition 5	0.09	0.10	0.06	0.11	0.08	0.00	0.13	0.09	0.30	0.04	0.12	0.14	0.39	0.06	0.06	**1.77**
System 04																
Repetition 1	0.00	0.04	0.16	0.09	0.18	0.35	0.28	0.09	0.07	0.11	0.08	0.04	0.16	0.21	0.16	**2.01**
Repetition 2	0.00	0.05	0.12	0.11	0.12	0.14	0.26	0.03	0.02	0.11	0.05	0.03	0.11	0.03	0.10	**1.27**
Repetition 3	0.00	0.18	0.15	0.13	0.20	0.30	0.37	0.16	0.14	0.10	0.04	0.07	0.37	0.00	0.15	**2.36**
Repetition 4	0.00	0.06	0.20	0.17	0.31	0.41	0.40	0.18	0.11	0.10	0.11	0.08	0.34	0.04	0.15	**2.68**
Repetition 5	0.00	0.10	0.21	0.27	0.33	0.53	0.54	0.20	0.11	0.16	0.04	0.01	0.28	0.04	0.09	**2.90**

Table 6-2. continued.

Commanded Application-Rate (kg/ha)	**0.00**	**336.24**	**0.00**	**504.36**	**0.00**	**672.48**	**0.00**	**336.24**	**504.36**	**672.48**	**504.36**	**336.24**	**672.48**	**336.24**	**0.00**	**Total (kg)**
Commanded quantity of fertilizer (kg)	**0.00**	**0.62**	**0.00**	**0.94**	**0.00**	**1.25**	**0.00**	**0.62**	**0.94**	**1.25**	**0.94**	**0.62**	**1.25**	**0.62**	**0.00**	**9.06**
System 05																
Repetition 1	0.01	0.02	0.04	0.03	0.08	0.11	0.09	0.03	0.07	0.08	0.09	0.09	0.21	0.02	0.05	**1.02**
Repetition 2	0.10	0.02	0.08	0.02	0.07	0.10	0.09	0.07	0.03	0.08	0.00	0.00	0.10	0.05	0.05	**0.88**
Repetition 3	0.00	0.01	0.06	0.02	0.07	0.13	0.08	0.00	0.07	0.12	0.01	0.03	0.13	0.12	0.04	**0.90**
Repetition 4	0.08	0.04	0.09	0.08	0.08	0.05	0.09	0.01	0.15	0.11	0.09	0.04	0.18	0.06	0.04	**1.18**
Repetition 5	0.00	0.05	0.08	0.06	0.07	0.20	0.09	0.02	0.04	0.11	0.05	0.08	0.15	0.04	0.07	**1.10**
System 06																
Repetition 1	0.00	0.26	0.18	0.41	0.26	0.51	0.46	0.24	0.12	0.04	0.12	0.03	0.24	0.25	0.08	**3.19**
Repetition 2	0.00	0.23	0.24	0.32	0.31	0.54	0.51	0.31	0.24	0.22	0.01	0.03	0.26	0.24	0.08	**3.53**
Repetition 3	0.00	0.27	0.23	0.37	0.28	0.63	0.40	0.23	0.13	0.03	0.01	0.02	0.36	0.15	0.09	**3.21**
Repetition 4	0.01	0.22	0.21	0.41	0.28	0.61	0.43	0.30	0.15	0.04	0.11	0.05	0.27	0.24	0.10	**3.43**
Repetition 5	0.01	0.27	0.21	0.36	0.27	0.63	0.49	0.25	0.21	0.07	0.12	0.02	0.24	0.23	0.11	**3.49**
System 07																
Repetition 1	0.00	0.10	0.07	0.18	0.09	0.23	0.11	0.09	0.13	0.10	0.04	0.00	0.11	0.06	0.06	**1.38**
Repetition 2	0.00	0.12	0.06	0.22	0.09	0.22	0.12	0.08	0.09	0.02	0.04	0.04	0.09	0.06	0.06	**1.31**
Repetition 3	0.01	0.15	0.07	0.11	0.10	0.20	0.13	0.13	0.16	0.12	0.10	0.06	0.15	0.04	0.07	**1.60**
Repetition 4	0.00	0.12	0.06	0.16	0.08	0.19	0.13	0.06	0.05	0.04	0.01	0.03	0.06	0.01	0.06	**1.06**
Repetition 5	0.00	0.14	0.08	0.23	0.08	0.13	0.13	0.15	0.09	0.05	0.08	0.02	0.14	0.05	0.07	**1.42**
System 08																
Repetition 1	0.00	0.25	0.10	0.45	0.12	0.79	0.11	0.26	0.09	0.13	0.14	0.16	0.27	0.23	0.07	**3.18**
Repetition 2	0.00	0.32	0.06	0.48	0.10	0.70	0.12	0.27	0.06	0.12	0.13	0.16	0.26	0.26	0.07	**3.10**
Repetition 3	0.00	0.26	0.09	0.56	0.09	0.69	0.11	0.31	0.20	0.20	0.14	0.17	0.23	0.26	0.07	**3.38**
Repetition 4	0.08	0.33	0.07	0.48	0.11	0.79	0.10	0.30	0.20	0.24	0.14	0.15	0.26	0.17	0.12	**3.54**
Repetition 5	0.05	0.26	0.08	0.55	0.09	0.79	0.11	0.26	0.13	0.12	0.03	0.17	0.24	0.27	0.07	**3.23**

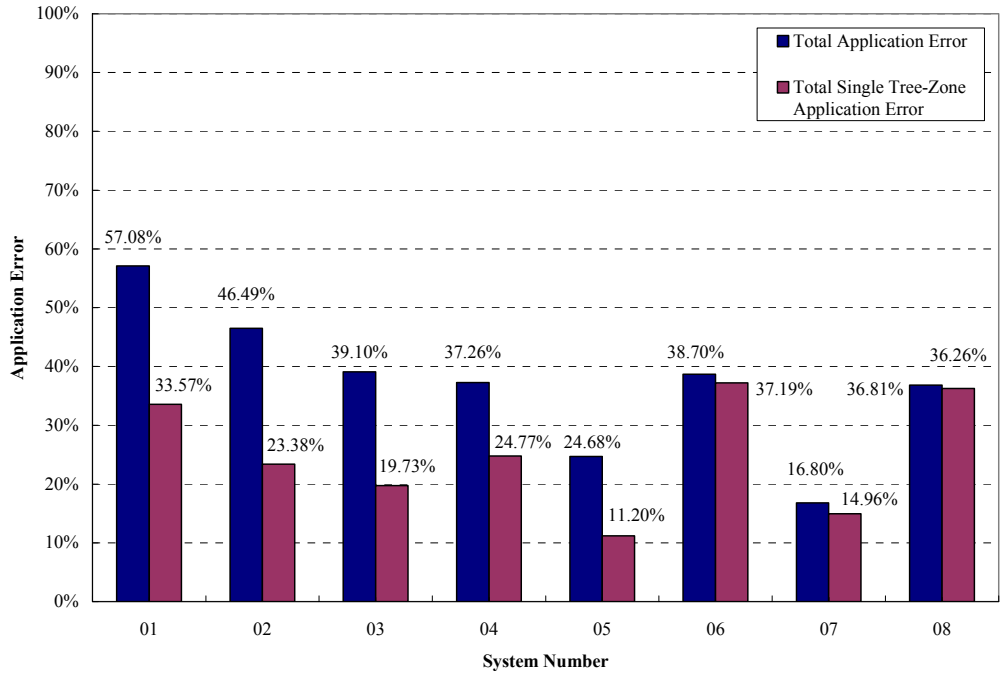

Figure 6-3. TAE and TSAE for the commercial systems expressed as a percentage of the total commanded fertilizer quantity.

ANOVA, at 95% confidence, was performed on TAE and TSAE in Table 6-3

calculated from the experimental datasets of the commercial system configurations listed

in Table 2-2. The errors were compared in kilograms and not as percentages noted previously in Figure 6-3. The results from the ANOVA concluded that there was significant difference in means of both the TAE and the TSAE of various commercial systems' configuration and therefore the null hypothesis was rejected in both the cases. Hence, Duncan's multiple range test was performed at 95% confidence to obtain all pairwise comparisons among the sample means of the TAE and TSAE datasets for the commercial controller systems.

Table 6-3. Data for ANOVA and Duncan's multiple-range test for the commercial controller systems.

	Total Application Error (kg)							
System Number →	**01**	**02**	**03**	**04**	**05**	**06**	**07**	**08**
Replication - 1	5.42	4.26	3.47	3.09	2.14	3.27	1.51	3.23
Replication - 2	5.50	4.02	3.43	2.53	2.16	3.65	1.47	3.15
Replication - 3	4.37	4.33	3.53	3.66	2.22	3.45	1.71	3.44
Replication - 4	5.36	4.22	3.63	3.80	2.36	3.56	1.34	3.54
Replication - 5	5.21	4.24	3.65	3.79	2.29	3.59	1.58	3.31
Mean TAE (kg) and Duncan Grouping [1]	5.17 a	4.21 b	3.54 c	3.38 c	2.24 d	3.51 c	1.52 e	3.34 c
CV (%)	8.88	2.77	2.78	16.41	4.03	4.23	9.06	4.78
	Total Single Tree Zone Application Error (kg)							
System Number →	**01**	**02**	**03**	**04**	**05**	**06**	**07**	**08**
Replication - 1	3.26	2.05	1.65	2.01	1.02	3.19	1.38	3.18
Replication - 2	3.17	2.39	1.76	1.27	0.88	3.53	1.31	3.10
Replication - 3	2.61	1.96	1.88	2.36	0.90	3.21	1.60	3.38
Replication - 4	3.10	2.13	1.88	2.68	1.18	3.43	1.06	3.54
Replication - 5	3.07	2.06	1.77	2.90	1.10	3.49	1.42	3.23
Mean TSAE (kg) and Duncan Grouping [1]	3.04 a	2.12 bc	1.79 c	2.24 b	1.02 d	3.37 a	1.36 d	3.29 a
CV (%)	8.37	7.70	5.36	28.54	12.68	4.64	14.53	5.29

[1] TAE and TSAE of the commercial controller systems with the same letter in Duncan Grouping are not significantly different ($\alpha = 0.05$).

Table 6-3 lists the results of the Duncan's multiple range test for both TAE and TSAE for the commercial systems. It is observed that there was not significant difference between the TAE of System Number 03, 04, 06 and 08. System Number 07 was the

lowest ranked for TAE criterion. On comparison of TSAE of the commercial systems, System Number 05 and 07 were not significantly different from each other and were the lowest ranked. Therefore it can be concluded that the commercial system with the Commercial controller module-1, proportional solenoid flow control valve and Encoder-1 had similar performance as compared to commercial controller module-2 with proportional solenoid flow control valve with Encoder-2 for TSAE criterion. System Number 07 had low error levels for both TAE and TSAE criteria and was selected as the best performing commercial system configuration for comparisons with experimental configurations.

Benchmarking of Commercial Controller Systems

Trigger Mode

The VRT controller configured with Commercial Controller Module-1, proportional solenoid flow control valve and Encoder-1, was triggered in GPS (System Number 04) and real-time mode (System Number 05). These results are graphed in Figure 6-4. It was observed that the delay in the response of the controller was longer when triggered in GPS mode. This delay time is the sum of the delay time of the response of the proportional solenoid flow control valve and the inherent controller delay in response to generate the application rate change command.

The extended controller delay in GPS trigger mode can be attributed to the search algorithm that the controller implements to determine the application rate from the prescription map at a particular spatial location. However, this could not be substantiated as no information was available in this regard from the manufacturer. The time delay of the Commercial Controller Module-1, after subtracting for the proportional solenoid flow control valve delay time (0.04 s) noted in Table 4-2, averaged 0.38 s when operating in

GPS mode and 0.075 s when operating in real-time mode. In all of the above tests the GPS refresh rates were set at 5Hz. The effect of the change in GPS refresh rates was not studied but a 5 Hz rate is representative of current GPS units on mobile equipment which operate at 1 to 10 Hz.

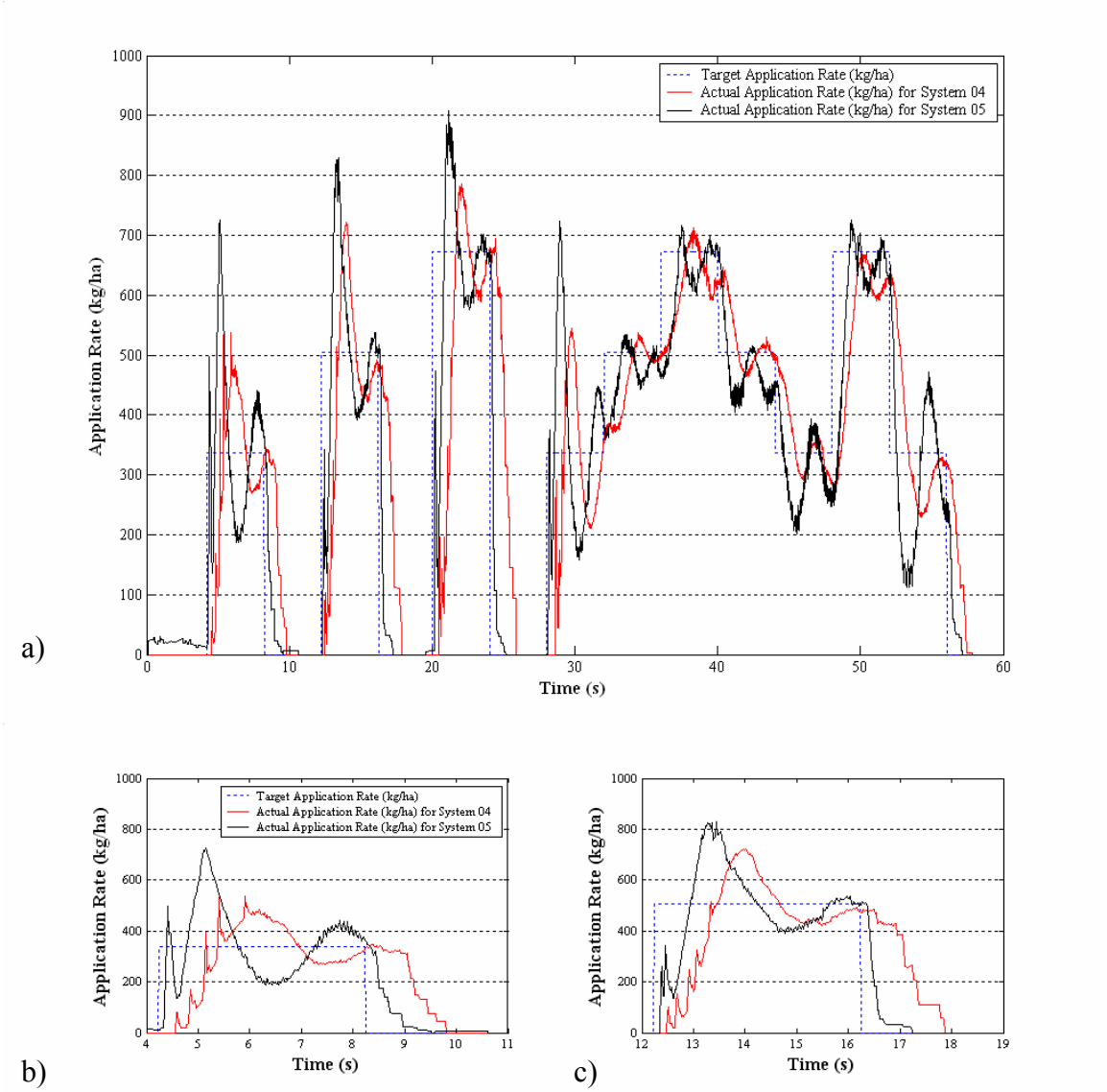

Figure 6-4. Commercial Controller-1 with system configurations 04 and 05 triggered in GPS and real-time mode. a) Complete test run. b) Step change from 0 to 336.24 kg/ha and c) Step change from 0 to 504.36 kg/ha.

The VRT controller configured with Commercial Controller Module-2, proportional solenoid flow control valve and Encoder-2 was triggered in both GPS

(System Number 06) and real-time mode (System Number 07). These results are plotted in Figure 6-5. The delay in the response was higher when the controller was triggered in GPS mode. The time delay of the Commercial Controller Module-2, after subtracting for the proportional solenoid flow control valve delay time (0.04 s), as listed in Table 4-2, was found to average 1.145 s when operating in GPS mode and, in real-time mode, only 0.14 s.

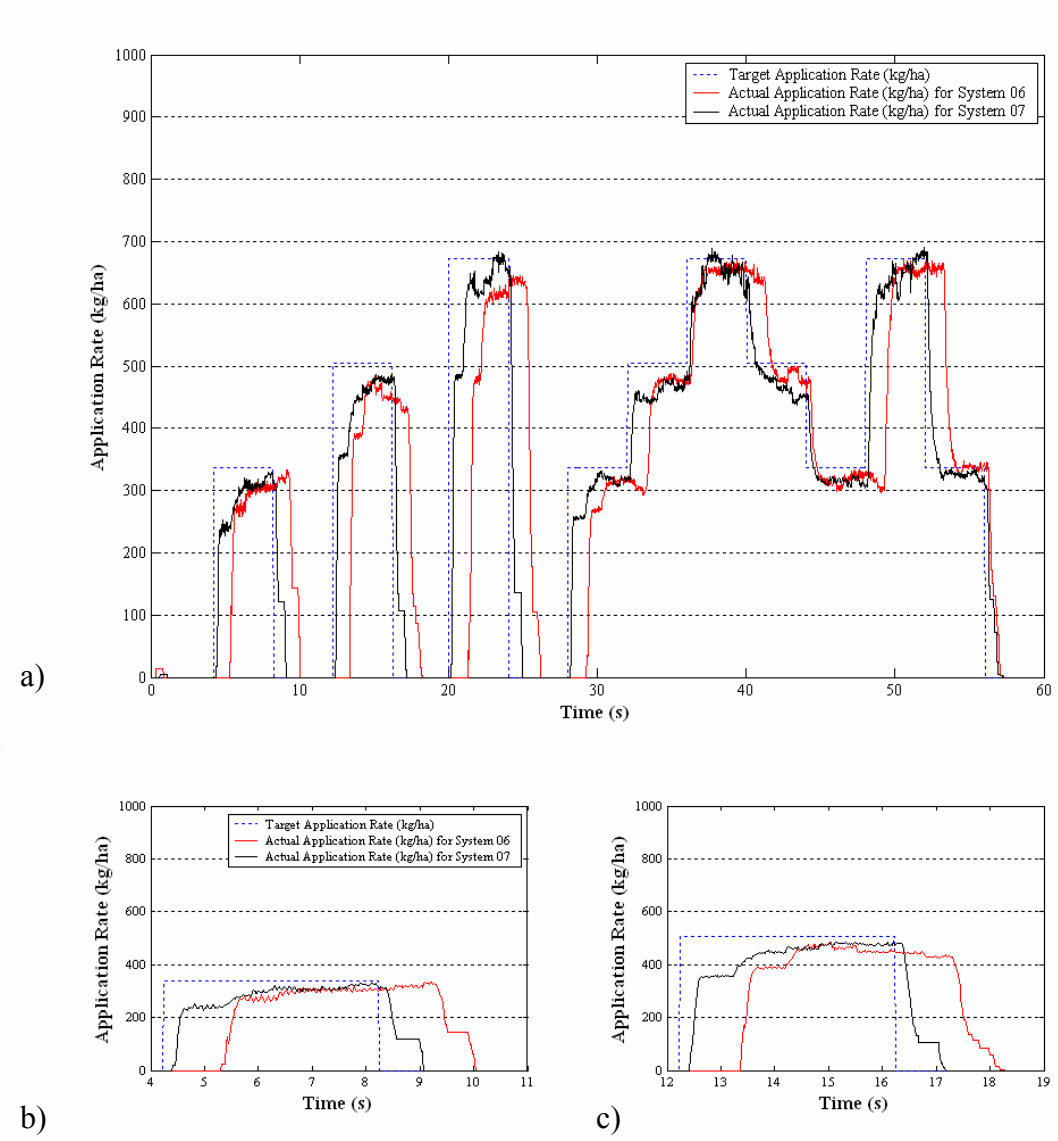

Figure 6-5. Commercial Controller-2 with system configurations 06 and 07 triggered in GPS and real-time mode. a) Complete test run. b) Step change from 0 to 336.24 kg/ha and c) Step change from 0 to 504.36 kg/ha.

Delay time in real-time trigger mode for Commercial Controller Module-2 (0.14 s) was 0.065 s (0.14 s − 0.075 s) greater than the delay time of Commercial Controller Module-1 (0.075 s). The delay time of Commercial Controller Module-2 (1.145 s) was markedly greater than of Commercial Controller Module-1 (0.38 s). One possible reason is that the Commercial Controller Module-2 can be operated in the GPS triggered mode through external PDA running Farmworks software, interfaced on RS232 port of the controller. This additional communication between the controller and the PDA can produce a delay of 0.7 s (1.145 s − 0.38 s − 0.065 s) in the response. These types of initial delays can be compensated for by implementing the delay algorithm described in Chapter 5.

By evaluating Duncan's grouping (Table 6-3) for the TAE and TSAE criteria, the System Number 05, was ranked less than System Number 04, and System Number 07 was ranked less than System Number-06. Therefore the performances of commercial systems triggered by real-time sensors were superior compared to the same systems triggered by GPS.

GPS

Figure 6-6 depicts the performance of the systems triggered in GPS mode (System Number 02, 04 and 06). The longer initial delays in System Number 02 observed during the application rate change from 0 kg/ha (Figure 6-6 b and 6-6 c) are due to a design characteristic where the DC motor operated flow control valve has no flow during the first 3° of rotation. The Commercial Controller Module-1 in combination with the proportional solenoid flow control valve and Encoder-1 provided the best performance when operating in GPS triggered mode.

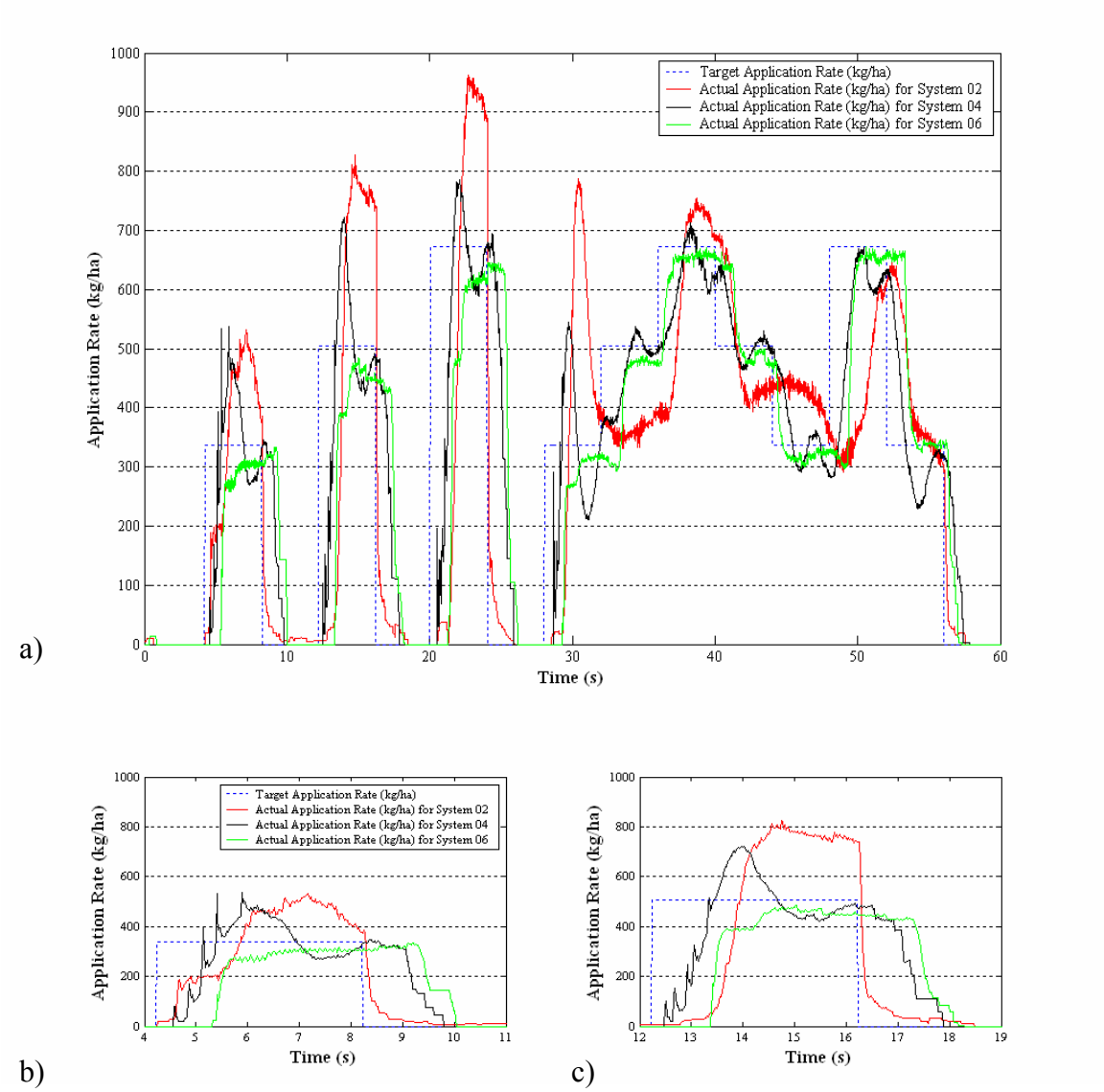

Figure 6-6. Performance comparison of systems 02, 04 and 06 triggering in GPS mode. a) Complete test run. b) Step change from 0 to 336.24 kg/ha and c) Step change from 0 to 504.36 kg/ha.

Real-time

Figure 6-7 a-c are plots of the performance of the systems triggered in real-time mode. It can be again observed that the DC motor operated flow control valve stem has no flow during the first 3° of rotation (Figure 4-14). On comparison of the Duncan's grouping for TAE and TSAE, System Number 07 had significantly better performance (Table 6-3).

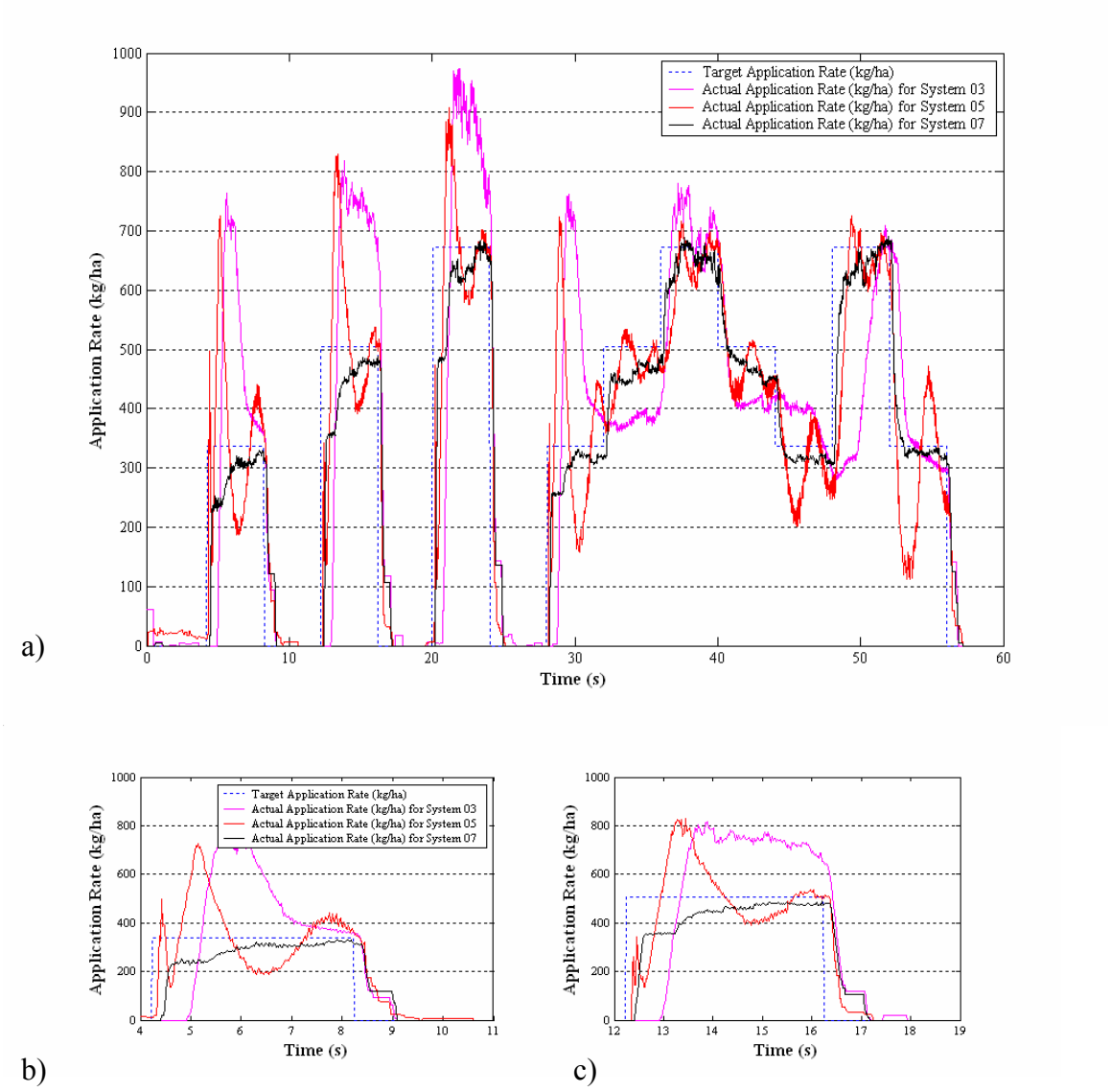

Figure 6-7. Performance comparison of systems 03, 05 and 07 triggering in real-time mode. a) Complete test run. b) Step change from 0 to 336.24 kg/ha and c) Step change from 0 to 504.36 kg/ha.

Flow Control Valves

The only components different when configuring System Number 03 and 05 were the flow control valves. This comparison (Figure 6-8) proved that the proportional solenoid flow control valve's performance was better than DC motor operated flow control valve. A lower initial valve delay time and shorter time constant (Table 4-2) contributed to the better performance of the proportional solenoid flow control valve.

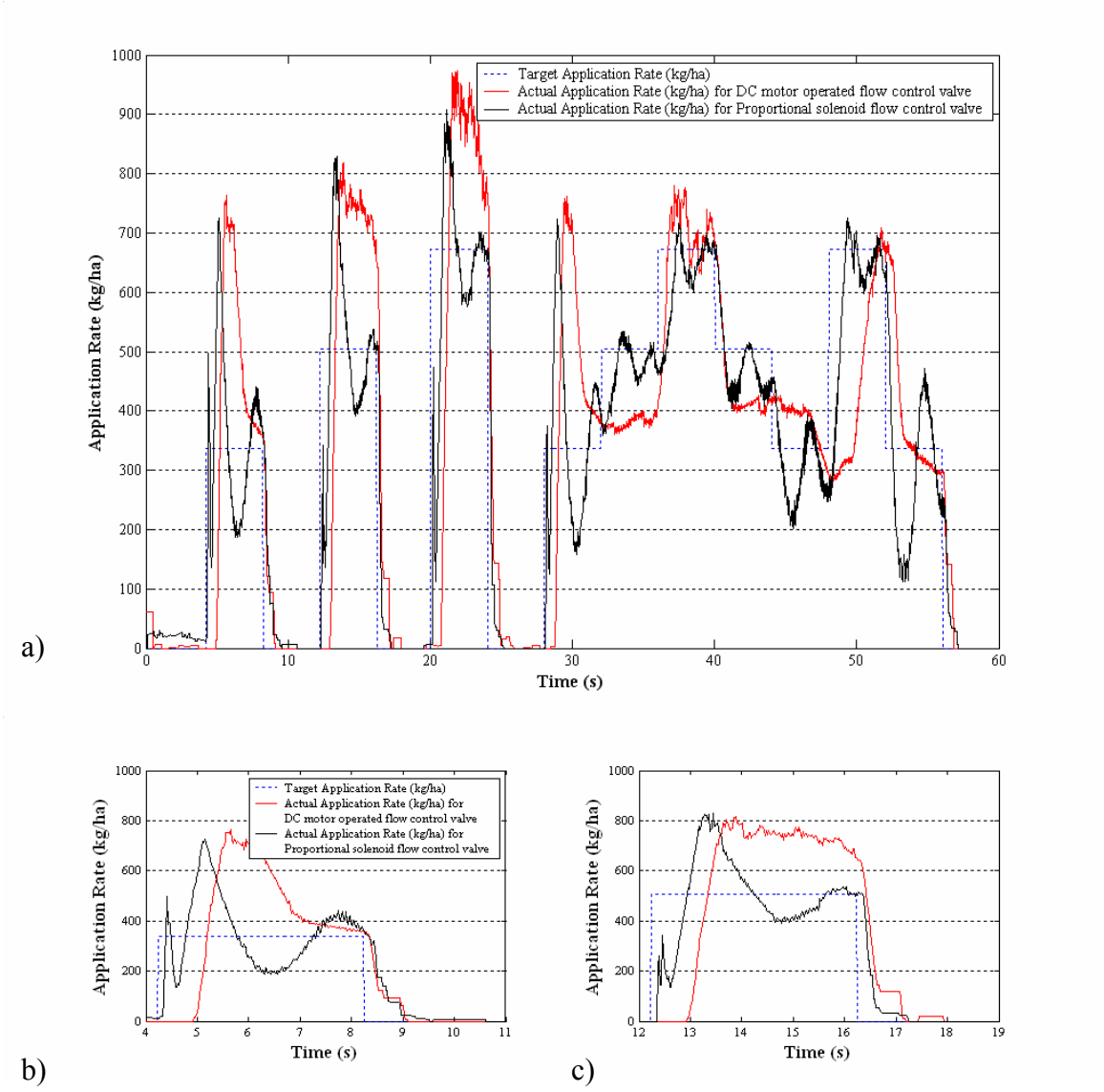

Figure 6-8. Performance comparison of the two flow control valves. a) Complete test run. b) Step change from 0 to 336.24 kg/ha and c) Step change from 0 to 504.36 kg/ha.

TAE of 39.10% for System Number 03 and 24.68% for System Number 05 indicated a 36% improvement in performance with the proportional solenoid flow control valve. The TSAE of 19.73% for System 03 and 11.20% for System 05 (Figure 6-3) provided results indicating that performance of the proportional solenoid flow control valve was better by 43%. System Number 05 was significantly better (Table 6-3) than System Number 03 in the Duncan's multiple range test for both TAE and TSAE criteria.

Encoders

These tests were performed using the Commercial Controller Module-2 and the proportional solenoid flow control valve. When Encoder-2 was used the System configuration was assigned System Number 07 and when Encoder-1 was used the configuration was assigned System Number 08. Again by observing the TAE and TSAE, 1.52 kg and 1.36 kg, respectively for System Number 07 and 3.34 kg and 3.28 kg, respectively for System Number 08, it was concluded that higher encoder resolution had a positive effect on the performance of the system. System Number 07 and 08 were significantly different in the Duncan's multiple range test and System Number 07 was ranked lesser than System Number 08 for both TAE and TSAE criteria. However, it is important that the encoder resolution be chosen such that the time required to have enough encoder counts to accurately measure the motor-gearbox combination's lowest shaft speed is less than the time required for execution of a single control loop.

A system with the configuration Encoder-1 (67 p/rev), along with the proportional solenoid flow control valve (time constant of 0.024 s and delay time of 0.04 s) is considered as an example. When System Number 08 was commanded in an open loop, to a flowrate of 6 L/min from 0 L/min, the system requires approximately 0.1 s to reach this state. The speed of the motor-gearbox combination shaft at this point would be 2.7 rev/min. Therefore, the Encoder-1 will generate a pulse train with a frequency of 2.96 Hz $\left(\frac{2.7\times 67}{60}\right)$. If the control loop was being executed at a rate of 50 Hz, it would be only after approximately 17 control loop executions that the controller obtains the first feedback pulse from the encoder. Hence proper design in selecting encoder resolution is

critical. The encoder should provide at least one pulse for every execution of the control loop at the lowest operating speed of the split conveyor chain roller.

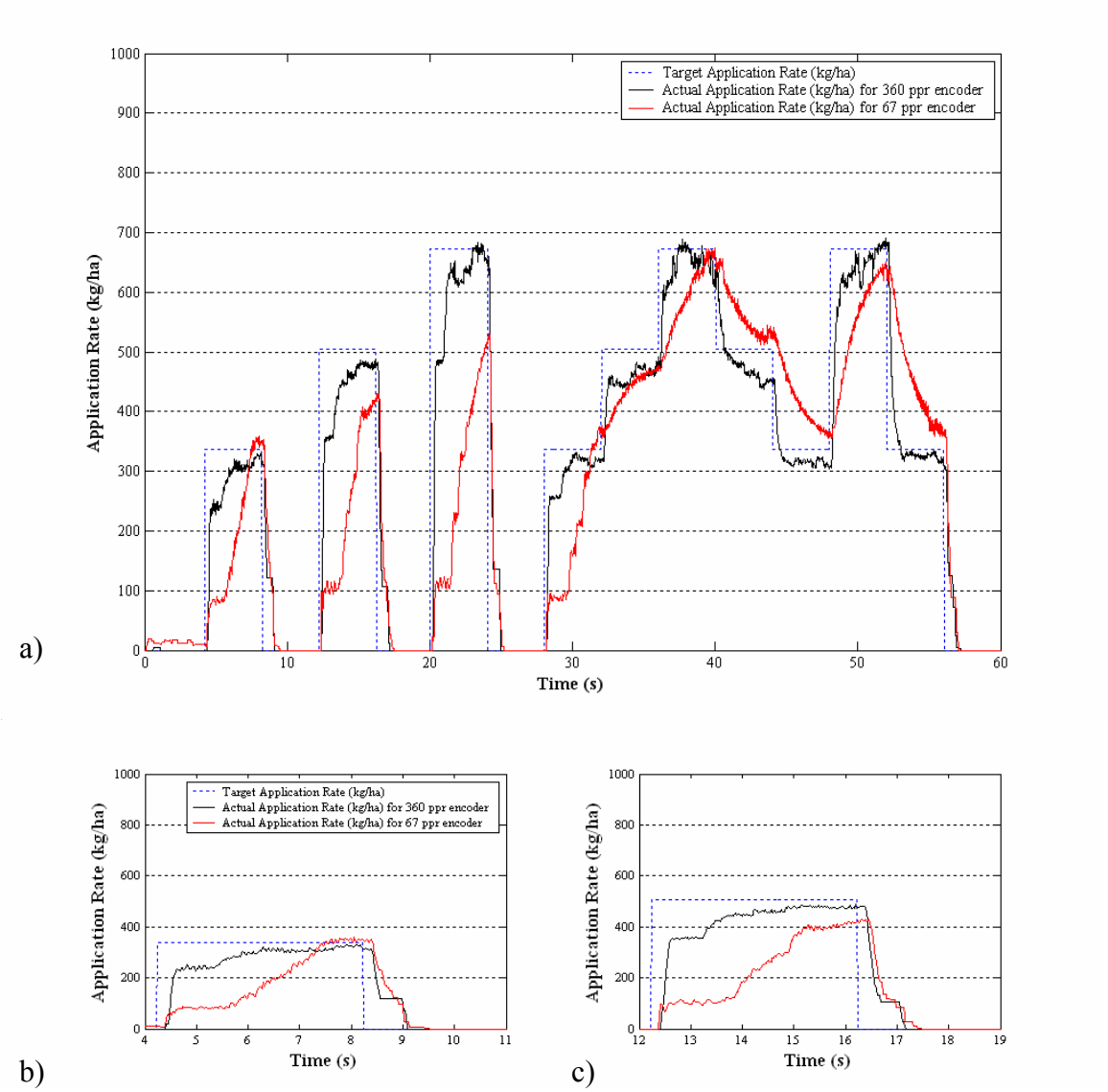

Figure 6-9. Performance comparison of the two encoders (System 07 and 08). a) Complete test run. b) Step change from 0 to 336.24 kg/ha and c) Step change from 0 to 504.36 kg/ha.

Commercial Controller Modules

A comparison of the performance (Figure 6-10) of System Number 05 and 08 showed that the TAE was 2.24 kg and 1.02 kg respectively for System Number 05 and 3.34 kg and 3.29 kg respectively for System Number 08. Hence, it can be inferred that

Commercial Controller Module-1 performed better. The performance result may also have measured the effect of the use of Encoder-1 (lower resolution) with Commercial Controller Module-2.

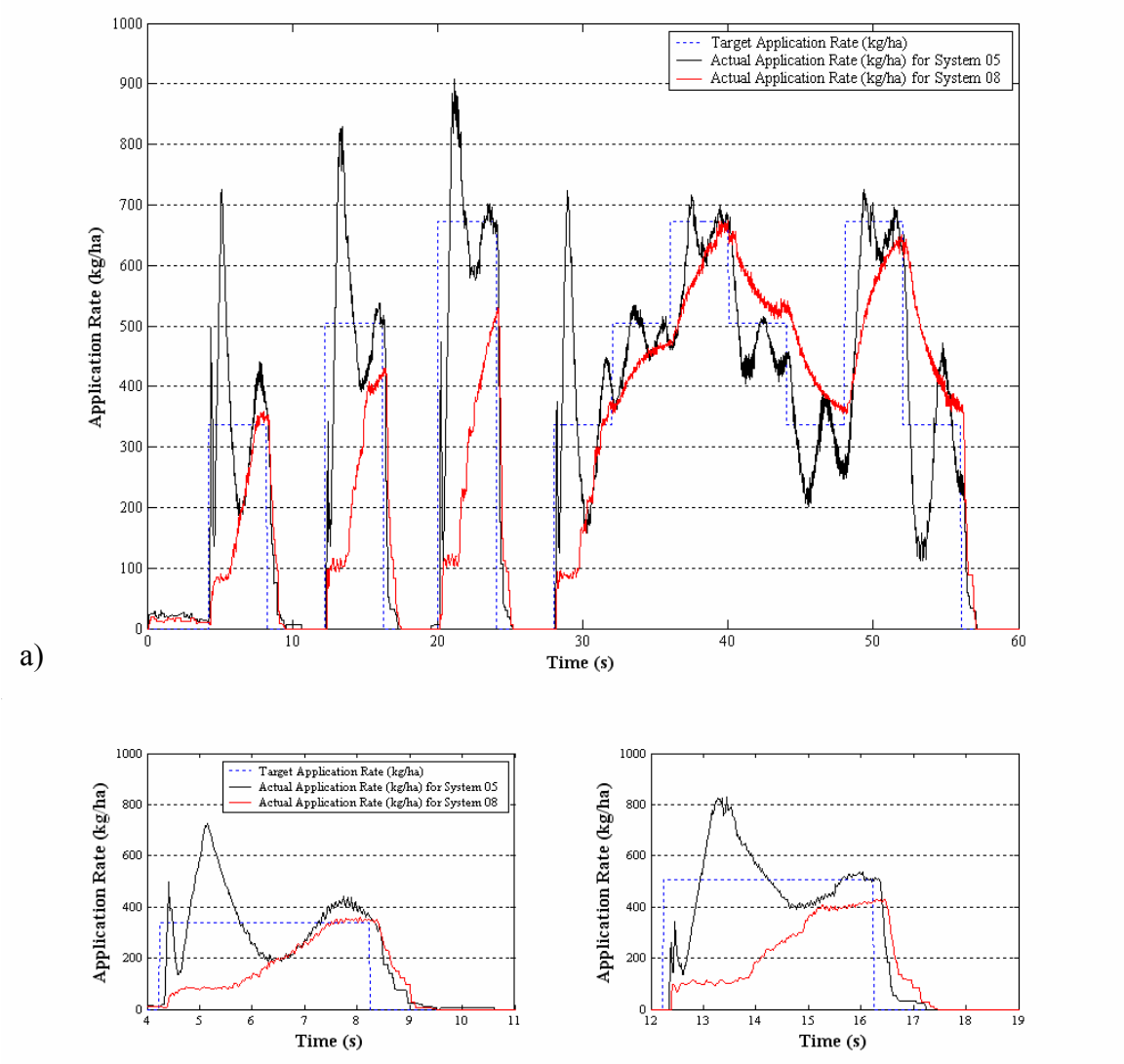

Figure 6-10. Performance comparison of the commercial controller modules (System 05 and 08). a) Complete test run. b) Step change from 0 to 336.24 kg/ha and c) Step change from 0 to 504.36 kg/ha.

However, in order to confirm the above inference, another test run with a new configuration with the Commercial Controller Module-1, proportional solenoid flow control valve and Encoder-2 should be performed to completely understand the

interaction of using Encoder-1 with Commercial Controller Module-2 in System Number 08.

Model Based PID Controllers

A total of six tuning rules were proposed to develop a model based PID controller to control the proportional solenoid flow control valve. The PID gains obtained from these six tuning rules were incorporated into the LabView PID controller. Five replications of the experiment for each of the six tuning rules (Table 5 -3 and 5-4) were conducted as detailed in the previous chapter. Tables 6-4 and 6-5 summarize the TAE and the TSAE for five repetitions of the experiment for all six PID tuning rules.

Table 6-4. TAE for the LabView PID controller using tuning rules from Tables 5-3 and 5-4.

Commanded Application-Rate (kg/ha)	**0.00**	**336.24**	**0.00**	**504.36**	**0.00**	**672.48**	**0.00**	**336.24**	**504.36**	**672.48**	**504.36**	**336.24**	**672.48**	**336.24**	**0.00**	**Total (kg)**
Commanded quantity of fertilizer (kg)	**0.00**	**0.62**	**0.00**	**0.94**	**0.00**	**1.25**	**0.00**	**0.62**	**0.94**	**1.25**	**0.94**	**0.62**	**1.25**	**0.62**	**0.00**	**9.06**
PID Tuning Rule	**Application Error (kg) ↓**															
Rule 01																
Repetition 1	0.00	0.06	0.04	0.04	0.07	0.07	0.13	0.04	0.03	0.03	0.03	0.02	0.03	0.04	0.08	**0.71**
Repetition 2	0.00	0.05	0.03	0.06	0.06	0.04	0.07	0.05	0.04	0.03	0.02	0.03	0.04	0.04	0.06	**0.62**
Repetition 3	0.00	0.04	0.05	0.04	0.06	0.06	0.06	0.04	0.03	0.03	0.02	0.02	0.03	0.04	0.03	**0.56**
Repetition 4	0.01	0.06	0.04	0.05	0.06	0.06	0.05	0.05	0.03	0.03	0.03	0.04	0.03	0.04	0.06	**0.64**
Repetition 5	0.00	0.05	0.04	0.05	0.05	0.06	0.08	0.04	0.03	0.03	0.03	0.03	0.03	0.04	0.03	**0.59**
Rule 02																
Repetition 1	0.00	0.06	0.03	0.04	0.04	0.07	0.06	0.04	0.02	0.03	0.02	0.03	0.03	0.04	0.07	**0.58**
Repetition 2	0.00	0.05	0.11	0.06	0.07	0.05	0.14	0.04	0.03	0.03	0.03	0.02	0.04	0.03	0.08	**0.78**
Repetition 3	0.00	0.03	0.09	0.05	0.10	0.05	0.06	0.05	0.03	0.03	0.03	0.03	0.04	0.03	0.05	**0.66**
Repetition 4	0.00	0.04	0.06	0.04	0.05	0.04	0.05	0.04	0.03	0.03	0.03	0.03	0.04	0.04	0.04	**0.56**
Repetition 5	0.00	0.05	0.09	0.06	0.06	0.06	0.08	0.06	0.03	0.03	0.02	0.04	0.04	0.03	0.09	**0.76**
Rule 03																
Repetition 1	0.00	0.05	0.03	0.06	0.06	0.05	0.06	0.05	0.03	0.03	0.03	0.02	0.04	0.04	0.06	**0.61**
Repetition 2	0.00	0.04	0.03	0.04	0.04	0.06	0.06	0.04	0.03	0.03	0.03	0.03	0.04	0.04	0.03	**0.55**
Repetition 3	0.04	0.04	0.03	0.04	0.04	0.04	0.05	0.06	0.04	0.03	0.02	0.03	0.03	0.03	0.05	**0.58**
Repetition 4	0.00	0.04	0.04	0.05	0.05	0.06	0.05	0.05	0.04	0.03	0.03	0.03	0.04	0.04	0.03	**0.57**
Repetition 5	0.00	0.04	0.03	0.04	0.06	0.06	0.07	0.05	0.03	0.03	0.03	0.03	0.03	0.04	0.07	**0.61**
Rule 04																
Repetition 1	0.00	0.04	0.05	0.06	0.04	0.05	0.04	0.03	0.03	0.03	0.02	0.03	0.03	0.04	0.03	**0.51**
Repetition 2	0.00	0.03	0.03	0.04	0.06	0.05	0.05	0.04	0.03	0.03	0.02	0.03	0.04	0.03	0.07	**0.56**
Repetition 3	0.00	0.05	0.07	0.05	0.06	0.04	0.05	0.04	0.04	0.03	0.03	0.03	0.04	0.04	0.05	**0.63**
Repetition 4	0.01	0.06	0.03	0.05	0.07	0.06	0.07	0.03	0.03	0.04	0.02	0.03	0.04	0.03	0.03	**0.60**
Repetition 5	0.00	0.03	0.05	0.04	0.06	0.05	0.05	0.03	0.02	0.03	0.02	0.03	0.04	0.04	0.03	**0.52**
Rule 05																
Repetition 1	0.00	0.05	0.05	0.05	0.04	0.05	0.07	0.06	0.04	0.04	0.04	0.05	0.05	0.05	0.10	**0.73**
Repetition 2	0.00	0.05	0.05	0.06	0.04	0.06	0.09	0.06	0.05	0.04	0.04	0.05	0.05	0.04	0.04	**0.74**
Repetition 3	0.00	0.05	0.08	0.05	0.03	0.06	0.04	0.05	0.03	0.03	0.03	0.03	0.03	0.04	0.04	**0.58**
Repetition 4	0.00	0.06	0.04	0.06	0.04	0.06	0.05	0.05	0.03	0.04	0.03	0.04	0.04	0.04	0.04	**0.63**
Repetition 5	0.00	0.05	0.03	0.06	0.08	0.05	0.06	0.06	0.04	0.03	0.03	0.04	0.04	0.04	0.08	**0.70**
Rule 06																
Repetition 1	0.00	0.05	0.05	0.07	0.04	0.07	0.07	0.07	0.06	0.03	0.04	0.04	0.04	0.04	0.04	**0.71**
Repetition 2	0.00	0.11	0.03	0.08	0.08	0.05	0.11	0.09	0.04	0.04	0.03	0.03	0.03	0.05	0.03	**0.82**
Repetition 3	0.00	0.16	0.03	0.06	0.06	0.07	0.05	0.11	0.06	0.03	0.03	0.03	0.05	0.09	0.03	**0.86**
Repetition 4	0.00	0.08	0.03	0.05	0.04	0.06	0.12	0.06	0.04	0.03	0.03	0.03	0.03	0.09	0.04	**0.74**
Repetition 5	0.00	0.05	0.04	0.04	0.12	0.06	0.06	0.20	0.04	0.04	0.03	0.04	0.04	0.05	0.04	**0.85**

Table 6-5. TSAE for the LabView PID controller using various tuning rules from Tables 5-3 and 5-4.

Commanded Application-Rate (kg/ha)	**0.00**	**336.24**	**0.00**	**504.36**	**0.00**	**672.48**	**0.00**	**336.24**	**504.36**	**672.48**	**504.36**	**336.24**	**672.48**	**336.24**	**0.00**	**Total (kg)**
Commanded quantity of fertilizer (kg)	**0.00**	**0.62**	**0.00**	**0.94**	**0.00**	**1.25**	**0.00**	**0.62**	**0.94**	**1.25**	**0.94**	**0.62**	**1.25**	**0.62**	**0.00**	**9.06**
PID Tuning Rule	**Single Tree-Zone Application Error (kg) ↓**															
Rule 01																
Repetition 1	0.00	0.01	0.04	0.00	0.07	0.01	0.13	0.00	0.00	0.00	0.00	0.00	0.00	0.01	0.08	**0.35**
Repetition 2	0.00	0.00	0.03	0.01	0.06	0.00	0.07	0.01	0.00	0.00	0.01	0.00	0.00	0.01	0.06	**0.26**
Repetition 3	0.00	0.00	0.05	0.00	0.06	0.00	0.06	0.00	0.00	0.01	0.00	0.00	0.00	0.01	0.03	**0.23**
Repetition 4	0.01	0.00	0.04	0.00	0.06	0.00	0.05	0.00	0.00	0.00	0.00	0.00	0.00	0.01	0.06	**0.25**
Repetition 5	0.00	0.01	0.04	0.01	0.05	0.01	0.08	0.00	0.00	0.00	0.01	0.00	0.00	0.01	0.03	**0.25**
Rule 02																
Repetition 1	0.00	0.02	0.03	0.00	0.04	0.01	0.06	0.00	0.00	0.00	0.00	0.00	0.00	0.01	0.07	**0.25**
Repetition 2	0.00	0.01	0.11	0.02	0.07	0.01	0.14	0.00	0.00	0.00	0.00	0.00	0.01	0.01	0.08	**0.47**
Repetition 3	0.00	0.00	0.09	0.01	0.10	0.01	0.06	0.00	0.00	0.00	0.00	0.00	0.00	0.01	0.05	**0.34**
Repetition 4	0.00	0.00	0.06	0.00	0.05	0.00	0.05	0.00	0.00	0.00	0.00	0.00	0.01	0.01	0.04	**0.24**
Repetition 5	0.00	0.01	0.09	0.01	0.06	0.01	0.08	0.02	0.00	0.01	0.00	0.00	0.00	0.01	0.09	**0.42**
Rule 03																
Repetition 1	0.00	0.00	0.03	0.01	0.06	0.01	0.06	0.00	0.00	0.00	0.00	0.00	0.01	0.01	0.06	**0.26**
Repetition 2	0.00	0.00	0.03	0.00	0.04	0.00	0.06	0.00	0.00	0.00	0.00	0.00	0.00	0.01	0.03	**0.20**
Repetition 3	0.04	0.00	0.03	0.00	0.04	0.00	0.05	0.02	0.01	0.00	0.00	0.00	0.00	0.01	0.05	**0.25**
Repetition 4	0.00	0.00	0.04	0.01	0.05	0.00	0.05	0.01	0.00	0.01	0.00	0.00	0.01	0.01	0.03	**0.22**
Repetition 5	0.00	0.00	0.03	0.00	0.06	0.00	0.07	0.00	0.00	0.00	0.00	0.00	0.00	0.01	0.07	**0.25**
Rule 04																
Repetition 1	0.00	0.01	0.05	0.01	0.04	0.00	0.04	0.00	0.00	0.00	0.00	0.00	0.01	0.01	0.03	**0.20**
Repetition 2	0.00	0.00	0.03	0.00	0.06	0.00	0.05	0.00	0.00	0.00	0.00	0.00	0.01	0.01	0.07	**0.24**
Repetition 3	0.00	0.00	0.07	0.00	0.06	0.00	0.05	0.00	0.00	0.01	0.01	0.00	0.00	0.01	0.05	**0.28**
Repetition 4	0.01	0.02	0.03	0.00	0.07	0.00	0.07	0.01	0.00	0.01	0.01	0.00	0.00	0.01	0.03	**0.27**
Repetition 5	0.00	0.01	0.05	0.00	0.06	0.01	0.05	0.00	0.00	0.00	0.00	0.00	0.00	0.01	0.03	**0.23**
Rule 05																
Repetition 1	0.00	0.00	0.05	0.00	0.04	0.00	0.07	0.00	0.00	0.00	0.01	0.00	0.01	0.01	0.10	**0.29**
Repetition 2	0.00	0.00	0.05	0.00	0.04	0.00	0.09	0.00	0.00	0.00	0.00	0.00	0.01	0.01	0.04	**0.27**
Repetition 3	0.00	0.00	0.08	0.00	0.03	0.01	0.04	0.00	0.00	0.00	0.00	0.00	0.00	0.01	0.04	**0.23**
Repetition 4	0.00	0.01	0.04	0.00	0.04	0.00	0.05	0.00	0.00	0.00	0.00	0.00	0.00	0.01	0.04	**0.21**
Repetition 5	0.00	0.00	0.03	0.01	0.08	0.00	0.06	0.01	0.00	0.00	0.00	0.00	0.01	0.01	0.08	**0.30**
Rule 06																
Repetition 1	0.00	0.00	0.05	0.02	0.04	0.01	0.07	0.02	0.01	0.00	0.00	0.00	0.01	0.01	0.04	**0.30**
Repetition 2	0.00	0.05	0.03	0.03	0.08	0.00	0.11	0.02	0.00	0.01	0.01	0.00	0.00	0.01	0.03	**0.39**
Repetition 3	0.00	0.07	0.03	0.01	0.06	0.01	0.05	0.05	0.02	0.00	0.00	0.00	0.01	0.02	0.03	**0.37**
Repetition 4	0.00	0.01	0.03	0.00	0.04	0.00	0.12	0.00	0.00	0.00	0.00	0.00	0.00	0.02	0.04	**0.28**
Repetition 5	0.00	0.00	0.04	0.00	0.12	0.00	0.06	0.12	0.00	0.01	0.00	0.00	0.01	0.02	0.04	**0.42**

Analysis

The average of TAE and TSAE of all six tuning rules are compared in Figure 6-11. It was observed that the error measurement of all six tuning rules varied by very small values, between 6.22% and 8.75% for TAE and between 2.61% and 3.87% for TSAE. The average errors for the model-based tuning rules are expressed as a percentage of the total commanded fertilizer quantity.

ANOVA was performed at 95% confidence on the two datasets (TAE and TSAE) listed in Table 6-7. The errors were compared in kilograms and not as percentages noted in Figure 6-11. The results from the ANOVA indicated a significant difference in means of both the TAE and the TSAE of the commercial system and the null hypothesis was rejected for both the criteria. Hence, Duncan's multiple range test was performed at 95%

confidence to obtain all pair wise comparisons among the sample means of the TAE and TSAE datasets for the model-based PID controller systems.

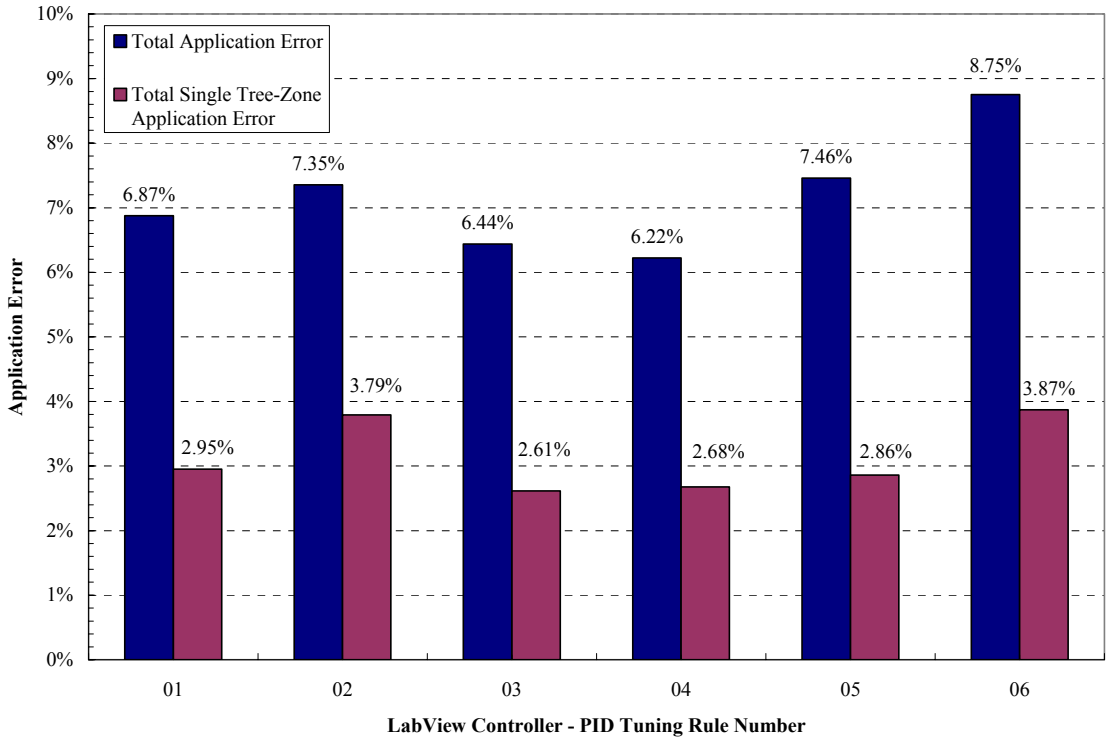

Figure 6-11. TAE and TSAE for the LabView Controller, implementing PID Tuning rules, expressed as a percentage of the total commanded fertilizer quantity.

Table 6-6 lists the results of the Duncan's multiple range test for both TAE and TSAE for the model-based PID controller systems. It can be observed that the Tuning Rule 03 and 04 were ranked the lowest for TAE criterion and Tuning Rule 01, 05, 04 and 03 were ranked the lowest for TSAE criterion. Model-based PID Tuning Rule 03 was ranked the lowest for both TAE and TSAE criteria and had the lowest variance and therefore designated as the best performing model-based PID controller system configuration.

The configuration with LabView implemented controller (LabView Controller-1) with the PID gains obtained from Tuning Rule 03, controlling the proportional solenoid

flow control valve with the feedback from Flowmeter-2 is referred to as System Number 09 from Table 2-2.

Table 6-6. Data for ANOVA and Duncan's multiple range test for the model-based PID controller tuning rules.

	Total Application Error (kg)					
PID tuning Rule →	**01**	**02**	**03**	**04**	**05**	**06**
Replication - 1	0.71	0.58	0.61	0.51	0.73	0.71
Replication - 2	0.62	0.78	0.55	0.56	0.74	0.82
Replication - 3	0.56	0.66	0.58	0.63	0.58	0.86
Replication - 4	0.64	0.56	0.57	0.60	0.63	0.74
Replication - 5	0.59	0.76	0.61	0.52	0.70	0.85
Mean TAE (kg) and Duncan Grouping [a]	0.62 bc	0.67 b	0.58 bc	0.56 c	0.68 b	0.79 a
CV (%)	9.44	15.21	4.81	8.94	10.00	8.58
	Total Single Tree Zone Application Error (kg)					
Replication - 1	0.35	0.25	0.26	0.20	0.29	0.30
Replication - 2	0.26	0.47	0.20	0.24	0.27	0.39
Replication - 3	0.23	0.34	0.25	0.28	0.23	0.37
Replication - 4	0.25	0.24	0.22	0.27	0.21	0.28
Replication - 5	0.25	0.42	0.25	0.23	0.30	0.42
Mean TSAE (kg) and Duncan Grouping [1]	0.27 b	0.34 a	0.23 b	0.24 b	0.26 b	0.35 a
CV (%)	17.99	29.54	10.09	12.04	15.56	16.88

[a] TAE and TSAE of the model-based PID controller systems with the same letter in Duncan Grouping are not significantly different ($\alpha = 0.05$).

Simulation

The Simulation Toolkit of the LabView software was used to conduct all simulations. The experiment explained previously in Chapter 5 to verify the PID control tuning rules was simulated. The values of the PID controller parameters obtained from the best performing tuning rule in Table 5-2 were substituted in the simulation and the data were acquired. Figure 6-12 is the snapshot of the simulation screen. Data were collected for the commanded flowrate and the simulated flowrate. The above data were converted to commanded and actual application rates using Equation 2.1 for further analysis assuming the vehicle speed to be 1.34 m/s, swath width to be 3.81 m, fertilizer

density as 1031 kg/m^3, chain roller diameter as 0.10 m, chain width and gate height as 0.25 m and 0.047 m respectively. Table 6-7 lists the Application Error and the Single Tree-Zone Application Error calculated for each rate change in the test run.

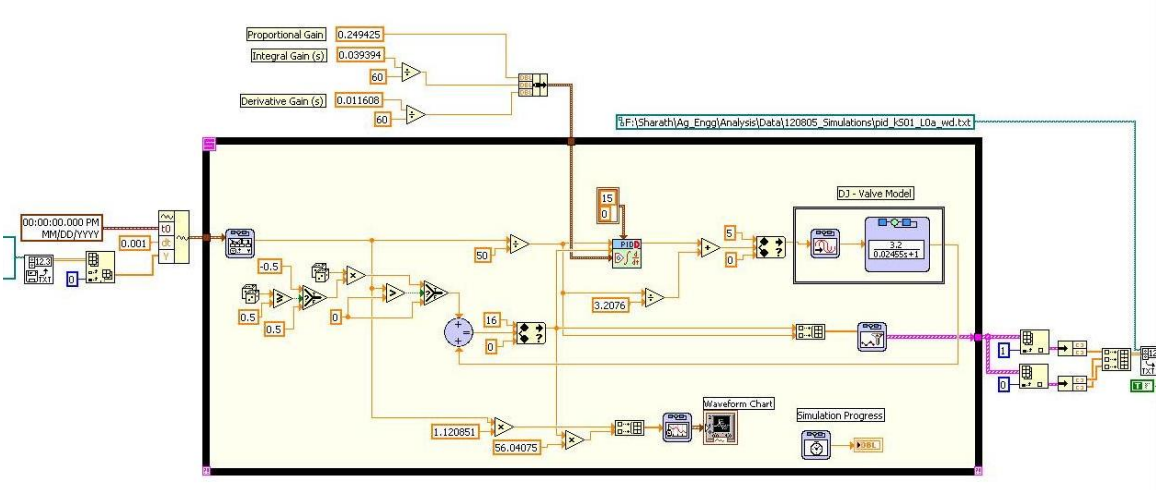

Figure 6-12. Screenshot of the PID controller simulation program. (LabView Simulation Toolkit).

Table 6-7. Simulated and experimental Application Error and Single Tree-Zone Application Error for Tuning Rule 03.

	Application Error (kg)														
Commanded Application-Rates (kg/ha)	**0**	**336.24**	**0**	**504.36**	**0**	**672.48**	**0**	**336.24**	**504.36**	**672.48**	**504.36**	**336.24**	**672.48**	**336.24**	**0**
Simulated	0.00	0.02	0.01	0.03	0.01	0.04	0.01	0.02	0.01	0.01	0.00	0.00	0.01	0.01	0.01
Experimental (average)	0.01	0.04	0.03	0.05	0.05	0.05	0.06	0.05	0.03	0.03	0.03	0.03	0.04	0.04	0.05
	Single Tree-Zone Application Error (kg)														
Commanded Application-Rates (kg/ha)	**0**	**336.24**	**0**	**504.36**	**0**	**672.48**	**0**	**336.24**	**504.36**	**672.48**	**504.36**	**336.24**	**672.48**	**336.24**	**0**
Simulated	0.00	0.01	0.01	0.01	0.01	0.01	0.01	0.01	0.00	0.00	0.00	0.00	0.00	0.01	0.01
Experimental (average)	0.01	0.00	0.03	0.00	0.05	0.00	0.06	0.01	0.00	0.00	0.00	0.00	0.00	0.01	0.05

Figure 6-13 are resultant plots of the simulation performed for the PID controller with gains obtained from the Tuning Rule 03. The simulation generated a data point for every 0.001 s. The experimental errors compiled in Table 6-7 are an average of five

repetitions of the test (Table 6-4 and 6-5) for the PID controller with gains determined from Tuning Rule 03.

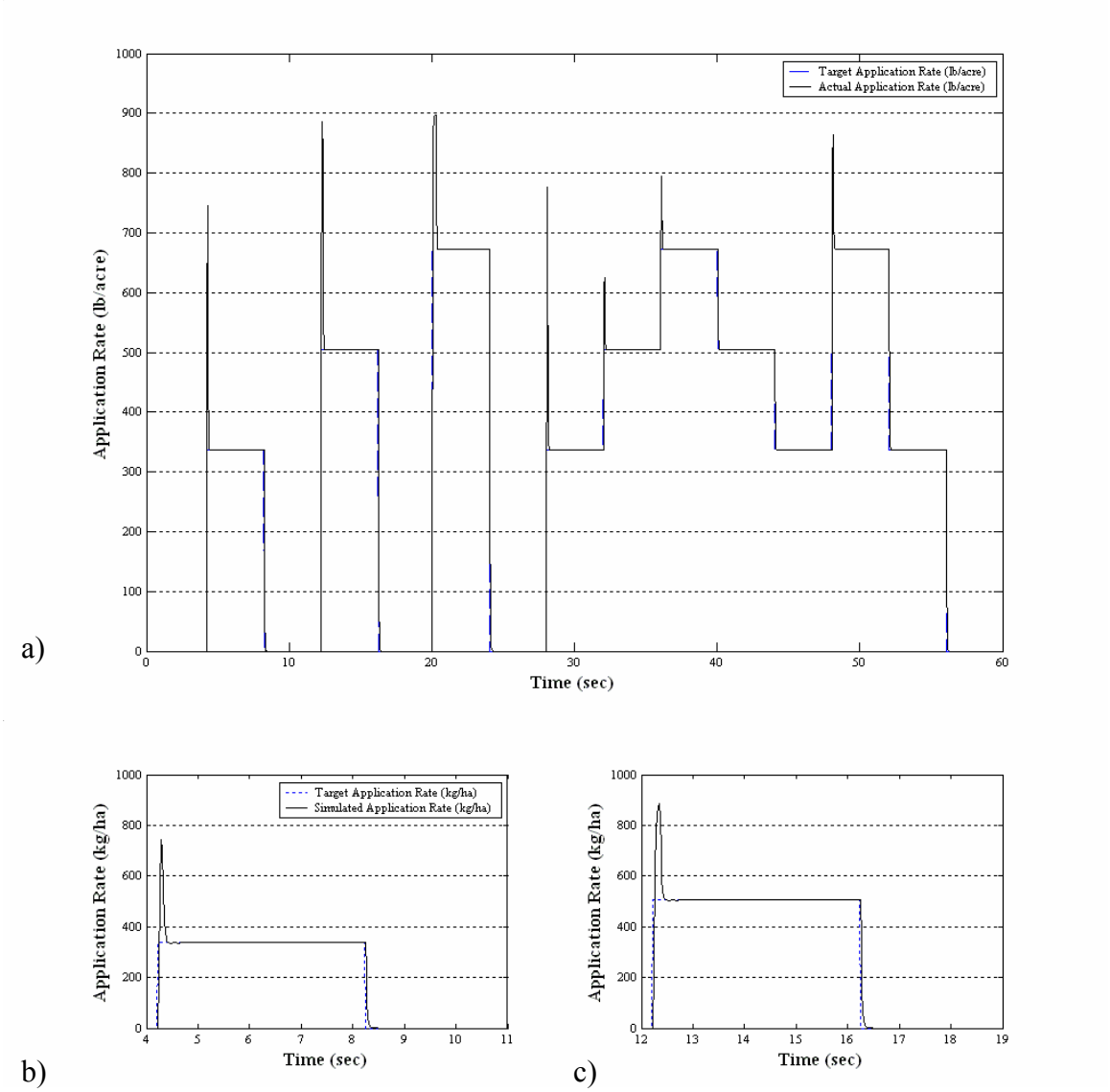

Figure 6-13. Simulation results for model-based PID controller implementing Tuning Rule 03. a) Complete test run. b) Step change from 0 to 336.24 kg/ha and c) Step change from 0 to 504.36 kg/ha.

The experimental Application Error (kg) for each application-rate change in the test run with the PID Tuning Rule 03 was plotted against the simulation Application Error (kg) (Figure 6-13) determined in Table 6-9 excluding the application rate changes

to 0 kg/ha. The relationship between the simulation and experimental Application Error was defined by the equation:

Experimental Application Error = 0.6943× (Simulated Application Error) + 0.0286 (6.3)

The R^2 value for this linear fit was found to be 0.85. Similar comparison was made between the experimental and the simulated Single Tree-Zone Application Error. However, the relationship between the simulated and the experimental Single Tree-Zone Application Error exhibited a poor linear relationship, $R^2 = 0.16$.

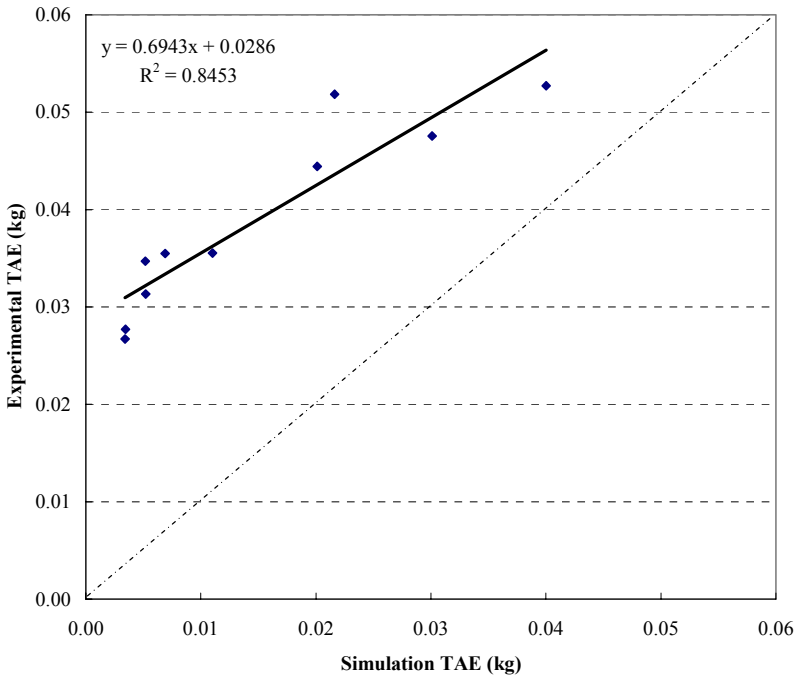

Figure 6-14. Plot of simulation TAE vs. experimental TAE for 10 tree zones, excluding zero kg/ha application rate, in the test run for PID controller implementing Tuning Rule 03.

Commercial Controller vs. Model based PID Controller

Proportional Solenoid Flow Control Valve

The performance of the LabView implemented model based PID controller system with the best performing commercial system was compared. System Number 07 in Table 2-2 had the least TAE (Figure 6-3) with respect to all other commercial system configuration and hence considered to be the best performing commercial controller configuration. Figure 6-15 depicts the performance of the commercial controller and the model based PID controller. From Figure 6-16, the TAE and the TSAE were 6.44% and 2.61% for the model based PID controller as compared to 16.80% and 14.96% for the commercial controller respectively.

Hence, the model based PID controller performed markedly better than the commercial controllers currently available. On comparison using TAE and TSAE, the model-based PID controller performed 62% and 82.5% better than the commercial controller with the same system configuration. Similar performance may be achieved by implementing a proper auto-tune algorithm or by further gain adjustment of the Commercial Controller Module-2.

Delay Algorithm Implementation: The experimental results for delay algorithm explained in the previous chapter are shown below. This algorithm in conjunction with the PID controller was used to compensate for the sensor offset distances, various delay times and varying travel speed of the applicator. The results in Figure 6-17 are presented in terms of flowrates. The application rates at these flowrates and vehicle speed can be calculated using the Equation 2.2. In Figure 6-17 it can be observed that the control algorithm compensates the delay time and the flowrate proportional to the speed of the vehicle.

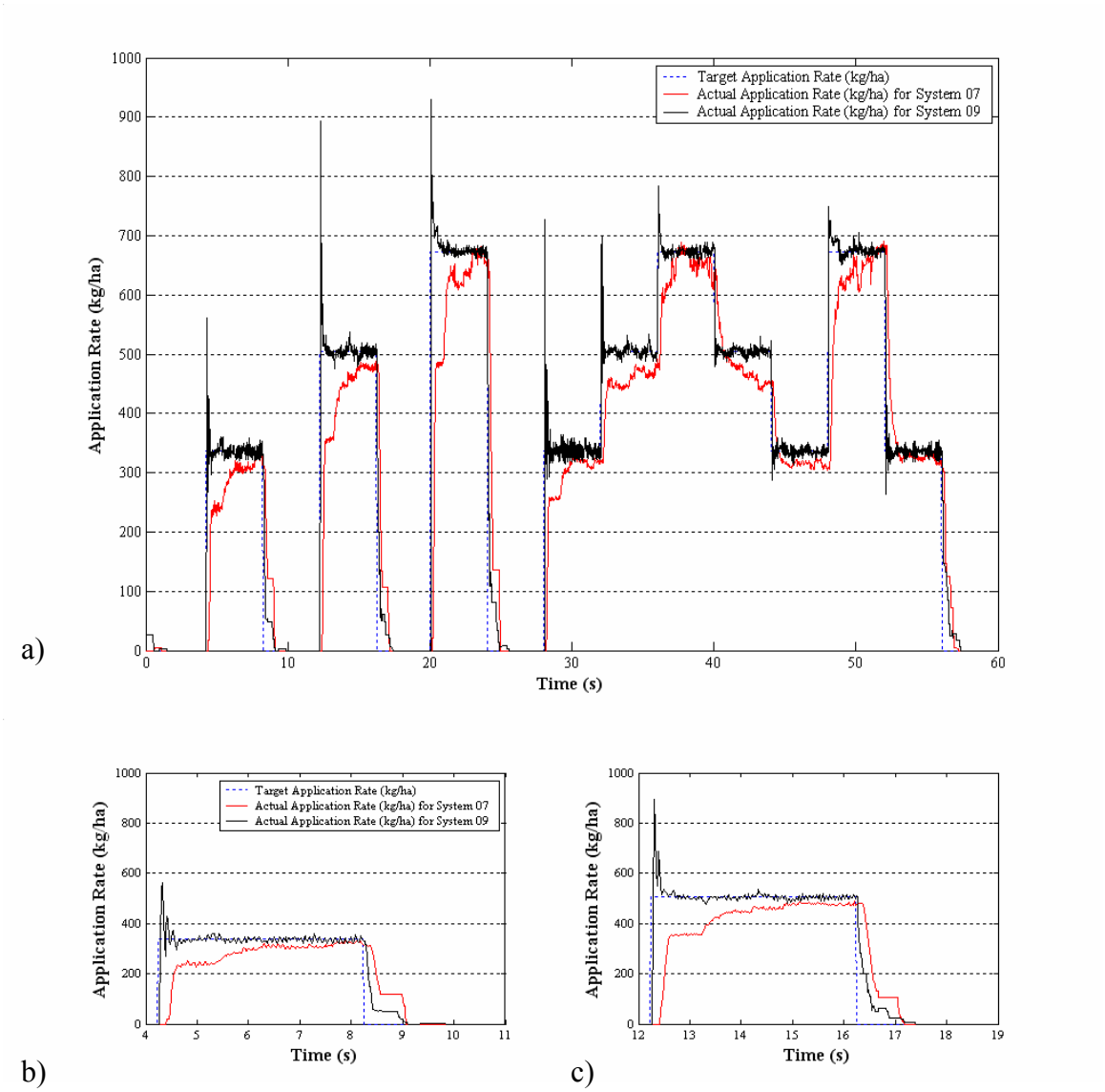

Figure 6-15. Performance comparison of the best performing commercial controller (System 07) versus LabView Controller-1 (System 09) for the proportional solenoid valve control. a) Complete test run. b) Step change from 0 to 336.24 kg/ha and c) Step change from 0 to 504.36 kg/ha.

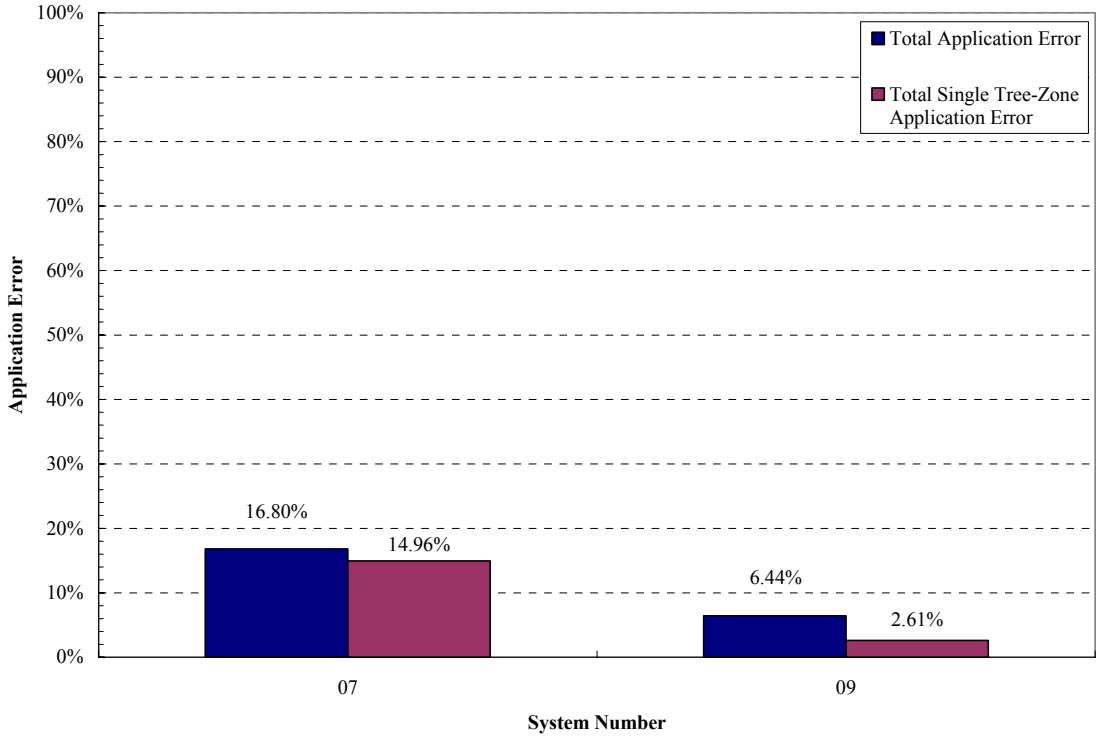

Figure 6-16. Comparison of the performance of the model-based PID controller with best performing commercial controller.

The commanded and the actual application rate calculated from Equation 2.2 are plotted versus the distance traveled in Figure 6-18. Also, the control algorithm changes to the new commanded application rate after the vehicle has traveled 2 m into the application zone. This was due to the real-time sensor's offset of 2 m. Provision was made in the control algorithm to measure the current vehicle speed for compensation implemented for every control loop execution. No comparative studies could be made with a commercial controller as the commercial controllers do not have an adaptive 'look-ahead' feature which compensates for distance offset, velocity and mechanical-pneumatic response time.

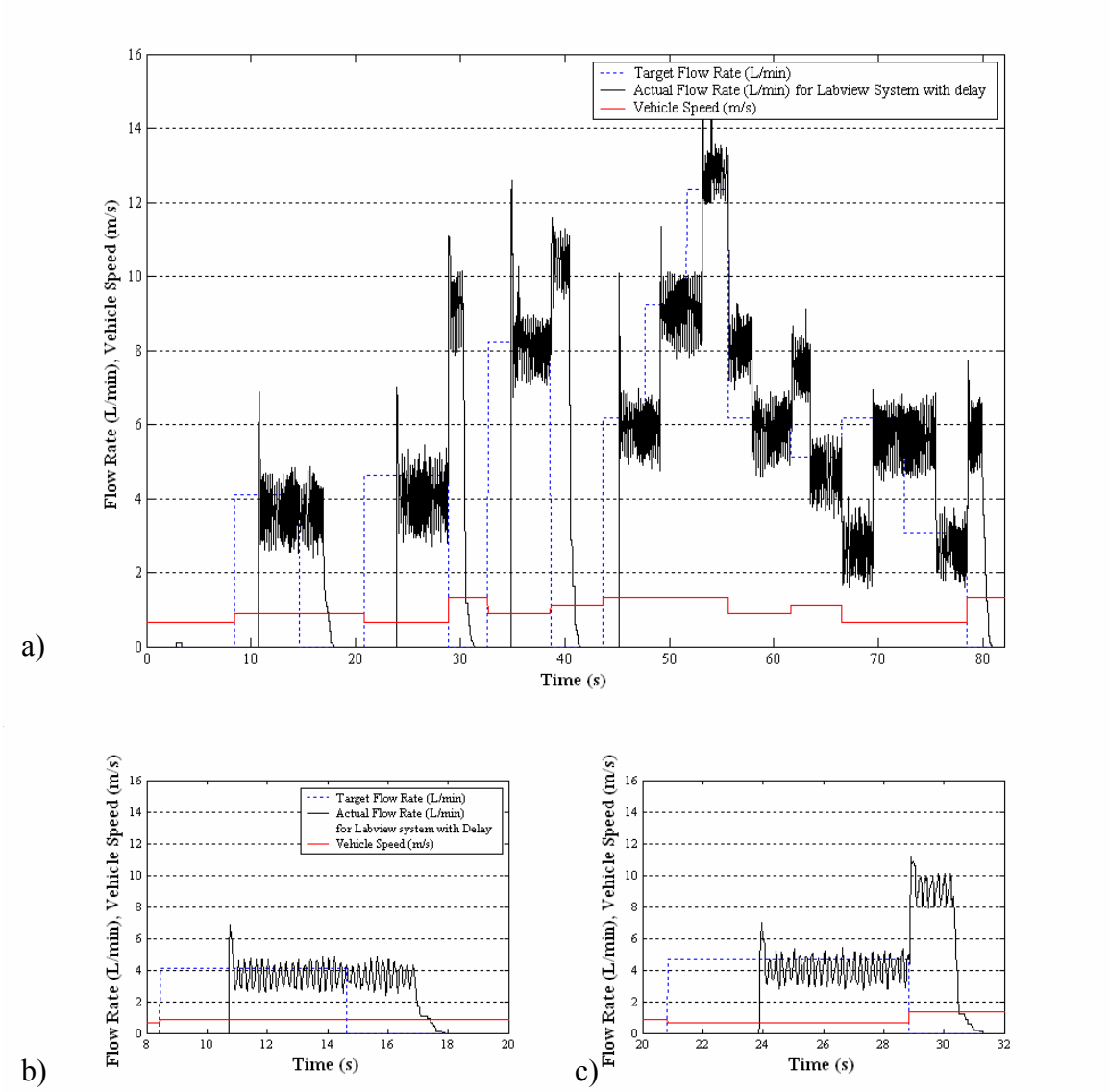

Figure 6-17. Target and actual flowrate and the vehicle speed. a) Complete test run. b) Step change from 0 to 336.24 kg/ha and c) Step change from 0 to 504.36 kg/ha.

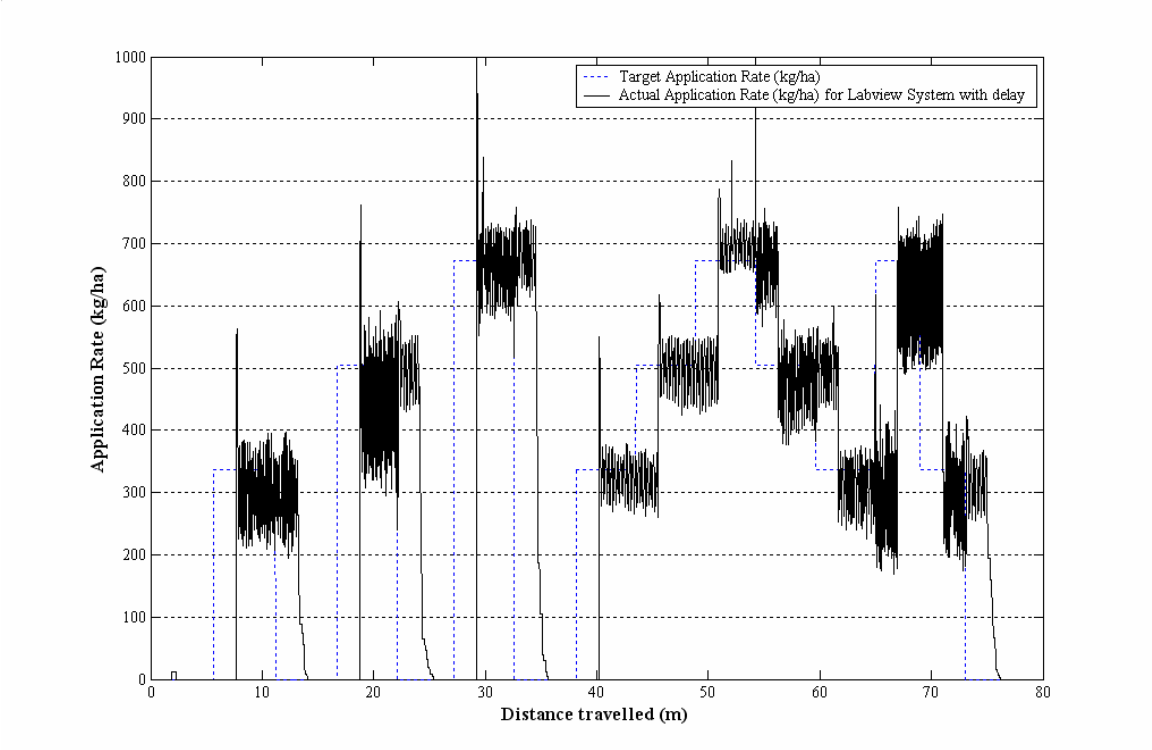

Figure 6-18. Commanded and target application-rate incorporating the delay times, sensor offsets and speed compensation.

DC Motor Operated Flow Control Valve

Results of the implementation of a simple control algorithm to control the DC motor operated flow control valve in comparison to the equivalent commercial controller system are shown in Figure 6-19. The commercial controller system was System Number 03 from Table 2-2. The configuration with the LabView controller controlling the DC motor operated flow control valve with feedback from the Flowmeter-2 was designated as System Number 10.

Table 6-8 detail the TAE and the TSAE of five replications of the experiment described in Chapter 3. Figure 6-20 illustrates the performance improvement achieved by implementing the LabView controller over the commercial controller. The TAE and the Single Tree-Zone Application Error were calculated as 39.1% and 14.53%, respectively

for the commercial controller and 19.73% and 11.44%, respectively for the LabView controller.

Table 6-8. TAE and TSAE for System Number 03 and 10

Commanded Application-Rate (kg/ha)	**0.00**	**336.24**	**0.00**	**504.36**	**0.00**	**672.48**	**0.00**	**336.24**	**504.36**	**672.48**	**504.36**	**336.24**	**672.48**	**336.24**	**0.00**	**Total (kg)**
Commanded quantity of fertilizer applied (kg)	**0.00**	**0.62**	**0.00**	**0.94**	**0.00**	**1.25**	**0.00**	**0.62**	**0.94**	**1.25**	**0.94**	**0.62**	**1.25**	**0.62**	**0.00**	**9.06**
Application Error (kg) ↓																
System 03																
Repetition 1	0.00	0.35	0.05	0.55	0.13	0.58	0.13	0.38	0.19	0.13	0.21	0.06	0.50	0.18	0.06	**3.47**
Repetition 2	0.00	0.44	0.06	0.53	0.14	0.54	0.13	0.43	0.19	0.11	0.14	0.11	0.40	0.13	0.07	**3.43**
Repetition 3	0.00	0.36	0.06	0.53	0.11	0.53	0.14	0.42	0.26	0.13	0.18	0.12	0.45	0.17	0.07	**3.53**
Repetition 4	0.00	0.42	0.07	0.50	0.13	0.57	0.16	0.41	0.21	0.16	0.21	0.10	0.40	0.24	0.05	**3.63**
Repetition 5	0.09	0.38	0.06	0.50	0.08	0.59	0.13	0.36	0.30	0.18	0.17	0.14	0.40	0.20	0.06	**3.65**
System 10																
Repetition 1	0.00	0.09	0.07	0.14	0.10	0.20	0.13	0.10	0.04	0.04	0.04	0.03	0.07	0.09	0.07	**1.22**
Repetition 2	0.00	0.09	0.08	0.15	0.08	0.20	0.16	0.07	0.06	0.05	0.05	0.05	0.06	0.04	0.19	**1.33**
Repetition 3	0.02	0.10	0.06	0.17	0.11	0.21	0.14	0.11	0.04	0.04	0.05	0.05	0.08	0.05	0.05	**1.27**
Repetition 4	0.00	0.11	0.06	0.15	0.12	0.20	0.19	0.10	0.04	0.03	0.04	0.03	0.08	0.09	0.07	**1.31**
Repetition 5	0.00	0.10	0.08	0.14	0.21	0.19	0.21	0.09	0.03	0.05	0.05	0.05	0.07	0.07	0.11	**1.45**
Single Tree-Zone Application Error (kg) ↓																
System 03																
Repetition 1	0.00	0.08	0.05	0.13	0.13	0.01	0.13	0.11	0.19	0.03	0.17	0.02	0.49	0.06	0.06	**1.65**
Repetition 2	0.00	0.16	0.06	0.09	0.14	0.09	0.13	0.16	0.19	0.03	0.02	0.11	0.40	0.12	0.07	**1.76**
Repetition 3	0.00	0.09	0.06	0.08	0.11	0.10	0.14	0.14	0.26	0.05	0.08	0.09	0.44	0.15	0.07	**1.88**
Repetition 4	0.00	0.16	0.07	0.06	0.13	0.05	0.16	0.15	0.21	0.02	0.16	0.10	0.39	0.17	0.05	**1.88**
Repetition 5	0.09	0.10	0.06	0.11	0.08	0.00	0.13	0.09	0.30	0.04	0.12	0.14	0.39	0.06	0.06	**1.77**
System 10																
Repetition 1	0.00	0.08	0.07	0.12	0.10	0.18	0.13	0.09	0.02	0.02	0.01	0.00	0.04	0.04	0.07	**0.98**
Repetition 2	0.00	0.08	0.08	0.13	0.08	0.19	0.16	0.04	0.02	0.03	0.00	0.00	0.03	0.03	0.19	**1.06**
Repetition 3	0.02	0.08	0.06	0.12	0.11	0.17	0.14	0.08	0.02	0.02	0.00	0.01	0.04	0.04	0.05	**0.96**
Repetition 4	0.00	0.08	0.06	0.11	0.12	0.18	0.19	0.08	0.03	0.01	0.02	0.01	0.04	0.01	0.07	**1.00**
Repetition 5	0.00	0.08	0.08	0.12	0.21	0.18	0.21	0.08	0.02	0.00	0.01	0.02	0.04	0.05	0.11	**1.18**

From Figure 6-20 it was determined that the simple LabView control algorithm performed 50% better than the best performing commercial controller when TAE were evaluated and a 21% improvement when TSAE were compared.

It was found that significant improvement in the performance can be achieved by properly studying the dynamics of the components of the VRT systems and implementing model-based tuning rules for the PID controllers. Proper selection of the feedback sensor also contributed to increased performance of the system.

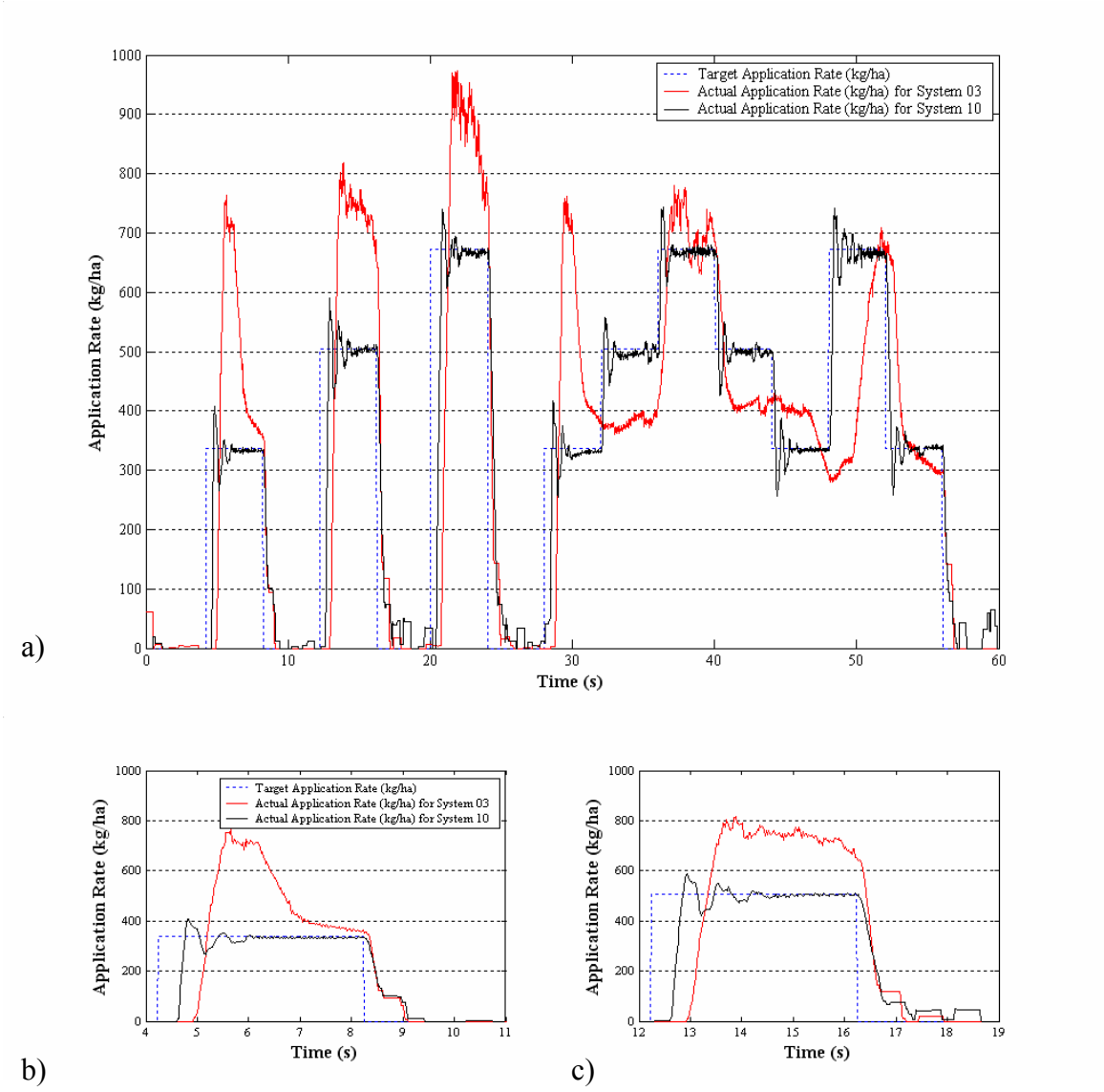

Figure 6-19. Performance comparison of the best performing commercial controller (System 03) versus LabView Controller-2 (System 10) with the proportional DC motor operated valve control. a) Complete test run. b) Step change from 0 to 336.24 kg/ha and c) Step change from 0 to 504.36 kg/ha.

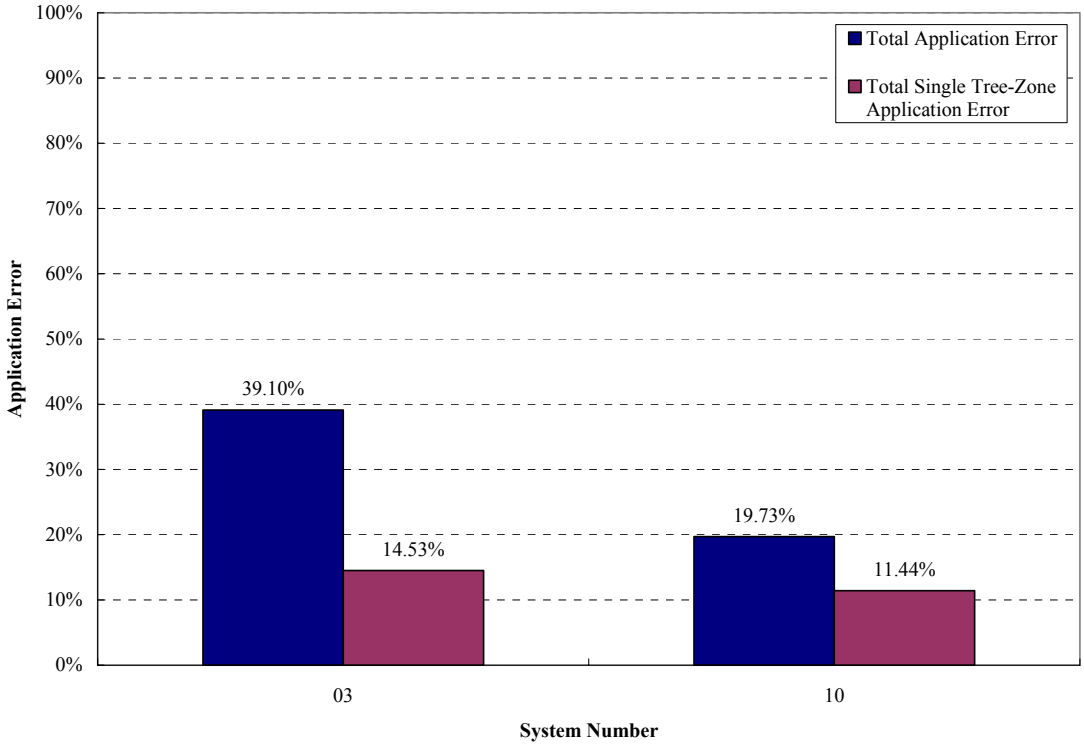

Figure 6-20. Comparison of the TAE and the TSAE for System Number 03 and 10.

Error Analysis

An attempt was made to estimate the overall accuracy in the performance of the VRT system which is comprised of individual components. It is assumed that the system was being operated using the PID controller module where the gains are obtained by the Tuning Rule 03. The application rate (kg/m^2) at any given point of the applicator is determined by Equation 2.1. The equation below is a representation of Equation 2.1 in units of kg/m^2,

$$\text{Application Rate} = \left(\frac{\omega \times h \times w \times \rho}{s \times v} \right) \tag{6.4}$$

where,

ω = Linear speed of the motor-gearbox shaft (m/s)

h = Gate height = 0.047 ± 0.001 m

w = Conveyor chain width = 0.25 ± 0.001 m

ρ =Fertilizer material density = 1031 ± 50 kg/m^3

s = Swath width = 3.81 ± 0.005 m

v = Speed of the applicator = 1.34 ± 0.05 m/s

The individual measurement accuracies for the gate height and conveyor chain width were assumed to be ± 0.001 m. However, this will be compensated by the controller when it is subjected to the calibration procedure. It was assumed that there is minimum interference from the tree canopy to the fertilizer particles exiting out of the applicator and that the speed of the spinner disc is stable enough to set the accuracy on the swath width to ± 0.005 m. The accuracy on the fertilizer material density was set to 50 kg/m^3 which is a commercial specification for the type of fertilizer being applied. The speed of the motor-gearbox combination in Equation 6.4 is defined by Equation 6.5. The accuracy on the speed of the motor-gearbox combination was explained in the following paragraph.

$$\omega = \pi \times k \times D \times q \tag{6.5}$$

where,

ω = Linear speed of the motor-gearbox shaft = 0.021 m/s

k = Gain of the hydraulic motor-gearbox combination = 0.44 ± 0.013 rev/L

D = Conveyor roller diameter = 0.1 ± 0.001 m

q = Flowrate input = 0.15 ± 0.007 L/s

The term ω was calculated to be at 0.021 m/s for an application-rate of 504.36 kg/ha. The gain on the hydraulic motor was the steady-state slope of 0.44 from Figure 4-5. The standard deviation of all the three steady-state slopes (all data, full load

and no load) in Figure 4-5 was assigned as the accuracy. The steady-state experimental data was observed for the Tuning Rule 03 and the standard deviation for the flowrate was calculated to be ± 0.007 L/s. This was the accuracy of the variable q in Equation6.5.

Various partial derivatives (Equations 6.6, 6.7and 6.8) were computed in Equation 6.5, to determine the sensitivity of application-rate to changes in each of the variables in the Equation 6.5.

$$\frac{\partial(\omega)}{\partial k} = \pi \times D \times q = \pi \times 0.15 \times 0.2 = 0.047 \ \frac{\text{m.L}}{\text{s}} \tag{6.6}$$

$$\frac{\partial(\omega)}{\partial D} = \pi \times k \times q = \pi \times 0.44 \times 0.2 = 0.21 \ \frac{\text{rev}}{\text{s}} \tag{6.7}$$

$$\frac{\partial(\omega)}{\partial q} = \pi \times k \times D = \pi \times 0.44 \times 0.1 = 0.14 \ \frac{\text{rev.m}}{\text{L}} \tag{6.8}$$

The absolute Error e_a (m/s) and total uncertainty u (m/s) are denoted by,

$$\pm e_a = (0.047 \times 0.013) + (0.21 \times 0.001) + (0.14 \times 0.007) = \pm 0.002 \ \frac{\text{m}}{\text{s}} \tag{6.8}$$

$$u = \sqrt{(0.047 \times 0.013)^2 + (0.21 \times 0.005)^2 + (0.14 \times 0.007)^2} = \pm 0.001 \ \frac{\text{m}}{\text{s}} \tag{6.9}$$

Now substituting the value for the accuracy (u) of ω and computing the partial derivatives of the variables in Equation 6.4,

$$\frac{\partial(ApplicationRate)}{\partial \omega} = \frac{h \times w \times \rho}{s \times v} = \frac{0.047 \times 0.25 \times 1031}{3.81 \times 1.34} = 2.37 \ \frac{\text{kg.s}}{\text{m}^3} \tag{6.11}$$

$$\frac{\partial(ApplicationRate)}{\partial h} = \frac{\omega \times w \times \rho}{s \times v} = \frac{0.021 \times 0.25 \times 1031}{3.81 \times 1.34} = 1.05 \ \frac{\text{kg}}{\text{m}^3} \tag{6.12}$$

$$\frac{\partial(ApplicationRate)}{\partial w} = \frac{\omega \times h \times \rho}{s \times v} = \frac{0.021 \times 0.047 \times 1031}{3.81 \times 1.34} = 0.20 \ \frac{\text{kg}}{\text{m}^3} \tag{6.13}$$

$$\frac{\partial(ApplicationRate)}{\partial \rho} = \frac{\omega \times h \times w}{s \times v} = \frac{0.021 \times 0.047 \times 0.25}{3.81 \times 1.34} = 0.000048 \text{ m} \tag{6.14}$$

$$\frac{\partial(ApplicationRate)}{\partial s} = \frac{\omega \times h \times w \times \rho}{s^2 \times v} = \frac{0.021 \times 0.047 \times 0.25 \times 1031}{3.81^2 \times 1.34} = 0.012 \ \frac{\text{kg}}{\text{m}^3} \quad (6.15)$$

$$\frac{\partial(ApplicationRate)}{\partial v} = \frac{\omega \times h \times w \times \rho}{s \times v^2} = \frac{0.021 \times 0.047 \times 0.25 \times 1031}{3.81 \times 1.34^2} = 0.04 \ \frac{\text{kg.s}}{\text{m}^3} \quad (6.16)$$

The absolute error for the application rate of the VRT system is denoted below.

$$\pm E_a = (2.37 \times 0.001) + (1.05 \times 0.001) + (0.20 \times 0.001) + (0.000048 \times 50) + (0.012 \times 0.005) + (0.04 \times 0.05)$$
$$= \pm 0.0083 \ \frac{\text{kg}}{\text{m}^2} = \pm 83.05 \ \frac{\text{kg}}{\text{ha}} \quad (6.17)$$

The uncertainty of the complete system is given by:

$$\pm U = \sqrt{(2.37 \times 0.001)^2 + (1.05 \times 0.001)^2 + (0.20 \times 0.001)^2 + (0.000048 \times 50)^2 + (0.0127 \times 0.005)^2 + (0.04 \times 0.05)^2}$$
$$= \pm 0.0042 \ \frac{\text{kg}}{\text{m}^2} = \pm 42.24 \ \frac{\text{kg}}{\text{ha}} \quad (6.18)$$

From the above analysis it was determined that the speed of the motor-gearbox combination has the greatest effect on the accuracy of the entire system. The second most important variable was the density of the fertilizer material. Hence it is necessary to control the speed of the conveyor chain to achieve minimal error in VRT fertilizer application.

CHAPTER 7
CONCLUSIONS AND FUTURE WORK

Commercial Controller Systems

- The present commercial controllers are not customized for citrus VRT fertilization. Features such as real-time sensor offset compensations for speed variations in the field are not currently available. The controllers operate with the assumption that the vehicle travels under a constant speed which is typically not the case on the field. As a result, the fertilizer material deposition will be offset from the correct spatial location in the field.

Benchmarking Tests

- A test procedure to benchmark the VRT systems' performance in both GPS and real-time trigger mode for all possible configurations of the commercial VRT systems and also for the model-based PID controllers was developed. Two performance criteria, the "Total Application Error" (TAE) and the "Total Single Tree-Zone Application Error" (TSAE) were proposed. TAE provides a better representation of the VRT system's response for the application rate change pattern, while the TSAE provides an indication of the VRT system's performance of overall application for each tree zone. Duncan's new multiple range tests were performed on the data for both TAE and TSAE criteria.

- The delay in the response of the controller was higher when triggered in GPS mode as compared the same system being triggered in the real-time mode. The controller delay in GPS trigger mode can be attributed to the search algorithm that the controller implement to determine the application rate from the prescription map at a particular spatial location. Commercial Controller Module-1 and Commercial Controller Module-2 had a delay of 0.38 s and 1.145 s respectively when triggered in GPS mode and a delay of 0.075 s and 0.14 s respectively when triggered in real-time mode.

- The performance of the proportional solenoid flow control valve was 36% better than the DC motor operated flow control valve for TAE and by 43% for TSAE.

- Encoder-2 (360 p/rev) was 54% and 58% better than Encoder-1 (67 p/rev) for TAE and TSAE criteria respectively.

- System Number 07 in Table 2-2 was determined to be the best performing commercial system by a Duncan's multiple range test. Commercial systems performed significantly different under different configurations. The commercial

system with Commercial Controller Module-2, proportional solenoid flow control valve, Encoder-2 and triggered by real-time sensing was the best while the commercial system with Commercial Controller Module-1, DC motor operated flow control valve with Encoder-1 and triggered by GPS had poorest performance for both TAE and TSAE criteria.

Dynamic Modeling of the Electro-hydraulic Components

- The steady-state speed response of the motor-gearbox combination for the commanded input was determined to be 0.44 rev/L for flowrates from 2 to 19 L/min. The response of the motor was adequate to reflect the changes in the flow rates induced in the system by the flow control valves. Loading of the conveyor chain had no effect on the performance of the motor-gearbox combination.

- The 2-way, 2-position solenoid flow control valve has a delay time (τ) of 0.4 s from issuing an open command signal until the flow response started, and a delay time (τ) of 0.036 s from issuing a close command signal until the flow response began.

- For the DC motor operated flow control valve, there was no flow output for the rotation of valve stem from 0° to 3°. The flow rate was found to be linear in the range of 3° to 10.5° of the rotation of valve stem. The DC motor operated flow control valve has a delay time (τ) of 0.08 s from issuing a command signal until the flow response starts. The near linear transient response after this initial delay was modeled as approximately first order with a time constant (T) of 0.09 s for a commanded step change of 3 L/min.

- For the proportional solenoid flow control valve, the flow rate was found to be linear in the range of 0 V to 5 V of the command signal. The proportional solenoid flow control valve has a delay time (τ) of 0.04 s from the issuing of a command signal until the flow response starts. The near linear transient response after this initial delay can be modeled as approximately first order with a time constant (T) of 0.024 s for a commanded step change of 3 L/min.

- The resolution of the encoder should be chosen such that the time required to have enough encoder counts to accurately measure the motor-gearbox combination's lowest shaft speed is less than the time required for execution of a single control loop.

Model Based PID Controller

- A total of six tuning rules were proposed to develop a model based PID controller to control the proportional solenoid flow control valve. Duncan's new multiple range test for both TAE and TSAE criteria indicated that PID Tuning Rule 03 provided the optimal PID control gain constants for the model based PID control implementation. Tuning Rule 06 had the poorest performance for both TAE and TSAE criteria.

- Performance comparison of the model based PID controller (System Number 09) with the best performing commercial controller (System Number 07) concluded that a reduction of 62% in TAE and 82% in TSAE can be achieved by implementing the model based PID controller.

- A linear fit, with $R^2 = 0.85$, was obtained between the simulation and experimental TAE values for the model based PID controller with gains obtained from Tuning Rule 03. It can be concluded that it was possible to predict the overall experimental TAE outcome of the PID controller implementation through simulation.

- The delay compensation algorithm in conjunction with the model based PID controller used to compensate for the sensor offset distances, other delays such as transport delays, valve delays and the varying travel speed of the applicator was demonstrated.

- In case of the DC motor operated flow control valve operation, a simple proportional speed control algorithm was implemented in LabView to control the position of the valve stem rotation. It was concluded that the TAE can be reduced by 50.5% compared to the best performing commercial controller by implementing this simple proportional speed control algorithm.

- The two most important variables whose accuracies had an effect on the application rate determined by error analysis were the conveyor chain speed and the density of the fertilizer material. Since density of the fertilizer material is an external factor which cannot be controlled the only other variable whose accuracy can be maximized is the conveyor chain speed by implementing better control algorithm.

Future Work

- A multi-variate control algorithm for speed and position control of the DC motor operated flow control valve can be implemented to compare its performance versus the controller proposed in the present study.

- Detailed study of delay times involved in the in transportation of the fertilizer material from the hopper onto the field needs to be studied so that it can be properly compensated for in the delay algorithm.

- Benchmarking tests to study effect of GPS refresh rates need to be conducted.

- The control of the spread pattern parallel to the direction of travel of the applicator was performed in this study. The spread pattern perpendicular to the direction of travel of the applicator can be controlled by the spinner discs and the cross-section of the exit orifice of the applicator. Future modifications can be implemented into the applicator to measure and vary the speed of the spinner discs and the cross-sectional discharge opening to control the spread pattern in the direction perpendicular to the direction of travel and a study commissioned to determine its effects.

- A feasibility study should be conducted to determine if the entire hydraulic motor and the flow control valves could be replaced by a faster electric motor and driver.

Summary

Existing VRT fertilization technologies available for citrus production were evaluated. The definition of the benchmarking test and the performance criteria could be a basis on which new standardized evaluation procedures could be developed to benchmark VRT controllers and their sub-components. The electro-mechanical components were mathematically modeled which served as the parameters in developing tuning rules and gain constants to be implemented in a PID control algorithm to optimize the performance of the VRT applicator to respond to the varying fertilizer needs of each tree in citrus groves. This provides a tool to the industry to implement efficient and optimally tuned control algorithms in the VRT systems. Additional features such as the real-time offset, delay time and speed compensation which greatly enhance the performance of the applicator were presented and experimentally proven for commercial scale implementation with the existing technologies.

APPENDIX
CONTROLLER SETUP, ANOVA RESULTS AND MISCELLANEOUS FIGURES

Nomenclature

A = ampere
ha = hectare
Hz = hertz
kg = kilogram
L = liter
m = meter
min = minute
N = nitrogen
p = pulses
Pa = pascal
rad = radians
rev = revolutions
s = second
s = complex frequency variable (Laplace transform)
V = volts

Commercial Controller Configuration

Table A-1. Commercial Controller Module-1 setup for DC motor operated flow control valve.

Implement Settings			PCM 1 Settings		Product Setup for PCM 1	
Implement Width	6.25	ft	Favorite	Loaded		
Number of Sections	2		Application	Granular	PCM 1	
Sections	3		App. Name	Main_Bin	In Use	
Section 1 switch	1		Config Standard	Standard	Prescription	0250500L
Boom 1 Width	6.25	ft	PCM Link	None	Layer	
Section 2 Switch	2		Drive Type	Servo	Product	Gran
Boom 2 Width	3.125	ft	Gain	7	Initial Quantity	
Section 3 Switch	3		Start Up Drive	20%	Rate A	500
Boom 3 Width	3.125	ft	Master Switch	Hold	Rate B	
Offset Direction Y	Back		Implement Status	Hold	Rate C	
Offset Distance Y	0	ft	Valve Delay	0.0 s	Rate D	
Offset Direction X	Right		Valve Location	Inline	Rate E	
Offset Distance X	0	ft	Units	lb/ac	Product Density	64.4 lb/ft^3
PCM Assignment	PCM 2		Primary Sensor	Granular		
Sections	3		Input	A		
Section 1 switch	4		Sensor Name	-		
Boom 1 Width	6.25	ft	Cal. #	509 p/ft^3		

Table A-1 continued

Implement Settings			PCM 1 Settings		Product Setup for PCM
Section 2 Switch	5		Secondary Sensor	None	
Boom 2 Width	3.125	ft	Monitor 1	"	
Section 3 Switch	6		Monitor 2	"	
Boom 3 Width	3.125	ft	Monitor 3	"	
Offset Direction Y	Back		Monitor 4	"	
Offset Distance Y	0	ft	Favorite	Loaded	
Offset Direction X	Left		Application	Granular	
Offset Distance X	0	ft	App. Name	Main_Bin	
PCM Assignment	PCM 1				

[a] Calibration Number for Encoder-1. This number is different for different encoders.

Table A-2. Commercial Controller Module-1 setup for proportional solenoid flow control valve.

Implement Settings			PCM 1 Settings		Product Setup for PCM 1	
Implement Width	6.25	ft	Favorite	Loaded		
Number of Sections	2		Application	Granular	PCM 1	
Sections	3		App. Name	Main_Bin	In Use	
Section 1 switch	1		Config Standard	Standard	Prescription	0250500L
Boom 1 Width	6.25	ft	PCM Link	None	Layer	
Section 2 Switch	2		Drive Type	PWM	Product	
Boom 2 Width	3.125	ft	Gain	1	Initial Quantity	
Section 3 Switch	3		Frequency	110 Hz	Rate A	500
Boom 3 Width	3.125	ft	Min. duty cycle	10%	Rate B	
Offset Direction Y	Back		Max. duty cycle	50%	Rate C	
Offset Distance Y	0	ft	Ramp Time	0.1 sec.	Rate D	
Offset Direction X	Right		Dither	5%	Rate E	
Offset Distance X	0	ft	Master Switch	Hold	Product Density	64.4 lb/ft^3
PCM Assignment	PCM 2		Implement Status	Hold		
Sections	3		Valve Delay	0.0 sec.		
Section 1 switch	4		Units	lb/ac		
Boom 1 Width	6.25	ft	Primary Sensor	Granular		
Section 2 Switch	5		Input	A		
Boom 2 Width	3.125	ft	Sensor Name	-		
Section 3 Switch	6		Calibration No. [a]	509 p/ft^3		
Boom 3 Width	3.125	ft	Secondary Sensor	None		
Offset DirectionY	Back		Monitor 1	None		
Offset Distance Y	0	ft	Monitor 2	None		
Offset Direction X	Left		Monitor 3	None		
Offset Distance X	0	ft	Monitor 4	None		
PCM Assignment	PCM 1					

[a] Calibration Number for Encoder-1. This number is different for different encoders.

Table A-3. Commercial Controller Module-2 setup for proportional solenoid flow control valve.

Configuration			**Channel Setup**		
Channel	Channel 1		Channel	Channel 1	
Type	Granular		Application Rate	600	lb/ac
Drive Type			Spreader Constant [a]	2735	pul/ft^3
Drive Frequency	100 Hz		Density	64.4	lb/ft^3
Input Filter	0.5		Inc/Dec Step	5	lb/ac
Boom Assignment	1		Minimum Rate	0	lb/ac
Drag Belt	Dual		Maximum Rate	600	lb/ac
Boom 1 Configuration			System Gain	Auto Gain	
Type	Granular				
Sections	1,2 and 3				
Section 1 Width	6.25	ft			
Section 2 Width	3.125	ft			
Section 3 Width	3.125	ft			

[a] Calibration Number for Encoder-2. This number is different for different encoders.

ANOVA Results

Table A-4. ANOVA for TAE for the commercial systems.

Source of Variation	*SS*	*df*	*MS*	*F*	*P-value*	*F crit*
Between Groups	43.5154	7	6.2165	**80.7813**	1.61E-18	**2.3127**
Within Groups	2.4625	32	0.0770			
Total	45.9779	39				

Table A-5. ANOVA for TSAE for the commercial systems.

Source of Variation	*SS*	*df*	*MS*	*F*	*P-value*	*F crit*
Between Groups	27.5094	7	3.9299	**50.6705**	1.58E-15	**2.3127**
Within Groups	2.4819	32	0.0776			
Total	29.9912	39				

Table A-6. ANOVA for TAE for the six PID Tuning Rules.

Source of Variation	*SS*	*df*	*MS*	*F*	*P-value*	*F crit*
Between Groups	0.1694	5	0.0339	**7.7486**	0.0002	**2.6207**
Within Groups	0.1050	24	0.0044			
Total	0.2744	29				

Table A-7. ANOVA for TSAE for the six PID Tuning Rules.

Source of Variation	*SS*	*df*	*MS*	*F*	*P-value*	*F crit*
Between Groups	0.0643	5	0.0129	**4.0254**	0.0086	**2.6207**
Within Groups	0.0767	24	0.0032			
Total	0.1410	29				

Miscellaneous Figures

Figure A-1. VRT applicator with all instrumentation.

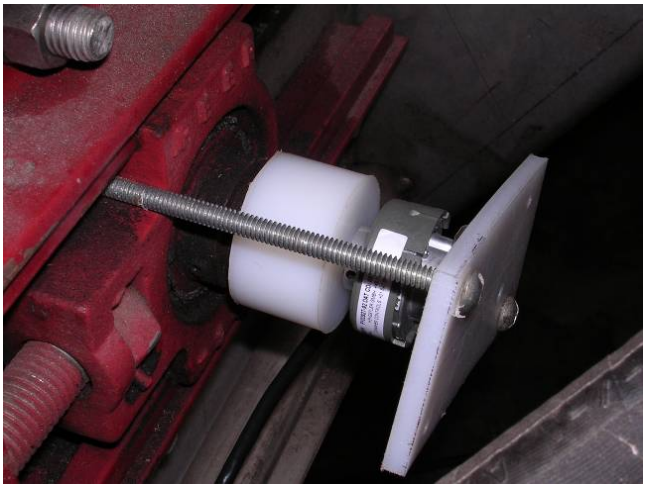

Figure A-2. Encoder-3 mounted on the conveyor chain roller shaft.

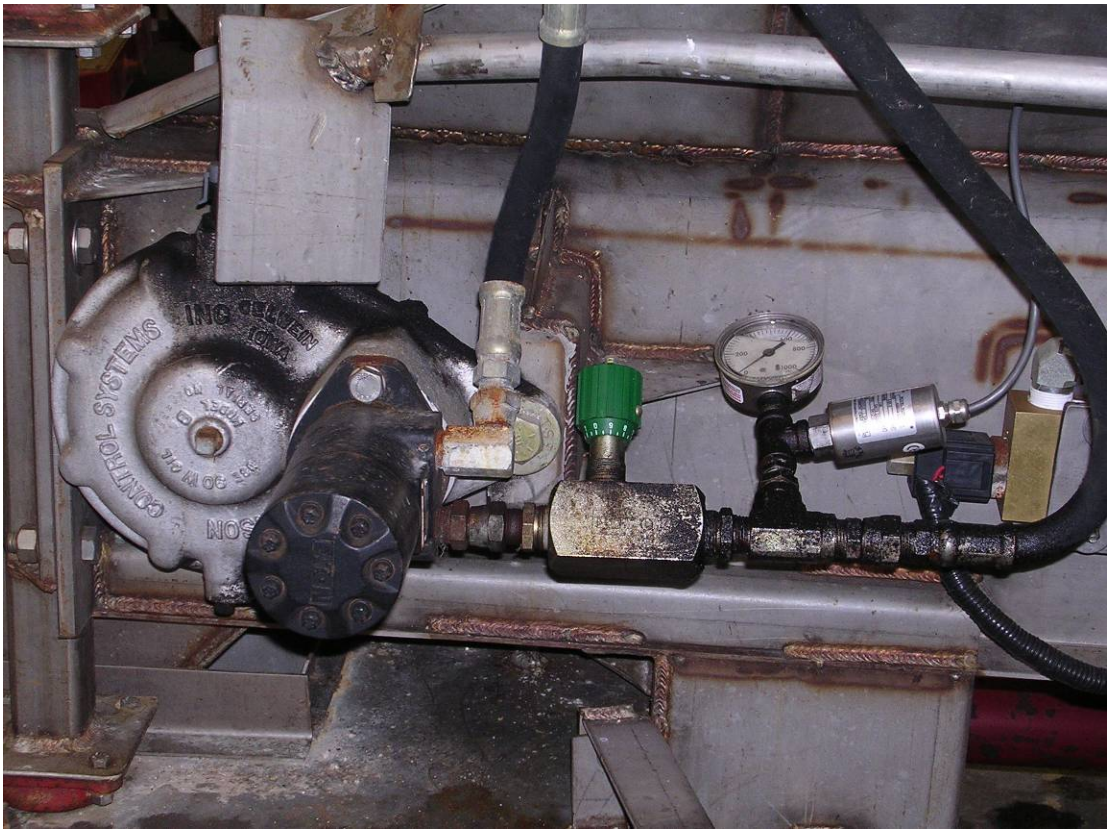

Figure A-3. Needle valve and the pressure transducer.

a) 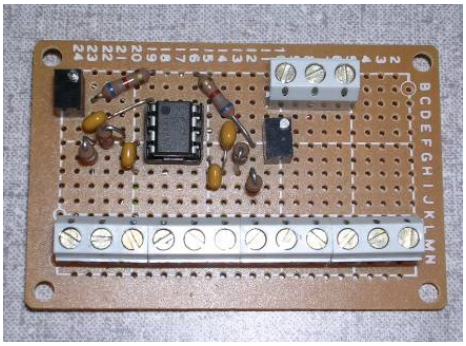

b) 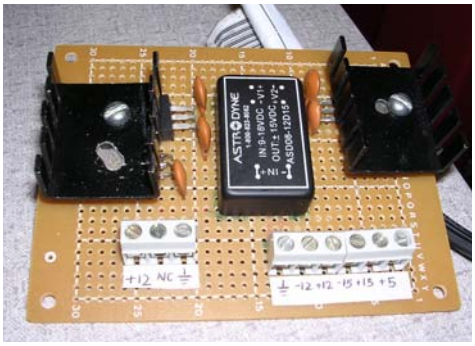

Figure A-4. Circuit boards. a) 100 Hz Low-pass filter and b) Power supply board.

a) 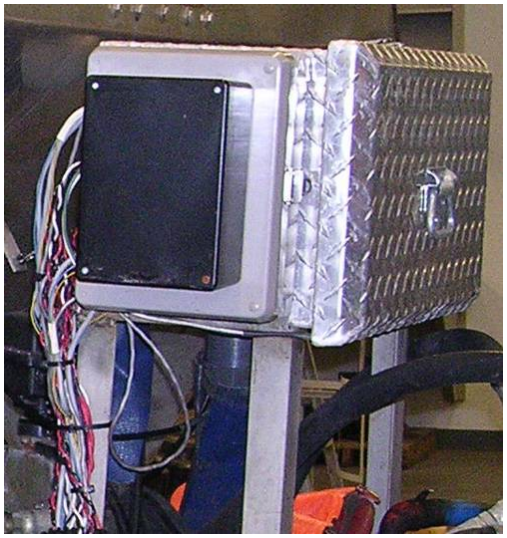 b) 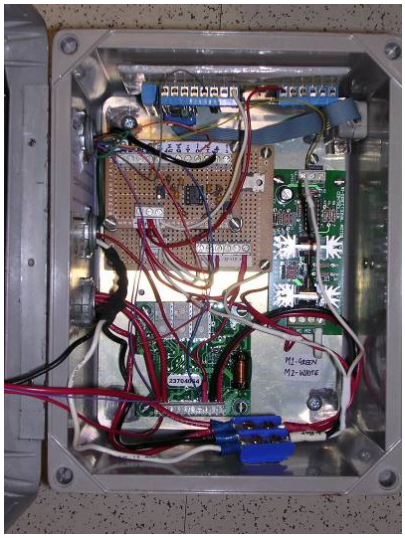

Figure A-5. Instrumentation box. a) Outer view of the instrumentation box and b) Power supply board, low-pass filter board and control boards for flow control valves.

Figure A-6. Proportional solenoid and DC motor operated flow control valves

LIST OF REFERENCES

Aphale, A, Bolander, N, Park, J, Shaw, L, Svec, J, Wassgren, C. 2003, "Granular fertiliser particle dynamics on and off a spinner spreader," *Biosystems Engineering* Vol. 85, no. 3, pp. 319-329.

American Society of Agricultural and Biological Engineers (ASABE). 2004, *ASAE standards 2004*, ASABE, St. Joseph, Michigan.

Auernhammer, H. 2002. "The role of mechatronics in crop product traceability," *Agricultural Engineering International: the CIGR Journal of Scientific Research and Development*, invited overview paper. Vol. IV. October, 2002, presented at the Club of Bologna meeting, July 27, 2002, Chicago, Illinois., USA, p. 6.

Chan, C, Schueller, J, Miller, W, Whitney, J, Cornell, J. 2003, "Error sources of nitrogen fertilizer variable rate application," *Precision Agriculture,* Vol. 5, no. 6, pp. 601-616.

Cointault, F, Sarrazin, P, Paindavoine, M. 2003, "Measurement of the motion of fertilizer particles leaving a centrifugal spreader using a fast imaging system," *Precision Agriculture,* Vol. 4, no. 3, pp. 279-295.

Cugati, S, Miller, W, Schueller, J. 2003, "Automation concepts for the variable rate fertilizer applicator for tree farming," *Programme Book of the joint conference of ECPA-ECPLF*, Wageningen Academic Publishers, Wageningen, pp. 391-392.

Cugati, S, Miller, W, Schueller, J. 2005a, "Dynamic modeling of the hydraulic system of a variable-rate spinner disc granular fertilizer spreader," *ASAE Annual International Meeting*, American Society of Agricultural Engineers, Tampa, paper no. 051126.

Cugati, S, Miller, W, Schueller, J. 2005b, "Dynamic modeling of variable rate granular applicator hydraulic flow control valve," in *Precision Agriculture '05*, Wageningen Academic Publishers, Wageningen, pp. 691-697.

DICKEY-john Corporation. 2003, *Land Manager® Version 1.3 Operator's Manual*, DICKEY-john Corporation, Auburn, Illinois.

Dorf, R. 1996, *The engineering handbook*, CRC Press Inc, Boca Raton, Florida.

Ehrl, M, Demmel, M, Stemfhuber, W, Maurer, W, Wunderlich, T. 2002, "Spatio-temporal quality of precision farming applications," *ASAE Annual International Meeting*, American Society of Agricultural Engineers, Chicago, Illinois, paper no. 023084.

Ess, D, Morgan, M. 2003, *The precision-farming guide for agriculturists*, John Deere Publishing, Moline, Illinois.

Food and Resource Economics Department. 2006, *Acreage, production and utilization*, Institute of Food and Agricultural Sciences, University of Florida, , viewed 23 May 2004, <http://www.fred.ifas.ufl.edu/citrus/pubs/ref/acre.htm#t21>.

Fulton, J, Shearer, S, Chabra, G, Higgins, S. 2001, "Performance assessment and model development of a variable-rate, spinner-disc fertilizer applicator," *Transactions of ASAE*, Vol. 44, no.5, pp. 1071-1081.

Johnson, C. 1977, *Process control instrumentation technology*, John Wiley & Sons, Inc, New York.

Johnson, M, Moradi, M. 2005*, PID control: New identification and design methods*, Springer-Verlag London Limited, London.

Mennel, R, Reece, A. 1963, "The theory of a centrifugal distributor, III: Particle trajectories," *Journal of Agricultural Engineering Research*, Vol. 8, no.1, pp. 78-84.

Miller, W, Whitney, J, Schumann, A, Buchanon, S. 2003, "A test program to assess VRT granular fertilizer applications for citrus," in *ASAE Annual International Meeting*, American Society of Agricultural Engineers, Las Vegas, paper no. 031126.

Miller, W, Schumann, A, Whitney, J. 2004, "Evaluating variable rate granular fertilizer technologies in Florida citrus," *Proceedings of the Florida State Horticultural Society*, no. 117, pp.161-166.

Midwest Technologies. n.d., *Fieldware for the Legacy 6000*, Midwest Technologies LLC, Illinois.

Office of Agricultural Water Policy. 2006, *Nitrogen best management practices (BMPs) for Florida ridge citrus*, viewed 12 February 2006, <http://www.floridaagwaterpolicy.com/PDFs/BMPs/Ridge_BMP_manual.pdf>.

O'Dwyer, A. 2003, *Handbook of PI and PID controller tuning rules*, Imperial College Press, Covent Garden, London.

Olieslagers, R, Ramon, H, De Baerdemaeker, J. 1996, "Calculation of fertilizer distribution patterns from a spinning disc spreader by means of a simulation model," in *Journal of Agricultural Engineering Research (1996),* no. 63, pp. 137-152.

Parish, R. 2002, "Broadcast spreader pattern sensitivity to impeller/spout height and PTO speed," *Applied Engineering in Agriculture*, Vol. 18, no.3, pp. 297-299.

Persson, K, Skøvsgaard, H, Weltzien, C. 2003, "Technical solutions for variable rate fertilization," in *Precision Agriculture*, Wageningen Academic Publishers, Wageningen, pp. 545-557.

Schueller, J. 1992, "A review and integrating analysis of spatially-variable control of crop production," *Nutrient Cycling in Agroecosystems,* Vol. 33, no.1, pp.1-34.

Schumann, A, Miller, W, Zaman, Q, Hostler, K, Buchanon, S, Perkins, G, Cugati, S. 2006, "Variable rate granular fertilization of citrus groves: spreader performance with single-tree prescription zones," in *Applied Engineering in Agriculture*, Vol. 22, no.1, pp. 19-24.

Shearer, S, Stombaugh, T, Fulton, J, Mueller, T. 2002, "Considerations for development of variable-rate controller test standard," *ASAE Annual International Meeting*, American Society of Agricultural Engineers, Chicago, paper no. 021191.

Task force on building a science roadmap for agriculture. 2001, "A science roadmap for agriculture," National association of state universities and land-grant colleges, experiment station committee on organisation and policy.

Tilman, D, Fargione, J, Wolff, B, D'Antonio, C, Dobson, A, Howarth, R, Schindler, D, Schlesinger, W, Simberloff, D, Swackhamer, D. 13 April 2001, "Forecasting agriculturally driven global environmental change," *Science*, Vol. 292, Issue 5515, pp.281-284.

Trimble Navigation Limited. Feb 2004, *NMEA-0183 Messages: Guide for AgGPS receivers*, Trimble Navigation Limited, Overland Park, KS.

Tucker, D, Alva, A, Jackson, L, Wheaton, T. 1995, *Nutrition of Florida Citrus Trees: SP 169*, University of Florida, Institute of Food and Agricultural Sciences, p. 22, Gainesville, Florida.

Tumbo, S, Whitney, J, Miller, W, Wheaton, T. 2001, "Design and testing of a site-specific citrus yield monitor," *ASAE Annual International Meeting*, American Society of Agricultural Engineers, Sacramento, paper no. 01-01183.

Wang, F, Juang, W, Chan, C. 1995, "Optimal tuning of PID controllers for single and cascade control loops," *Chemical Engineering Communications*, Vol. 132, pp.15-34.

Whitney, J, Harrell, R. 1989, "Status of citrus harvesting in Florida." *Journal of Agricultural Engineering Research*, Vol. 42, pp.285-299.

Whitney, J, Miller, W, Wheaton, T, Salyani, M, Schueller, J. 1999, "Precision farming applications in Florida Citrus," *Applied Engineering in Agriculture*, Vol. 15, no.5, pp.399-403.

Yildirim, Y, Kar, M. 2003, "Effect of vane height on distribution uniformity in rotary fertilizer spreaders with different flow rates," *Journal of Agricultural Engineering Research*, Vol. 19, no.1, pp. 19-23.

Zhuang, M, Atherton, D. May 1993, "Automatic tuning of optimum PID controllers," *IEEE Proceedings-D*, Vol. 140, no. 3, pp.216-224.

BIOGRAPHICAL SKETCH

Sharath Aswathanarayan Cugati was born on February 11, 1976, in Kollegal, India. He grew up in Bangalore, India, where he had his initial schooling. He attended the BMS College of Engineering in Bangalore, which was affiliated with the Bangalore University. He earned the Bachelor of Science degree in mechanical engineering in 1998. After this, he worked for 11 months as a management trainee at Kirloskar Toyoda Textile Machinery Limited, Bangalore, a joint venture between the Kirloskar Group, India, and the Toyota Industries Corporation, Japan. After a voluntary resignation from this post he moved to Gainesville, Florida, to pursue his Master of Science degree in mechanical engineering at the University of Florida. After his completion of his master's degree, he enrolled for Doctor of Philosophy degree in the Department of Agricultural and Biological Engineering. The aim of his research was to improve precision agriculture technologies for Florida citrus.